Faculty of Engineering and Science

Department of Mechanical Engineering

Characterisation and Properties of Biomass Compost Pellets

Sim Yun Kiat

This thesis is presented for the Degree of

Doctor of Philosophy

of

Curtin University

September 2016

ABSTRACT

As Malaysia is one of the largest palm oil producers and exporters around the globe, significant amount of biomass wastes is produced from this industry. Large portion of these biomass wastes are empty fruit bunches (EFB) which were typically either burned or converted into energy sources. An alternative means to recycle the waste is through composting. However, these composts are generally loose, wet, and bulky in its original which can be difficult to handle. Pelleting compost improves efficiency of by densifying them into a dense and solid compost pellets. Although the pellets may have been utilised in practice, the characterisation of the production and the properties of EFB compost pellets yet to be well documented and studied. As a result, it is not known if and how the pellets can be optimised for improved performance. In this project, the relationships between the processing parameters and material property, mechanical strength, and nutrient release characteristics of compost pellets were studied.

The first study was to investigate the compaction behaviour by compacting ground EFB compost powder into pellets using the instrumented die. Specific energy of compaction was found to be decreased with increased moisture content. Compaction data were obtained by two methods: “in-die” method and “out-of-die” method. These data were analysed using Heckel model and Kawakita-Ludde model. The Kawakita-Ludde model provided the best fit of data for all pressure range and conditions tested. Decreasing particle size and increasing moisture content improved compaction behaviour of the ground EFB compost; however, moisture content above 15% was deleterious on pellet porosity.

The second study was to investigate the properties of the EFB compost pellets including the physical strength and nutrient release characteristics. The effect of compaction pressure, particle size, moisture content and storage were evaluated. The physical strength of the produced pellet was studied by mechanically crush the pellets in diametrical direction. The diffusion characteristics of the EFB compost pellets were studied based on the change in conductivity with the pellets submerged in distilled water. The pellet strength increased with the applied compaction pressure but plateaued when the pellets achieved zero porosity during the compaction. Increasing the moisture content resulted in pellets with higher strength at lower compaction pressures but a lower maximum strength. Pellets with smaller particle size exhibited slightly higher strength. The influence of storage appears to affect the final strength of the pellets differently dependent on the initial moisture content. Despite the

increase in porosity after storage, pellets with higher moisture content exhibited an increase in strength after storage, and loses strength with 5% moisture content. Highest pellets strength was attained with 15% moisture content. In the nutrient release study, the increase in nutrient release rate is correlated to the final strength of the pellets. The nutrient release rate plateaued when the diametrical compressive strength achieved in approximate 0.2 MPa. The nutrient release rate is significantly decreased with smaller particle size due to the deceased effective pathway for diffusion.

The third study was to investigate the underlying compaction mechanism of pellet mill. The friction build-up in the die channels of a pellet mill was found to be the principal pelleting compaction pressure and was modelled using the elemental slice approach. The proposed model predicted the pelleting compaction pressure for the given die geometry and the physical parameters: radial-axial pressure transmission ratio K, residual stress σ_{res}, and coefficient of friction during ejection μ_e. The proposed model was in good agreement with experimental results. The physical parameters of the proposed model were independently studied using a customised instrumented die which incorporates measurements of top, bottom and radial pressure. The following observations were made: increasing moisture content increased K and μ_e, and decreased σ_{res}; increasing particle size has no significant effect on σ_{res} , slightly decreased K and μ_e; Values of σ_{res}, K and μ_e correlated with compact porosity corresponding to the applied compaction pressure.

In the fourth study, an iterative approach which combines the proposed pellet mill compaction model and Kawakita-Ludde model to predict the steady-state pellet mill compaction pressure were developed. Results from previous studies were consolidated to allow prediction of pellet porosity and properties of the pellet based on given parameters of moisture content, particle sizes and die geometry. Results showed that the steady state pelleting pressure increased with the increased moisture content and increased die geometry which followed experimental trends from existing literature. This approach able to show the primary cause of clogging in pellet mill was due to the excessive moisture content from the increased adhesion of the raw material on the die wall. Clogging can be avoided by reducing the moisture content or the length of the die channel.

DECLARATION

To the best of my knowledge and belief this thesis contains no material previously published by any other person except where due acknowledgment has been made.

This thesis contains no material which has been accepted for the award of any other degree or diploma in any university.

Signature : ______________________

Date : 9/9/2016

ACKNOWLEDGEMENT

I wish to express my sincere gratitude and thank to Dr. Aaron Goh Suk Meng, who has been my mentor and source of inspiration for me to embark on this PhD journey. This thesis would not have been possible without his continuous support and guidance, and for this I am deeply indebted.

I would like to thank my main supervisor Dr. Chua Han Bing, co-supervisor Dr Wong Kwong Soon, and thesis chairperson Dr Amandeep Sidhu. Dr Chua Han Bing and Dr Wong Kwong Soon provided me invaluable ideas and help which is indispensable in bringing this work to culmination.

I would like to express my appreciation to Celtex Resources Sdn Bhd and the Faculty of Engineering School for the financial support. Special thanks to the Dean of Faculty of Engineering, Prof. Michael Cloke, and Dean of Graduate School, Prof. Marcus Lee, for kindly granting me an extension in thesis completion and extended monetary support.

I would also like to thank all the laboratory personals, Mr. Michael Ding, Mr. Gideon Darias, Mr. George Edmund, Mr. Denn Alladin, Mr. Kevin Wong, and Ms. Magdalene Bangkang Joing, for their assistance in my experimental work. I am thankful as well to my family, friends, and colleagues for their motivation and companionship.

Finally, I would like to express my gratitude to my wife, Michelle Phua Siew Huei for her unconditional love and unwavering support throughout my graduate studies.

In dedication to my mom, Chai Siew Chin who lives eternally with Him.

TABLE OF CONTENTS

ABSTRACT i

DECLARATION iii

ACKNOWLEDGEMENT iv

TABLE OF CONTENTS v

LIST OF FIGURES x

LIST OF TABLES xviii

LIST OF NOMENCLATURE xix

CHAPTER 1: INTRODUCTION 1

1.1 Palm oil 1

1.2 Palm oil by-products 3

1.3 Composting process 3

1.4 Pelleting compost 6

1.5 Challenges and research needs 6

1.6 Objectives 8

1.7 Overview of thesis 9

CHAPTER 2: BACKGROUND AND LITERATURE REVIEW 11

2.1 Densification process 11

2.1.1 Binding mechanism 12

2.1.2 Density 14

2.1.3 Porosity 15

2.1.4 Elastic recovery 16

2.2 Biomass composition 17

2.3 Pellet mill 18

2.3.1 Pellet mill densification process 19

2.4 Existing models describing pellet mill compaction mechanism 21

2.4.1 Holm’s model 22

2.5 Characterisation of biomass compost pellets 25

2.5.1 Compactability 25

2.5.2 Compressibility 29

2.5.3 Nutrient release behaviour 30

2.6 Factors affecting densification behaviour 34

2.6.1 Effects of compaction pressure 34

2.6.2 Effects of die channel dimension 35

2.6.3 Effects of moisture content 36

2.6.4 Effects of particle size 38

2.6.5 Effects of storage time and conditions 39

2.7 Conclusions 40

CHAPTER 3: COMPACTION BEHAVIOUR OF GROUND EFB COMPOST 43

3.1 Introduction 43

3.2 Material preparation 44

3.2.1 Measurement of moisture content and water activity 45

3.2.2 Moisture adjustment 45

3.2.3 Measurement of true density of powder 46

3.3 Experimental setup 46

3.3.1 Design of instrumented die 47

3.3.2 Powder compaction procedure 51

3.4 Property of ground EFB Compost 53

3.4.1 Microscopy and Particle Size Analysis 53

3.4.2 Particle density, moisture content and water activity 54

3.5 Results and discussions 55

3.5.1 Loading and unloading 55

3.5.2 Porosity 59

3.5.3 Compaction models 65

3.6 Conclusions 78

CHAPTER 4: PROPERTIES OF EFB COMPOST PELLETS 80

4.1 Introduction 80

4.2 Materials and Methods 82

4.2.1 Pellet preparation 82

4.2.2 Mechanical strength test 83

4.2.3 Nutrient release tests 84

4.2.4 Analysis of kinetic release data 85

4.3 Results and discussion 86

4.3.1 Mechanical properties 86

4.3.2 Nutrient release 97

4.4 Conclusions 106

CHAPTER 5: MODELLING OF THE PELLET MILL COMPACTION MECHANISM 107

5.1 Introduction 107

5.2 Theory 108

5.3 Materials and methods 111

5.3.1 Materials 111

5.3.2 Compaction experiments 111

5.4 Results and discussions 114

5.4.1 Radial axial transmission ratio, K 114

5.4.2 Residual die wall pressure 118

5.4.3 Ejection force 122

5.4.4 Coefficient of friction during ejection 125

5.5 Validation of pellet mill compaction model 130

5.6 Conclusions 131

CHAPTER 6: STEADY-STATE PELLET MILL COMPACTION 133

6.1 Introduction 133

6.2 Iteration procedure 135

6.3 Results and discussion ... 137

6.3.1 Steady-state pelleting pressure ... 139

6.3.2 Porosity and pellet strength ... 141

6.4 Conclusions ... 144

CHAPTER 7: CONCLUSIONS, RECOMMENDATIONS, AND FUTURE WORK ... 145

7.1 Conclusions ... 145

7.2 Recommendations ... 149

7.3 Future work ... 149

CHAPTER 8: REFERENCES ... 151

LIST OF FIGURES

Figure 1.1: Oil palm tree bearing fruits (Lim 2014) 2

Figure 1.2: Simplified palm oil production flow chart (Hashim et al. 2012) 2

Figure 1.3: Production cycle of EFB compost pellets 4

Figure 1.4: Composting windrow 5

Figure 1.5: Matured EFB compost delivered with conveyor belt at the pelleting plant 5

Figure 1.6: Processing EFB compost into pellet with pellet mill 5

Figure 1.7: Relations between processing conditions & material properties, mechanical strength, and dissolution profile.. 8

Figure 2.1: Powder compaction curve. Adapted from Pietsch (2008)...................... 12

Figure 2.2: Pictorial representation of the binding mechanism. Adapted from Pietsch (2008). 14

Figure 2.3: Flat-die pellet mill (left), ring-die pellet mill (right) 19

Figure 2.4: Illustration of the pelleting process 20

Figure 2.5: Deformation of biomass powder under the roller of a pellet mill 21

Figure 2.6: Principal axes of wood with respect to grain direction. Adapted from Walker (2005) 23

Figure 2.7: Compaction behaviour of two different type of material with different particle size on Heckel plot (Hersey and Rees 1971). Type 1 indicates compaction by plastic deformation, and Type 2 indicates compaction by fragmentation. 27

Figure 2.8: Schematic diagram for pellet compressive strength tests compressed at the axial direction (left) and, diametrical direction (right).. 29

Figure 3.1: Schematic diagram of the instrumented die (i) Top view (ii) Sectional side view.. 48

Figure 3.2: The assembled instrumented die on a universal tensile compression testing machine. A separate LVDT was attached to the crosshead to synchronise data between separate data loggers. 49

Figure 3.3: Radial pressure calibration of the instrumented die with NBR elastomer. 50

Figure 3.4: Measurement of pellet height (a) during compaction process, (b) after ejection, and (c) after prolonged storage.. 52

Figure 3.5: Particle size distribution of ground EFB compost.................................. 53

Figure 3.6: Micrograph of the compost powder with particle sizes of 150-300 μm (left) and 300-600 μm (right). Granular particles as indicated by the arrow. 54

Figure 3.7: Typical compaction data from the instrumented die during loading and unloading. Pre-set compaction load of 8000 N with ground EFB compost particle size of 150-300 μm and 15% (w.b.) moisture content. 56

Figure 3.8: Typical radial-axial compaction curve of ground EFB compost in the instrumented die. Pre-set compaction load of 8000 N with EFB compost particle size of 150-300 μm.. 57

Figure 3.9: Compaction curve during loading and unloading obtained from Lloyd testing machine for the particle size of (a) 150-300 μm and (b) 300-600 μm with different moisture content tested at the highest pre-set load. The displacement data has been corrected for machine elasticity. 58

Figure 3.10: Specific energy requirement of compaction for EFB compost powder with different moisture content and particle size. 59

Figure 3.11: Relationship between porosity at different conditions and the applied compaction pressure for EFB compost powder with particle size of 150-300 μm and moisture content ■ 5%, ♦ 10%, ▲ 15%, ● 25% 61

Figure 3.12: Relationship between porosity at different conditions and the applied compaction pressure for EFB compost powder with particle size of 300-600 μm and moisture content ■ 5%, ♦ 10%, ▲ 15%, ● 25% 62

Figure 3.13: Schematic diagram of powder compaction in an instrumented die....... 63

Figure 3.14: Relationship between coefficient of friction during compaction and compact porosity with particle size of 150-300 μm and moisture content of (a) 5%, (b) 10%, (c) 15% and (d) 25% 64

Figure 3.15: Relationship between coefficient of friction during compaction and compact porosity with particle size of 300-600 μm and moisture content of (a) 5%, (b) 10%, (c) 15% and (d) 25% 65

Figure 3.16: In-die Heckel plot for EFB compost powder with particle size of (a) 150-300 μm and (b) 300-600 μm. Values in legend indicates the initial moisture content of the pellet. 67

Figure 3.17: Heckel plot for EFB compost powder with particle size of 150-300 μm and various moisture contents measured at different condition (a) after ejection, and (b) after prolonged storage. Values in legend indicate the initial moisture content of the pellet. 70

Figure 3.18: Heckel plot for EFB compost powder with particle size of 300-600 μm and various moisture contents measured at different condition (a) after ejection, and (b) after prolonged storage. Values in legend indicate the initial moisture content of the pellet. 70

Figure 3.19: Elastic recovery of pellet after storage particle size of (a) 150-300 μm (b) 300-600 μm at different moisture content. 71

Figure 3.20: Relationship between the mean elastic recovery and the difference in Heckel constant ***k*** between "in die" and "out of die" after storage result. 72

Figure 3.21: "In die" Kawakita plot for EFB compost powder with the particle size of (a) 150-300 μm and, (b) 300-600 μm at various moisture contents. Values in legend indicate the initial moisture content of the pellet. 74

Figure 3.22: "Out of die" Kawakita plot for EFB compost powder with particle size of 150-300 μm and various moisture contents measured (a) after ejection, and (b) after prolonged storage. Values in legend indicate the initial moisture content of the pellet. 76

Figure 3.23: "Out of die" Kawakita plot for EFB compost powder with particle size of 300-600 μm and various moisture contents measured (a) after ejection, and (b) after prolonged storage. Values in legend indicate the initial moisture content of the pellet. 76

Figure 3.24: Comparison of the "in die" and "out of die" Kawakita plot for EFB compost powder with 5% moisture content and 150-300 μm particle size 78

Figure 4.1: Schematic diagram for crushing of pellet in diametrical direction 84

Figure 4.2: Schematic diagram of the kinetic release experimental setup 85

Figure 4.3: Stress-strain curve for EFB compost pellets with 150-300 μm particle size and moisture content of (a) 5% (b) 10% (c) 15% and, (d) 25% tested immediately after ejection. The numbers in legend indicate the applied compaction pressure. 88

Figure 4.4: Stress-strain curve for EFB compost pellets with 300-600 μm particle size and moisture content of (a) 5% (b) 10% (c) 15% and, (d) 25% tested immediately after ejection. The numbers in legend indicate the applied compaction pressure. 89

Figure 4.5: Stress-strain curve for EFB compost pellets with 150-300 μm particle size and moisture content of (a) 5% (b) 10% (c) 15% and, (d) 25% tested after 1 week storage. The numbers in legend indicate the applied compaction pressure...... 89

Figure 4.6: Stress-strain curve for EFB compost pellets with 300-600 μm particle size and moisture content of (a) 5% (b) 10% (c) 15% and, (d) 25% tested after 1 week storage. The numbers in legend indicate the applied compaction pressure...... 90

Figure 4.7: Relationship between the diametrical compressive strength pellets and the applied compaction pressure with different moisture content. Top row shows particle size of 150-300 μm measured (1.a) after ejection, and (1.b) after storage. Bottom row shows particle size of 300-600 μm measured (2.a)) after ejection, and (2.b) after storage. The numbers in legend indicate the initial moisture content of the pellets. . 91

Figure 4.8: Relationship between maximum compressive strength and the initial moisture content of the compost pellets corresponding to the particle size and storage 91

Figure 4.9: Change in diametrical compressive strength after storage for particle size of (a) 150-300 μm, and (b) 300-600 μm. The numbers in legend indicate the initial moisture content of the pellets. 92

Figure 4.10: Comparison of diametrical compressive strength between pellets measured before storage (■), and after storage (□) against the pellet porosity with the moisture content of (a) 5%, (b) 10%, (c) 15% and, (d) 25% for particle size of 150-300 μm 93

Figure 4.11: Comparison of diametrical compressive strength between pellets measured before storage (■), and after storage (□) against the pellet porosity with the moisture content of (a) 5%, (b) 10%, (c) 15% and, (d) 25% for particle size of 300-600 μm 94

Figure 4.12: Example of deviation in Ryshkewitch – Duckworth plot. Solid line indicates the fitted Ryshkewitch – Duckworth to the linear region of the plot.......... 96

Figure 4.13: Conductivity at equilibrium for EFB compost powder with different particle sizes. Values in legend indicate the particle size range of the EFB compost powder. 98

Figure 4.14: Changes in the size of an EFB compost pellets with time when soaked in water 99

Figure 4.15: Kinetic release plot of EFB compost pellets with particle size of 150-300 µm and initial moisture content of (a) 5%, (b) 10%, (c) 15%, and (d) 25%. Values in legend indicate the applied compaction pressure. 100

Figure 4.16: Kinetic release plot of EFB compost pellets with particle size of 300-600 µm and initial moisture content of (a) 5%, (b) 10%, (c) 15%, and (d) 25%. Values in legend indicate the applied compaction pressure. 100

Figure 4.17: Typical plot of $\ln\frac{c_{\infty}}{c_{\infty}-c}$ against time for the diffusion of EFB compost pellets with initial moisture content of 25% compacted at 80 MPa. 101

Figure 4.18: Effect of compaction pressure on the diffusion rate constant of EFB compost pellets 103

Figure 4.19 Effect of pellet porosity on the diffusion rate constant of EFB compost pellets 104

Figure 4.20: Effect of pellet tensile strength on the diffusion rate constant of EFB compost pellets 105

Figure 5.1: Force balance analysis of a plane element within a cylindrical compact 109

Figure 5.2: Schematic diagram of forces measured with die-wall instrumentation. 112

Figure 5.3: Typical measurement obtained using instrumented die during compaction cycle. Pressures were measured during (a) compaction, (b) unloading, and (c) ejection phase. Label (d) indicates the residual die wall pressure measured 113

Figure 5.4: Relationship between the radial pressure on the die wall and the axial pressure at the position of the radial sensor with different moisture content and particle size of (a) 150-300 and, (b) 300-600 µm. Values in legend indicate the moisture content. 115

Figure 5.5: Relationship between the radial-axial transmission ratio and the compact porosity with different moisture content for particle size of (a) 150-300 µm and, (b) 300-600 µm. Values in legend indicate the moisture content. 117

Figure 5.6: Relationship between residual pressure and the applied compaction pressure with different moisture contents for particle size of (a) 150-300 µm and, (b) 300-600 µm. Values in legend indicate the moisture content. 119

Figure 5.7: Height measurement of in-die relaxed compact porosity 120

Figure 5.8: Relationship between residual pressure and in-die relaxed porosity with different moisture content with particle size of (a) 150-300 µm and, (b) 300-600 µm. Values in legend indicate the moisture content. 121

Figure 5.9: Machine crosshead-piston positioning in reference to the bottom surface of the compact 123

Figure 5.10: Change of friction during the ejection normalised with contact area due to the moisture content of compact with preload of 5000 N for particle size of (a) 150-300 µm and (b) 300-600 µm 124

Figure 5.11: Change of friction during ejection of compact with different range of compaction load for particle size of 300-600 µm and 11.5% (w.b.) moisture content 125

Figure 5.12: Change of friction during ejection of compact with different contact length for particle size of 300-600 µm and 15% (w.b.) moisture content 125

Figure 5.13: Relationship between friction force per contact area and the applied compaction pressure with different moisture content for particle size of (a) 150-300 µm and, (b) 300-600 µm. Values in legend indicate the moisture content. 126

Figure 5.14: Relationship between friction force per contact area and the residual die wall pressure with different moisture content for particle size (a) 150-300 μm and, (b) 300-600 μm. Values in legend indicate the moisture content. 127

Figure 5.15: Relationship between coefficient of friction during ejection and the in-die relaxed porosity with the different moisture content for particle size of (a) 150-300 μm and, (b) 300-600 μm. Values in legend indicate the moisture content. 128

Figure 5.16: Comparison between theoretical (solid line) and experimental results (data points) of pelleting pressure vs $\boldsymbol{HD}$ plot for (a) 10% moisture content, 300-600 μm particle size, (b) 15% moisture content, 300-600 μm particle size. 131

Figure 6.1: Schematic diagram of steady-state pelleting 134

Figure 6.2: Iteration algorithm for solving steady-state pelleting pressure 135

Figure 6.3: Example of relationship between the steady-state pelleting pressure and the die geometry for EFB compost powder with particle size of 150-300 μm and moisture content of 15% 138

Figure 6.4: Comparison of steady-state pelleting pressure with different moisture content for EFB compost with particle size (a) 150-300 μm and, (b) 300-600 μm. Results for 25% moisture content cropped for clarity. 140

Figure 6.5: Comparison of in-die compact porosity with different moisture content for EFB compost with particle size of (a) 150-300 μm and, (b) 300-600 μm 142

Figure 6.6: Comparison of pellet diametrical compressive strength with different moisture content for EFB compost with particle size of (a) 150-300 μm and, (b) 300-600 μm 143

LIST OF TABLES

Table 2.1: Composition of oil palm empty fruit bunches 18

Table 3.1: Properties of ground EFB compost powder.. 55

Table 3.2: Calculated "in-die" Heckel model physical constants for EFB compost . 67

Table 3.3: "Out of die" Heckel model physical constants for EFB compost with particle size of 150-300 µm 69

Table 3.4: "Out of die" Heckel model physical constants for EFB compost with particle size of 300-600 µm 69

Table 3.5: Calculated "in-die" Kawakita model parameter for EFB compost........... 75

Table 3.6: Calculated "out of die" Kawakita model parameter for EFB compost with particle size of 150-300 µm.. 77

Table 3.7: Calculated "out of die" Kawakita model parameter for EFB compost with particle size of 300-600 µm.. 77

Table 4.1: Physical changes of EFB compost pellets after a week storage 87

Table 4.2: Fit parameters of Ryshkewitch – Duckworth equation before storage..... 96

Table 4.3: Fit parameters of Ryshkewitch – Duckworth equation after storage........ 96

Table 4.4: Rate constant for the diffusion of the EFB compost pellets 102

Table 5.1: Values of $\boldsymbol{m}$ and $\boldsymbol{K0}$ obtained from linear fitting of Equation (5.12) 116

Table 5.2: Values of $\boldsymbol{\varphi}$ and $\boldsymbol{\sigma res0}$ obtained from the fitting of Equation (5.13) .. 121

Table 5.3: Values of $\boldsymbol{\gamma}$ and $\boldsymbol{\mu 0}$ obtained from the fitting of Equation (5.14) 129

Table 6.1: Values of physical parameter of the pellet mill compaction model used 136

LIST OF NOMENCLATURE

A	Heckel model constant
a	Kawakita-Lüdde model constant
a_w	Water activity
α	Kinetic release model constant
b	Kawakita-Lüdde model constant
C	Degree of volume reduction
c	Concentration of dissolved nutrient
c_∞	Concentration at equilibrium
D	Diameter of die channel
D_p	Diameter of the pellet
EFB	Empty fruit bunches
ϵ	Pellet strain
φ	Model constant for porosity and residual stress relationship
ε	Porosity
ER	Elastic recovery
F_e	Force needed for ejection
F_f	Friction force from the die channel
F_R	Pellet mill roller force
FFA	Free fatty acid
FFB	Fresh fruit bunches
γ	Model constant for porosity and coefficient of friction relationship
H_0	Height of compact during compaction
H_e	Height of the pellet after ejection
H_f	Final height of the pellet after storage
H_r	Height of compact after the release of compaction pressure
K	Radial-axial pressure transmission ratio
k	Heckel model constant
k_{obs}	Observed rate constant
K_0	Axial-radial transmission ratio at 0 porosity

M_f	Final moisture fraction
M_i	Initial moisture fraction
m_i	Initial mass of the EFB compost
m_w	Mass of water
$M.C.$	Moisture content
μ	Coefficient of friction during ejection
μ_0	Coefficient of friction during ejection at 0 porosity
μ_c	Coefficient of friction during compaction
μ_e	Coefficient of friction during ejection from Eq. (3.11)
η	Ryshkewitch-Duckworth model constant
n	Model constant for porosity and axial-radial ratio relationship
P_a	Axial pressure
P_{N0}	Pre-stress term from Holm's model
P_r	Radial pressure
P_x	Pellet compaction pressure from Holm's model
P_y	Mean yield pressure of the material
RD	Relative density of pellet
ρ_a	Apparent particle density
ρ_B	Bulk density of the powder volume
ρ_c	Maximum compact density
ρ_e	Ejected pellet density
ρ_f	Final pellet density
ρ_p	Density of pellet
ρ_r	Relaxed compact density
ρ_T	True density of powder particle
ρ_w	Density of water
σ	Pellet compressive strength
σ_0	Theoretical compressive strength at zero porosity
σ_A	Axial compressive strength
σ_{bottom}	Bottom axial pressure
σ_{rad_z}	Radial pressure at given height z
σ_{res}	Residual radial stress
σ_{res_0}	Residual stress at 0 porosity

σ_T	Diametrical compressive strength
σ_{top}	Top axial pressure
σ_y	Yield strength of the material
σ_z	Axial pressure at given height z
τ_z	Shear stress at given height z
ν	Poisson's ratio
ν_{LR}	Poisson's ratio in longitudinal-radial direction
V	Volume of powder under compaction
V_0	Initial volume of powder bed
w.b.	Moisture fraction in wet basis
x_w	Moisture content in fraction

CHAPTER 1: INTRODUCTION

1.1 Palm oil

Elaeis Guineensis or commonly called the oil palm is the world's top oil producing crop, surpassing soy bean at 35% production of world vegetable oil (USDA 2014). Currently, Malaysia is the second largest palm oil producer in the world and accounts for 32% of world's palm oil production and 40% of world's exports (USDA 2014). The oil palm industry has proven to be one of the major agricultural commodity in Malaysia, as the local production of palm oil has reached 19.2 million tons of crude palm oil and exported 17.6 million tons across the world in the year 2013 (MPOB 2015). This marks a great economic significance for Malaysia as the palm oil industry contributed 45.7% of gross domestic product in agricultural sector (Department of Statistics 2013).

As of December 2013, a total area of 5.22 million hectares has been planted with oil palms in Malaysia, with 2.59 million hectares in Peninsular Malaysia, 1.16 million and 1.46 million hectares in Sarawak and Sabah respectively (MPOB 2015). A total number of 433 palm oil mills in Malaysia built with the capacity to process 104 million tons of fresh fruit bunches harvested from the oil palms (MPOB 2015).

Throughout its economic life cycle, the oil palm continuously produces fresh fruit bunches in the axil of its fronds (Figure 1.1). The fruits usually ripen within six months after the anthesis as indicated by the change of fruit colour from black to bright orange or red. The ripen fruit bunches are harvested in between 7 to 14 days interval and delivered to the palm oil mill where the palm oil and palm kernels are extracted from the fresh fruit bunches (FFB). The fresh fruit bunches need to be processed as soon as possible to reduce the development of free fatty acid (FFA) which can be detrimental towards the quality of processed palm oil.

Figure 1.1: Oil palm tree bearing fruits (Lim 2014)

Figure 1.2 shows the typical process of palm oil production. To extract the palm oil, the collected fresh fruit bunches are first sterilised in a pressurised steam. This process is meant to prevent the rise of FFA and to assist stripping of palm oil fruits from the fruit bunches as well as to condition the mesocarp, the middle layer of the pericarp of the fruit for oil extraction. The sterilised bunches are then further processed in a rotating thresher drum to strip the oil palm fruits from the fruit bunches, leaving empty fruit bunches (EFB) as by-product and the stripped fruits are further processed for palm oil.

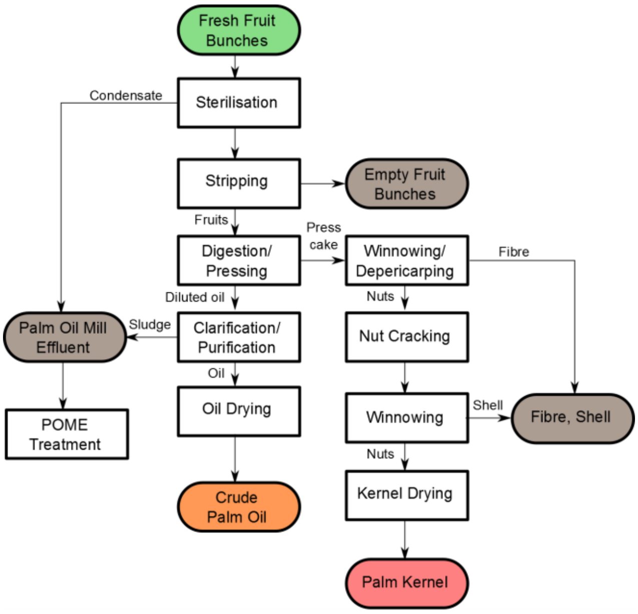

Figure 1.2: Simplified palm oil production flow chart (Hashim et al. 2012)

1.2 Palm oil by-products

The production of palm oil generates a substantial amount of by-products. It is estimated that 22% of empty fruit bunches (EFB), 13.5% of fibre and 5.5% of shell from the fresh fruit bunches left as solid residue (Yusoff 2006). This gives an estimated value of 20.9 million ton of empty fruit bunches were generated corresponding to a total area of 5,229,739 hectares of land planted with oil palm in Malaysia in the year 2013 (MPOB 2015). Traditionally, these empty fruit bunches were disposed by means of mulching or by incineration and recovered for ash for soil conditioner. However, mulching with EFB may provide rhinoceros beetle breeding sites which can cause irreversible damage to the oil palm tree (Heriansyah 2011). Open burning of EFB presents a considerable amount of air pollution problem and has been prohibited by the Malaysian government. Alternatively, EFB can be composted and return to the plantation as organic fertiliser (Abdullah and Sulaiman 2013a).

Composting empty fruit bunches provides higher efficiency in waste management and also economically beneficial as it potentially reduces dependency on inorganic fertilisers with the compost as an alternative source of nutrients for the plants. The volatile prices of the inorganic fertiliser further drive the effort to repurpose all biomass waste into biomass compost while to achieve zero waste emission to the environment in the palm oil industry.

1.3 Composting process

The composting process involves microbial activity to decompose organic matter into a humus residue *i.e.* stable organic material. Composting empty fruit bunches produces higher nutrient content while reduces the overall volume and weight (Heriansyah 2011). However, the composting process may take up 32 weeks for the compost to mature (Lim 1989). Various methodologies have been developed to improve on composting process by increasing the degradation rate and nutrient value of the final compost. Baharuddin et al. (2009) demonstrated a reduction of carbon to nitrogen (C/N) ratio from 45 to 15 after 48 days by co-composting empty fruit bunches with partially treated POME. Study on the addition of microbial to the EFB composting process saw a greater reduction rate on the C/N ratio (Mukhlis 2006). Nahrul et al. (2012) studied the feasibility of vermicomposting the EFB with the addition of POME and showed an increase in heavy metal concentration which may be essential for plant growth.

Figure 1.3 shows the typical production cycle of EFB compost. To produce compost with empty fruit bunches, the stripped fruit bunches are conveyed to the chipper shredder to process the fibrous strand of the fruit bunches into fine pieces with an approximate 3cm to 4cm in length. The shredded empty fruit bunches are then transported to the main composting plant where the fibres are piled in long rows of windrows (Figure 1.4). These rows are frequently turned with the windrow turner to redistribute the pile and sprayed with palm oil mill effluent. Microbial is added into the compost pile to further hasten the composting process. Upon maturity, the composts are transported to the pelleting plant where the composts are processed into dense pellets with pellet mills, repackaged and ready for distribution (Figure 1.5 & Figure 1.6).

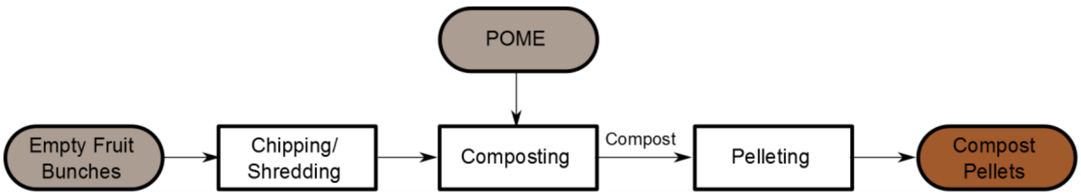

Figure 1.3: Production cycle of EFB compost pellets

Figure 1.4: Composting windrow

Figure 1.5: Matured EFB compost delivered with conveyor belt at the pelleting plant

Figure 1.6: Processing EFB compost into pellet with pellet mill

1.4 Pelleting compost

Due to the inherent characteristics of high moisture content and low bulk density of the EFB compost in its original form, distribution of the compost across the oil palm estate by means of manual labour can be costly and requires large amount of space to store. The unprocessed EFB composts may leach significant amount of nutrients to the environment, rendering it unsuitable to be used in an efficient manner. To resolve the aforementioned issues, the compost can be further densified into pellets using pellet mills. Pellet mill is one of the commonly used machines for forming and densification in the biomass processing industry. Processing the EFB compost into pellets has significant advantages which led to its widespread adoption in the industry. In the densification process, the application of external mechanical pressure enables the compost to bond together and reduces the overall bulk volume of the compost. This process produces higher net nutrient content per volume compost pellets in a consistent shapes and sizes which allow for ease of transportation, handling and storage. During usage, the EFB compost pellets may disintegrate slowly when in contact with water and releases the nutrients to the soil for plant absorption.

1.5 Challenges and research needs

Although the biomass densification has been investigated extensively in the last few decades, the mechanism behind pellet mill densification process is still not well understood primarily due to the complex interaction between material properties and machine processing conditions. In current trend of research, studies on the densification of biomass were primarily focused on the compaction behaviour of selected biomass, and the resulting pellet strength from the applied mechanical pressure. The biomass densification studies were typically conducted experimentally either with laboratory apparatus or pilot scale studies with actual pellet mill.

In laboratory studies, uniaxial compaction with piston-cylinder die is one of the most common methods in the literature for studying biomass densification. This method allows detailed analysis of compaction behaviour of biomass and small scale production of pellets for quality analysis. However, results from previous laboratory studies can hardly be extended to industrial setting (Xia et al. 2014), owing to the difficulties in quantifying the underlying applied compaction pressure in actual pellet mill.

In pilot scale studies with pellet mill, factorial design was used to test the effect of variables on the production of biomass pellets and the models describing the results were empirical in nature. This method which can be time consuming and inherently expensive as there is no complete model that sufficiently describe the pelleting process. Fundamental research on the pellet mill compaction process is necessary in order to develop applicable models to meet practical needs.

The compost pellets are subjected to frequent mechanical loading during production and transport. As the compost pellets are frequently handled from transporting the product to the oil palm estates, problems with broken pellets and fine dusts have often been reported. Current production of compost pellets still associated with pellets with low quality and high moisture content problem. To improve on the overall quality and effectiveness of the compost pellets, contributing factors such as the properties of the input material, and manufacturing process variables of the pellet mill should be studied extensively. These variables can be controlled to optimise production efficiency and improve on the overall quality of the EFB compost pellets. Hence the challenge to produce quality compost pellets requires the following characteristics:

- Mechanical behaviour
    - Able to withstand rigorous transportation and storage with minimal induced crumbs and fractures
    - Does not deteriorate during prolonged storage
- Nutrient release
    - Able to maintain shape in long term usage
    - Able to maintain sufficient controlled release of nutrients to the plant root in long period

The densification behaviour on EFB compost and its effect on mechanical strength and the nutrient release characteristics of the compost pellet are still relatively unknown. Therefore, the focus of this thesis is to determine the relationships between these factors so that the compost pellets can be optimised for their effectiveness (Figure 1.7).

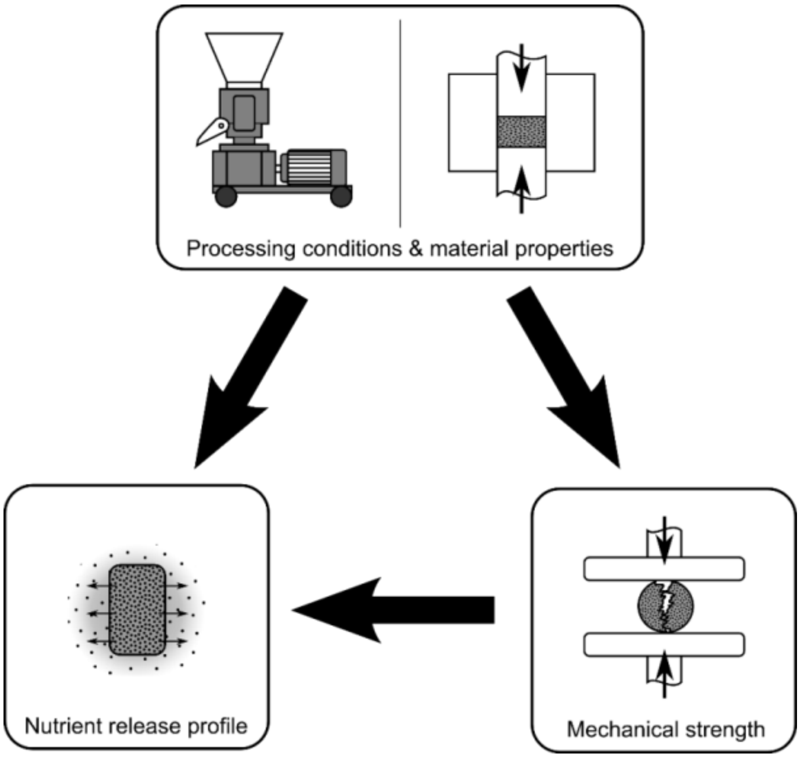

Figure 1.7: Relations between processing conditions & material properties, mechanical strength, and dissolution profile

1.6 Objectives

The overall objective of this thesis is to study the mechanism behind pellet mill densification as well as the densification behaviour of the EFB compost through experiments and modelling.

The specific objectives of this research are:

1) To characterise the compaction behaviour of the ground EFB compost.
2) To determine the effects of processing conditions and material properties including the effects of storage on the mechanical properties and nutrient release behaviour of EFB compost pellets.
3) To investigate and develop a theoretical model of the pellet mill densification mechanism using laboratory apparatus.

4) To investigate the effects of material properties on the physical parameters of the developed model from (3) above.
5) To develop new approach in predicting the compaction pressure of the pellet mill.

1.7 Overview of thesis

An overview of the rest of this thesis as summarised:

Chapter 2: Background and related literature for the densification of biomass is presented in this chapter. Information in this chapter includes the possible binding mechanism of EFB compost and the related parameter that describe the physical property of EFB compost pellets. Previous studies on the modelling the pellet mill compaction process is presented in this chapter. Reviews of previous studies related to the biomass densification are presented as well.

Chapter 3: Characterisation on the effect of moisture content, particle size and applied compaction pressure on the compaction behaviour of ground EFB compost is presented in this chapter.

Chapter 4: Analysis on the effect of moisture content, particle size, the applied compaction pressure, and storage time on the mechanical strength of the EFB compost pellets and nutrient release pattern of the EFB compost pellets is introduced in this chapter.

Chapter 5: An alternative theoretical modelling on the pellet mill compaction process is proposed in this chapter. The model was accompanied with new methodology that can be experimentally measures the physical parameters in the proposed model using an instrumented die.

Chapter 6: Prediction of steady-state pelleting pressure which reflects the actual compaction pressure of the pellet mill using an iterative approach. Results were briefly compared with existing literature to evaluate the predictive capabilities of the proposed approach.

Chapter 7: A conclusion of the completed experiments and result analysis is presented in this chapter, followed by recommendations and plans for future work.

CHAPTER 2:
BACKGROUND AND LITERATURE REVIEW

Powder densification, also known as pressure agglomeration, is a process that adhere powder particulates together with mechanical compaction pressure to achieve greater bulk density of a product. In densification of empty fruit bunch (EFB) compost, pellet mill was used to produce compost pellets which contain higher net nutrient content per unit volume in a consistent shape and size. The EFB compost in its pelleted form allows for ease of transportation, handling, and minimize storage space with the additional benefit of reduced nutrient leaching rate. Quality pellets must have the strength to withstand rigorous transportation and handling activities with minimal formation of crumbs and fractures.

This chapter provides the background information on the powder densification theory related to the biomass densification process. Additionally, the compaction mechanism of a pellet mill used in processing the empty fruit bunch compost is described. Following that, previous studies in the attempt to model the mechanism of pellet mill compaction process are discussed. Moreover, existing models that mathematically that describe the compactability and compressibility, and nutrient release behaviour are discussed. Finally, the relevant experimental works that study the effect of processing conditions and biomass material properties on the compactability and compressibility of the biomass are discussed.

2.1 Densification process

The powder densification process begins when a compaction pressure is applied to a powder bed in a constricted volume. The compaction pressure is defined as the applied force divided by the applied contact area. The applied compaction pressure increases exponentially as the bulk volume of the powder bed decreases with time as illustrated in Figure 2.1. In the initial process of densification, the powder particulates rearrange themselves and come into close proximity with each other. Subsequently, the empty spaces become more limited at higher pressure and preventing further rearrangement of particles. With additional compaction pressure beyond this point, the powder particulates undergo elastic and plastic deformation with malleable particles, or fragmentation with brittle particles (Duberg and Nyström 1986). Once the maximum pressure is reached, the compaction pressure is released and a powder compact is formed. During the release of compaction pressure, the powder compact experienced an elastic spring-back which is caused by the expansion of compressed air and the relaxation of elastic deformation (Pietsch 2008).

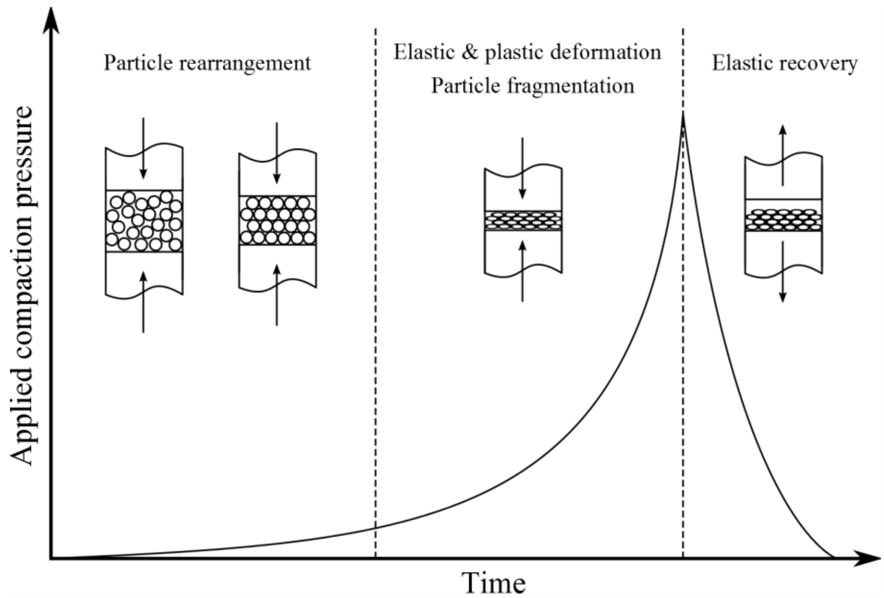

Figure 2.1: Powder compaction curve. Adapted from Pietsch (2008)

2.1.1 Binding mechanism

The strength of the powder compact depends on the physical forces that bind the particles together. According to Rumpf (1958), the binding mechanism between particles in a compacted body can be classified as:

i) solid bridges,
ii) adhesion and cohesion forces,
iii) surface tension and capillary pressure,
iv) attraction forces between solid particles, and
v) mechanical interlocking bonds.

According to Pietsch (2008), an elevated temperature during compaction may soften the solids and diffuses atoms or molecules from one particle to another at points of contact. The solid bridges which are developed at this manner are called sinter bridges. Heat caused by friction or pressure may also partially melt the particles and develop liquid bridges which solidify quickly and form solid bridges (Pietsch 2008). Also, solid bridges may also form due to crystallisation of some ingredients, chemical reaction or hardening of binders (Kaliyan and Morey 2010). Increase in temperature and compaction pressure may improve the reaction and potentially result in stronger bond formation (Pietsch 2008). Solid bridges are typically formed during cooling or drying of pellets (Kaliyan and Morey 2010).

The adhesion and cohesion forces between particles may form with the introduction of highly viscous binder such as bitumen, honey, pitch, and tar. The adhesion forces between the solid and binder and cohesion forces within the viscous binder provide agglomerate strength until weaker of the two fails (Pietsch 2008). Viscous binder may harden in the process of cooling or drying and form solid bridges (Kaliyan and Morey 2010).

Liquid bridge between particles may form with the presence of liquids developed from free water or by capillary condensation. They are normally prerequisite for the formation of solid bridges (Pietsch 2008). When the entire void space in a powder volume is saturated with liquid and concave menisci form at the interstices between particles on the surface of the volume, a negative capillary pressure may exist in the interior providing strength to the agglomerate (Pietsch 2008).

Attraction forces between solid particles such as molecular bond, electrostatic bond, and magnetic forces can cause particles to bond at extremely small distance. However, these effects diminish quickly with increasing distance between particles due to their short range effect (Pietsch 2008).

Mechanical interlocking bonds may form when particles have the shape of fibres, threads, or thin plate like structures that can twist, weave, bend or entangle between each other during compaction process.

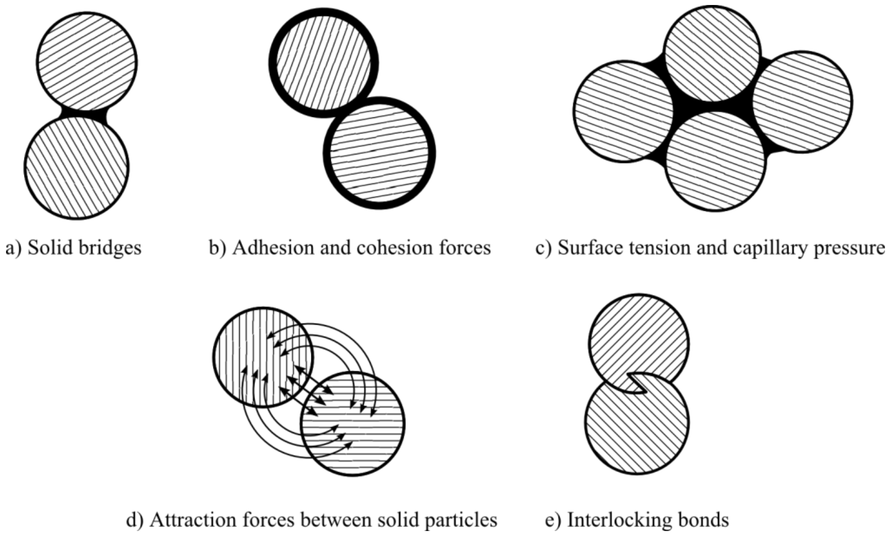

Figure 2.2: Pictorial representation of the binding mechanism. Adapted from Pietsch (2008).

2.1.2 Density

The density is universally defined as mass per unit volume of a substance. The true density of the biomass powder is obtained when the pores and void spaces within the particle is excluded in volume measurement. The true density of the powder is typically measured with the gas pycnometer or liquid pycnometer based on the Archimedes' principle (ASTM 2014; Lai et al. 2013; Mani et al. 2004b).

The bulk density refers to the total mass of the pellet per unit volume inclusive of void space in the pellet. For a cylindrical pellet, the bulk density is calculated by the following equation:

$$\rho_B = \frac{m}{\frac{\pi D^2 h}{4}} \tag{2.1}$$

Where m is the mass of the pellet, D is the diameter of the pellet and h is the height of the pellet.

The length of the pellet may vary at different stages of densification process due to stress relaxation result in different bulk density at respective stages. Different terminology was used to describe the bulk density of the pellet dependent on the stages of densification process:

Maximum compact density ρ_c refers to the bulk density of the compact when compaction pressure is applied.

Relaxed compact density ρ_r refers to the bulk density of the pellet when the compaction pressure is released during unloading.

Ejected pellet density ρ_e refers to the bulk density of the pellet measured immediately after ejection.

Final pellet density ρ_f refers to the bulk density of the pellet after a prolonged storage.

2.1.3 Porosity

Porosity is one the important physical characteristics that influence the strength and functional property of the biomass pellets. In pharmaceutical studies, the porosity of the tablet can affect the strength, dissolution and disintegration of the tablet (Panda and Mallick 2012; Johansson and Alderborn 2001; Kleinebudde 1994). Thus, studies on the effect porosity would be beneficial in determining the quality of the biomass pellet. Many researchers have attempted to characterise the relationship between the compaction pressure and the porosity of the compact (Kawakita and Lüdde 1971; Cooper and Eaton 1962; Heckel 1961). Porosity measurements were also used to correlate with the crushing or the compressive strength of the pellets (Ryshkewitch 1953; Duckworth 1953).

In densification studies, porosity refers to the ratio of total volume void spaces in a powder bed to the bulk volume of the powder bed (Lachman et al. 1986). During compaction process, the particles move closer to each other and reduce amount of void spaces in the powder volume. This led to the decrease in porosity of the powder bed. The porosity of the biomass pellet can be physically measured by determining the bulk density of the biomass pellet and the true density of the biomass particles in the powder bed in the following calculation.

$$\varepsilon = 1 - \frac{\rho_B}{\rho_T} \tag{2.2}$$

where ε is the porosity of the powder bed, ρ_B is the bulk density of the powder bed, and ρ_T is the true density of the powder. Some literature may express with the term relative density (RD), which is defined as the ratio of bulk density to the true density of the powder.

$$RD = \frac{\rho_B}{\rho_T} \tag{2.3}$$

2.1.4 Elastic recovery

The elastic recovery, also known as elastic relaxation of the pellet occurs from the onset of unloading stage where the compaction force is removed until the pellet has been ejected from the die. During the densification process, the elastic and plastic deformation of the material will occur to a certain degree depending on material characteristics and process parameters (Anuar and Briscoe 2009). It is believed that the elastic recovery of the pellet is caused by the release of relatively high amount of stored elastic energy in the pellet (Haware et al. 2010). The elastic recovery increases the final pellet porosity which may lead to weakening of the pellet strength and failures such as capping and lamination. Therefore, the final success of densification process will be determined by the ability of the pellet to withstand the release of stored elastic energy.

The elastic properties of the pellet can be accessed by the analysis of pellet expansion (Haware et al. 2010). The degree of elastic recovery (ER) can be obtained by comparing between the minimum height length during compaction and final height after ejection according to the following equation:

$$ER = \frac{H - H_c}{H_c} \tag{2.4}$$

where H is the height of the pellet and H_c is the height of the compact at the applied pressure during compaction.

2.2 Biomass composition

The chemical composition of the biomass typically includes compounds such as cellulose, hemicelluloses, protein, starch, lignin, crude fibre, fat and ash may affect the densification process (Tumuluru, Wright, Kenney, et al. 2010). Understanding the behaviour of these compounds changes during biomass densification can be useful in determining the bond characteristics of the biomass pellets. Under high pressure and temperature, the lignin and protein were expressed during densification process and act as natural binders that form solid bridges between particles (Kaliyan and Morey 2010) . The natural binders can be soften or plasticised at the presence of heat and moisture which improve the binding ability of biomass. Kong et al. (2012) investigated the biomass pellets made from wood sawdust and wrapping paper fibre as binder and revealed that the pellets were strengthened due to the interlocking bond of the fibre. The addition of paper fibre also resisted the disruptive force caused by elastic recovery and adding strength to the pellets.

Liu et al. (2014) investigated the compaction characteristics of biomass pellets made from pinewood sawdust, rice husk, coconut fibre and coconut shell and proposed that the bonding forces involved in biomass pellets are mainly related to the mechanical interlocking bonds and attraction forces such has hydrogen bonding and van der Waals forces. The lignin originated from the raw biomass cannot act as a binder due to low pelletisation temperature used in their study (Liu et al. 2014). It is further deduced that the strength of the biomass pellets is dependent on the amount of extractives in biomass (Liu et al. 2014). The presence of extractives such as wax and lipid interferes with the hydrogen bonds and van der Waals force by preventing close contact between adjacent bonding sites (Stelte et al. 2011a; Nielsen, Gardner, et al. 2009).

So far, no data is available in literature on the binding mechanism of biomass compost. However, the changes in chemical composition due to the composting process may suggest the binding mechanism involved in biomass compost densification. Table 2.1 indicates the chemical composition of the untreated palm oil empty fruit bunch and the composted empty fruit bunch from previous literatures. The untreated palm oil empty fruit bunch contains high cellulosic matters which are easily decomposed by the combination of physical, chemical and biological processes (Baharuddin et al. 2013). As shown in Table 2.1, there was a significant decrease in lignin, cellulose and hemicellulose content as the empty fruit bunches were subjected to the composting process. The lipid content in the biomass also rapidly degraded during the composting process (García-Gómez et al. 2005). The palm oil mill effluent sludge which is normally used to co-compost with the empty fruit bunch may provide the necessary bond between the biomass particles. The palm oil mill effluent contains high level of dissolved solids with concentration of 15500 to 29000 mg/l (Wu et al. 2010). The dissolved solids would recrystallise and forming solid bridges between particles, and giving strength to the biomass compost pellets.

Table 2.1: Composition of oil palm empty fruit bunches

	Lignin (%)	Cellulose (%)	Hemicellulose (%)
Untreated EFB	19.052[1]- 22.8[2]	52.581[1]-57.8[2]	25.456[1]-21.2[2]
Composted EFB	5.598[1]	26.771[1]	17.897[1]

Data taken from [1]Amira et al. (2011) and [2]Abdullah and Sulaiman (2013b)

2.3 Pellet mill

Over the past few decades, various biomass densification machines have been developed to produce densified biomass products such as pellet mill, briquette press, screw extruder, and roller press. Among these machineries, pellet mill is one of the common densification techniques used to produce biomass pellets. The earliest large capacity pellet mill patents were registered in 1930 and was primarily used to produce poultry feedstock (Meakid 1934). The patent describes the rollers which are mounted on the die plate used to compact and force the material through the die channels to form the pellets. The pellet mills were later used to produce wood pellets as an alternative fuel as price of fossil fuel spike in the 1970s. Pelleting animal manure and biomass compost as fertiliser pellets was soon followed to combat growing waste pollution problems.

In general, there are two types of pellet mill in the market: flat-die pellet mill and ring-die pellet mill. Both designs have the same basic components consists of multiple compaction rollers mounted on a die perforated with multiple cylindrical openings (Bhattacharya et al. 1989). The main difference between these designs is the die can be in the shape of a flat plate or a ring as illustrated in Figure 2.3.

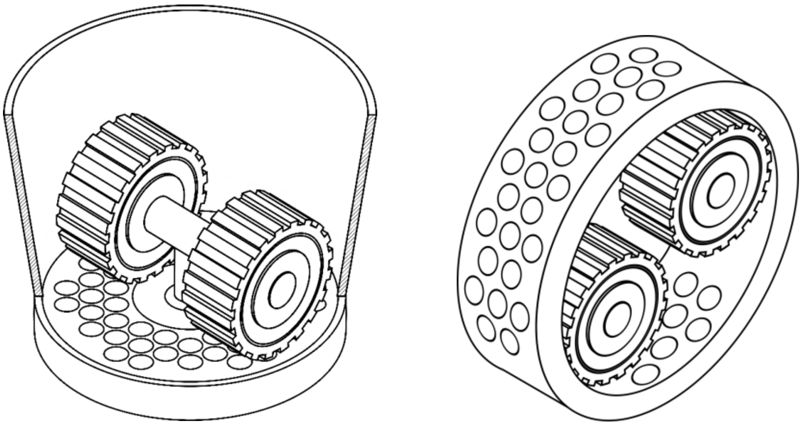

Figure 2.3: Flat-die pellet mill (left), ring-die pellet mill (right)

2.3.1 Pellet mill densification process

Figure 2.4 schematically illustrates the pelleting process in the cross section view of the pellet mill. During the pelleting process, the biomass powder is fed to pellet mill through the hopper. The rollers rotate and draw the powder towards the narrow gap between the roller and the die plate. The powder is thereby pressed by the roller into the die channels. The compacted powder extruded from the die channels is cut by a knife on the channel exit, and thus forming the final product of the pellets.

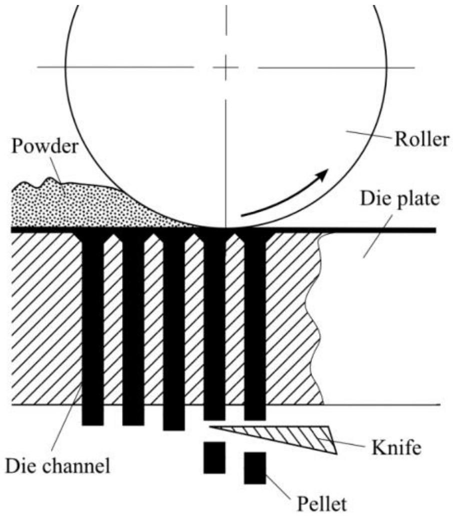

Figure 2.4: Illustration of the pelleting process

Figure 2.5 illustrate the deformation conditions for the biomass powder under the roller of a pellet mill. Clearance between the roller and the die plate is set so that a compact layer is formed on the running surface of the die plate (Sitkei 1987). At point A, the roller grabs and deforms the biomass powder between the roller force F_R and the friction force F_f induced from the die wall interface that resists the flow towards the die channel. The biomass powder with thickness of h_i gradually decrease to a minimum value of h_f as the roller rotates to point B. At this point, roller force F_R exceeds the limit of friction force F_f and begin to displace the compact layer into the die channel. The force exerted by the roller remains practically constant during pushing and decreases rapidly after point C. The biomass powder thus deforms into a new layer of compact on the surface of the die plate while the existing compact layer extruded out from the die channel. This process is repeated with every rotation as the biomass powder is loaded continuously.

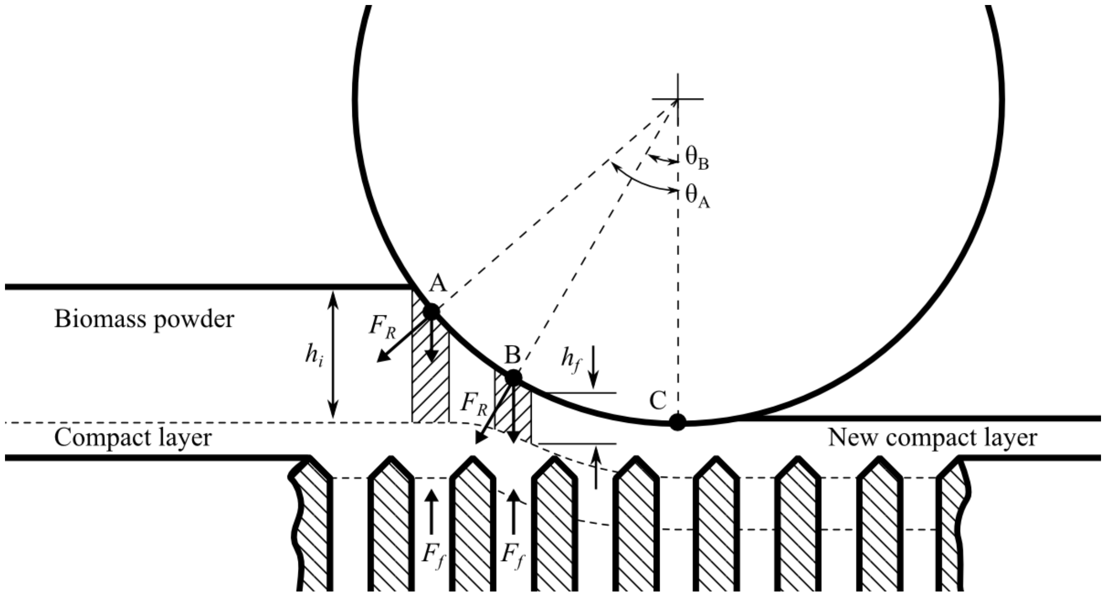

Figure 2.5: Deformation of biomass powder under the roller of a pellet mill

The degree of compaction force on the biomass powder with the pelleting process is therefore dependent on the friction force F_f generated from the die channel. The roller gradually exerts compaction force that deforms the biomass powder to the limit of friction force F_f before pushing the material into the die channel. The roll force F_R is limited by the operating size and power output of the pellet mill motor. If the friction force build up in the die channel F_f exceeded this limit, the pellet mill will be blocked since the rollers will not be able to provide the necessary force to push the material through the die channel (Holm et al. 2011). High F_f may also led to the increased risk of fire due to excessive heat developed by friction, lowers production efficiency, and increases the rate of wear and tear of the pellet mill (Stelte et al. 2012; Holm et al. 2011). The optimal magnitude of compaction force is therefore a balance between the necessary force to produce quality pellet and minimal energy consumption of the pellet mill.

2.4 Existing models describing pellet mill compaction mechanism

The magnitude of the pellet mill compaction force from can be determined by estimating the resistive friction force F_f generated in the die channel. However, information on friction force modelling in powder compaction was predominantly applied in powder metallurgy and pharmaceutical compaction to determine the density gradient within the powder compact due to the present of friction force. The increased popularity in biomass densification process placed a new emphasis on pelleting biomass materials with pellet mill.

Although pellet mill compaction process has been known since 1930s, it is only recently that fundamental aspects of friction in pelleting have been studied. The existing information on the pellet mill compaction was only of empirical nature. Most processes are developed with trial-and-error method which is time consuming and inherently expensive as there is no complete model that describe the pelleting process. Hence, there is a need for a mathematical model to describe the relationship between material properties, the die channel dimension and processing conditions to aid engineers and operators in design and operation for the pellet mill.

2.4.1 Holm's model

Holm et al. (2006) was one of the first to fill this gap by providing the means to determine the magnitude of the pellet mill compaction as pressure P_x corresponding to the generated friction force in the die channel as:

$$P_x = \frac{P_{N0}}{\nu_{LR}} \left(e^{4\frac{H}{D}\mu\nu_{LR}} - 1 \right) \tag{2.5}$$

Holms' model describes the exponential variation of pelleting pressure P_x along the die channel height H with woody biomass material properties such as pre-stress P_{N0}, coefficient of friction μ, and Poisson's ratio ν_{LR} which were attained experimentally. The subscript in ν_{LR}, L and R denotes longitudinal and radial deformation according to the fibre orientation as illustrated in Figure 2.6.

This model assumes the wood material expands perpendicularly to the direction of the applied pressure known as the Poisson's effect and mathematically characterised as the Poisson's ratio ν. The Poisson's ratio is defined as the negative ratio of radial strain to the axial strain caused by uniformly distributed axial pressure (Xu et al.

2015). When a body is compacted in the cylindrical rigid die, expansion is prohibited and therefore appears as radial pressure on the wall of die channel.

The wood biomass is also assumed to be inelastic material (i.e. plastic) which contributes to the pre-stress P_{N0} due to the irrecoverable pressure when the applied compaction force is removed. The presence of the pre-stress P_{N0} and the radial pressure P_r act as the normal force component to the friction component on the die wall, and give rise to the friction force when ejecting the powder compact out from the die.

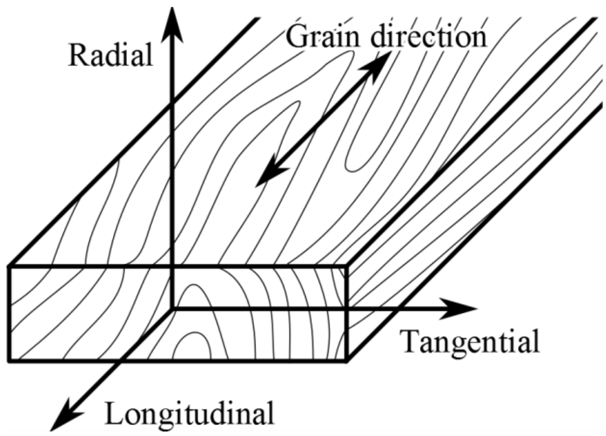

Figure 2.6: Principal axes of wood with respect to grain direction. Adapted from Walker (2005)

Holm's theory provided a method for predicting the compaction pressure of the pellet mill compaction process according to the geometry of the die channel which has been used in experimental investigation. Xia et al. (2014) conducted a pilot pellet mill compaction experiments on straw and used Holm's model to predict the compaction force and the torque exerted on the roller. The predicted values showed reasonable agreements with the experimental results with a deviation of 6.76%.

To obtain model parameters P_{N0}, ν_{LR} and μ, Holm et al. (2007) measured the pressure needed to eject the compact of differently length with a single pellet press solved the model parameters with the least-square fits method. However, there are limitations because solving three variable model parameters (P_{N0}, ν_{LR} and μ) with least-square fits to a single equation is inadequate and the model solution may not be representative to the actual value. Furthermore, the least-square fit method allows the model parameters to be determined only if the coefficient of friction μ is known and kept as constant. Moreover, properties of a powder compact may vary due to the changes in compact porosity and therefore the model parameters cannot be expected to be the same. Therefore, published values on solid wood material parameters such as μ and ν_{LR} on may not be applicable for Holm's model.

Holm et al. (2011) further simplified the model equation by combining the parameters P_{N0}, μ and ν_{LR} into two new parameters $U = \mu P_{N0}$ and $J = \mu \nu_{LR}$ which allowed estimation with fewer experimental trials using a single pellet press. While this approach allows faster testing of new types of biomass, the procedure remains unable to discern the factors such as moisture content, particle size and moisture content that influence the friction conditions, the Poisson's ratio and the prestressing pressure of the material.

Furthermore, the inclusion of Poisson's ratio ν_{LR} in Holm's model is still questionable as it is only applicable for elastic body where the radial pressure P_r would increase linearly with applied axial pressure P_a. Assuming a perfectly elastic behaviour of isotropic material, the radial pressure P_r and the axial pressure P_a is related to the Poisson's ratio ν by the relation:

$$P_r = \frac{\nu}{1-\nu} P_a \tag{2.6}$$

with a slope equals to $\frac{\nu}{1-\nu}$ in a radial-axial compaction pressure plot.

In practice, a compacted powder rarely behaves elastically as the applied compaction pressure P_a normally occurs beyond the yield point of the powder material. When the axial pressure exceeds the yield limit, yielding of the material occurs and the slope changes differently according to the failure behaviour of the material (Doelker and Massuelle 2004). The assumption of elastic body no longer valid beyond the yield point and therefore, slight modifications are required to Holm's model.

2.5 Characterisation of biomass compost pellets

Apart from analysing processing condition of the pelleting process, it is important to consider the effect of binding mechanism on the strength of the biomass pellets. There are two major aspects to be considered in densification studies. First is the compactability of the powder material. Compactability is defined by the deformation behaviour of the powder particle when under compaction pressure. It is usually carried out by correlating the outcome of the bulk density of the compact with the applied compaction pressure on a powder bed in a uniaxial die (Kawakita and Lüdde 1971; Heckel 1961). Secondly is the compressibility of the pellet. Compressibility defines the capability of the pellet to withhold external pressure before breakage. The physical strength of the pellet can be carried out by applying mechanical stress on the pellet until the pellet breaks.

2.5.1 Compactability

The compaction behaviour of biomass depends on the physical properties of the powder particles. Different biomass materials may possess different chemical composition, and therefore behave differently under compaction pressure. Thus it is essential to understand the basis of compaction mechanism involved through parameterisation of compaction profile to provide interpretation of physical quality of material involved. To further understand the compaction behaviour of biomass material, a number of models has been proposed that describe the relationship between compaction pressure and the physical properties of the biomass pellets (Kawakita and Lüdde 1971; Cooper and Eaton 1962; Heckel 1961; Walker 1923). Many of the compaction models applied on different biomass materials have been discussed in detail by Mani et al. (2004a).

2.5.1.1 *Heckel model*

Heckel (1961) proposed a model to express the relationship between density and pressure of the powder compact as:

$$\ln \frac{1}{1 - RD} = kP_a + A \quad (2.7)$$

Where P_a is the applied compaction pressure, RD is the relative density of the powder compact, k and A is the Heckel model constant. The constant k and A can be determined from the slope and the intercept respectively from the extrapolated linear region of the plot $\ln \frac{1}{1-RD}$ vs P_a. The constant A describes the particle movement and rearrangement and defined by the equation:

$$A = \ln \left(\frac{1}{1 - RD_0} \right) + B \quad (2.8)$$

Where B represents densification by individual particle movement and rearrangement, and $\ln(\frac{1}{1-RD_0})$ is densification by die filling.

The value of k was related by Heckel (1961) to the yield strength σ_y of the material by the expression $k = \frac{1}{3\sigma_y}$. Later, Hersey and Rees (1970) described the reciprocal of k was defined as the mean yield pressure P_y. The constant k is inversely related to the ability of the powder material to deform plastically under pressure. Additionally, Hersey and Rees (1971) used the Heckel model to differentiate materials that deform by fragmentation and by plastic deformation. They showed that the two compaction behaviour can be distinguished by plotting a function of the relative density against applied pressure with different particle size fraction of the material based on Heckel model (Figure 2.7).

For type 1 materials, the powder material exhibits different initial packing density depending on factors such as particle size. The densification with pressure would occur due to particle slippage and rearrangement, then plastic deformation. In Heckel plot, the type 1 material is represented by the initial curved portion followed by the parallel straight lines as the applied pressure increases.

For type 2 materials, the compaction largely occurs due to fragmentation. The particulate structure is progressively destroyed due to the applied pressure. And thus, the Heckel plot would show an initial curved portion followed by a linear line in which all curves converge onto the same line at certain pressure.

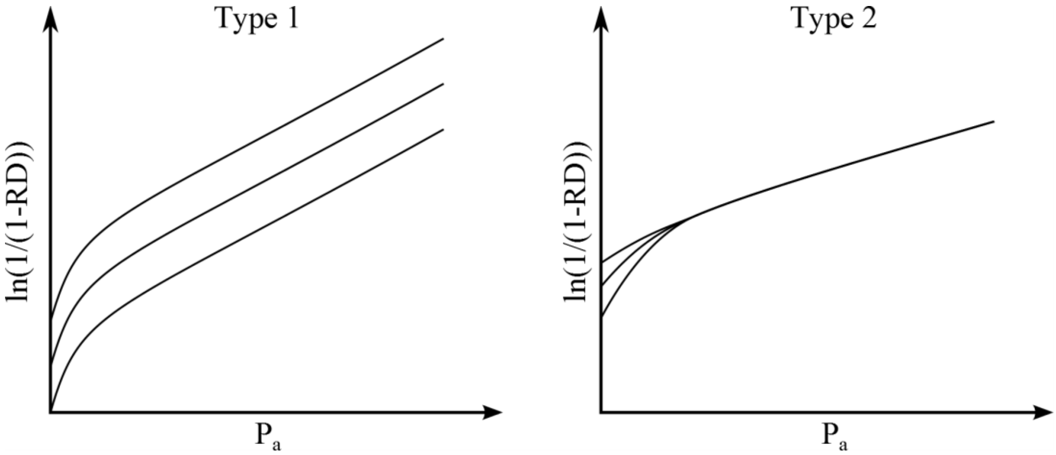

Figure 2.7: Compaction behaviour of two different type of material with different particle size on Heckel plot (Hersey and Rees 1971). Type 1 indicates compaction by plastic deformation, and Type 2 indicates compaction by fragmentation.

2.5.1.2 *Kawakita-Lüdde model*

Kawakita and Lüdde (1971) developed compaction model based from the observed relationship between applied pressure and the powder compact volume. The model is expressed as:

$$C = \frac{V_0 - V}{V_0} = \frac{abP_a}{1 + bP_a} \tag{2.9}$$

where C is degree of volume reduction, V_0 is initial apparent volume of the powder bed, V is powder bed volume under the applied pressure P_a, a and b is the model constants. The model equation (2.9) can be rearranged as:

$$\frac{P_a}{C} = \frac{1}{ab} + \frac{P_a}{a} \tag{2.10}$$

The constant a and b can be evaluated from the slope and intercept from the linear plot of $\frac{P_a}{C}$ versus P_a. The constant a is regarded equal to the initial porosity of the powder bed. In practice however, it has been found that the derived value does not fit well with the measured value due to the non-linearity of the plot (Denny 2002). The constant b is considered to be related to the resisting forces or the plasticity of the material (H. et al. 2008; Kawakita and Lüdde 1971).

Kawakita and Lüdde (1971) stated the linear relationship holds best for soft, fluffy and medical powders, however additional attention must be paid to the measurement of initial volume of powder bed V_0. Any fluctuation in measured value V_0 may led to deviation from the Kawakita-Lüdde model.

2.5.1.3 *Discussion of the compactability model*

Although none of these models was derived from the fundamental consideration of physical model of compaction, the constants in the equation shows close correlations with the input material formulation (Sheikh-Salem and Fell 1981).They were essentially curve fitting formulae *e.g.* exponential curve to describe the convergence value of the porosity in a porosity-applied compaction pressure plot. The models gained popularity as they show reasonable fit to compaction data over a wide range of pressure.

Mani et al. (2004a) studied the applicability of the models to four agricultural residues i.e. wheat, barley straws, corn stover and switch grass and concluded that the Kawakita model equation fitted well with the compaction data. Sun (2008) pointed that the increase of moisture content in microcrystalline cellulose powder decreased the parametric constant $\frac{1}{k}$ in the Heckel model or the mean yield pressure P_y which corresponds to a better plasticity or increased capability to form tablet. Variation in processing parameters such as the rate of compaction and hold time will influence also the results obtained from the compaction plot (Lai et al. 2013). Therefore, this thesis will examine the effects of different compaction cycles *e.g.* pellet mill compaction cycle, die geometry, as well as the material formulation *e.g.* input material particle size and its distribution and moisture content on the compactability of the input material *i.e.* rate of change of pellet density by the compaction pressure.

2.5.2 Compressibility

The produced biomass pellets are required to withstand rigorous transportation and impact with minimal amount of crumbs and fractures. The physical properties of the material and processing conditions are known to influence the compressibility of the produced pellets. Therefore, investigation on the effect of processing conditions and the starting material on the mechanical properties is crucial in obtaining a general understanding of pelleting process. Compressibility is a measurement of pellet hardness or strength which can be evaluated by the force required to fracture a pellet (Figure 2.8).

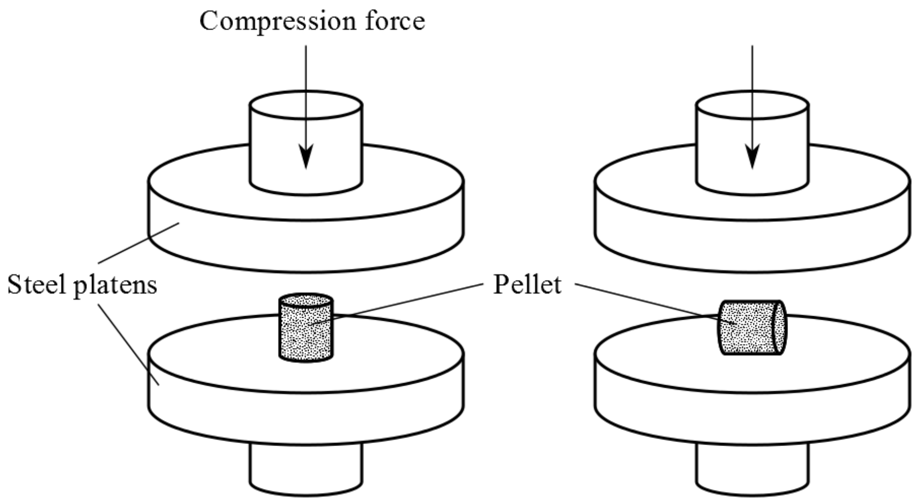

Figure 2.8: Schematic diagram for pellet compressive strength tests compressed at the axial direction (left) and, diametrical direction (right)

The strength of the pellet can be defined as the axial compressive strength σ_A and diametrical compressive strength σ_T (Fell and Newton 1970):

Axial compressive strength:

$$\sigma_A = \frac{F}{\frac{\pi D^2}{4}} \tag{2.11}$$

Diametrical compressive strength

$$\sigma_T = \frac{2F}{\pi DL} \tag{2.12}$$

where F is the maximum compression force to fracture the pellet, D is diameter of the pellet, and L is length of the pellet. A universal material testing machine will be used to compress the pellet to evaluate the mechanical properties of the pellets.

2.5.2.1 *Ryshkewitch-Duckworth model*

Several mathematical models have correlated the mechanical strength of pellets with changes in density or porosity of the pellets. Empirical models such as the Ryshkewitch-Duckworth equation are commonly used to describe the relationship between strength of compacts and porosity (Duckworth 1953; Ryshkewitch 1953):

$$\sigma = \sigma_0 e^{-\eta\varepsilon} \tag{2.13}$$

Where σ and σ_0 is compressive strength and compressive strength at theoretical zero porosity respectively, ε is the pellet porosity and η is the model constant.

The higher value of ηsignifies that the pellet strength increases rapidly with decreasing porosity and indicates the stronger bonding capacity of the particles(Maarschalk et al. 1996). The constant η has been found to be dependent on the material formulation *e.g.* particle size (Maarschalk et al. 1996) and moisture content (Sun 2008; Gupta et al. 2005). A more detailed model of the pellets will also be developed to take into account the different components of the compost. This model will characterize the effect of the shape and properties of the different components in relating to the overall strength of the pellets.

2.5.3 Nutrient release behaviour

The effectiveness of fertilizers depends on the capability of the fertilizer to maintain sufficient concentration of nutrients within the plant root zone for desired period of time (Friedman and Mualem 1994). Thus, a number of fertilizer products have been developed in the form of controlled release fertilizers such as incorporating hydrophobic coating or adding a binder in the materials formulation to reduce the dissolution rate of fertilizer (Whittington 2003; Stansbury 1971). Pharmaceutical studies also demonstrated controlled release tablets by means of tablet compaction strength and porosity (Fukami et al. 2006; Marais et al. 2003; Fassihi 1987). The use of controlled release fertilizers are beneficial as it allows nutrients to be used efficiently by the plants through the reduced leaching losses while maintaining constant supply of nutrients to the roots (Mikkelsen et al. 1994). The prolonged release of fertilizer may also reduce the frequency of fertilizer reapplication thus reducing labour expenses (Oertli 1980). As such, the chemical release rate of the fertilizer pellets will be one of key indicator of the fertilizer pellet quality. Literature on disintegration behaviour of the EFB compost pellets is scarce. However, studies on the disintegration of tablets from pharmaceutical and food industry could be applied in this study.

Forny et al. (2011) described the disintegration and dissolution process of food powder agglomerates as according to these steps:

1) the wetting of the agglomerate followed by the penetration of solute to the core through capillary forces,
2) immersion of agglomerate in solute,
3) dissolution of solid bridges between the particles followed by disintegration of particles around the solute, and
4) dissolution of particles.

The disintegration of tablets occurs when the force inside the tablet surpassed the sum of cohesive forces (Quodbach and Kleinebudde 2015a). The cohesive forces consist of hydrogen bond, capillary forces, van der Waals and electrostatic forces, solid bridges, and mechanical interlocking bond which contribute to the overall strength of the pellets (Quodbach and Kleinebudde 2015a). Disintegration increases the surface area available for dissolution or diffusion, which subsequently increases the release rate (Noyes and Whitney 1897).

Natural polymers such as starches and microcrystalline cellulose with disintegrating properties were commonly added to the pharmaceutical tablets its disintegration

(Nogami et al. 1969; Patel and Hopponent 1966). Quodbach and Kleinebudde (2015a) described several possible disintegration mechanism of pharmaceutical tablets which includes swelling, inter-particle repulsion force, shape recovery, wicking, heat of wetting, and effervescence. Disintegrating agents can be identified by their disintegration mechanism and their disintegrating effect may differently with the process conditions. For example, disintegration time for crospovidone, a synthetic polymer known to have a shape recovery mechanism, was found to be decreased with increasing compaction pressure despite the increase in tablet strength (Quodbach and Kleinebudde 2015b). Polymers with shape recovery may deform with the applied compaction pressure and remain in a high energy state, stabilised by the interlocking of polymer chains or crystallisation of polymer parts (Quodbach and Kleinebudde 2015a). When in contact with water, bonds may be destroyed and the stored energy is released by the recovery of the original particle shape. The amount of stored energy should increase with increased compaction pressure and may lead to decreased disintegration time (Quodbach and Kleinebudde 2015b). In contrast, polymers with wicking and swelling tendency such as glycine showed an increase in disintegration time with increased tablet hardness (Fukami et al. 2006). This tendency was postulated to be related to the water absorption rate that was inhibited by the smaller pores with low tablet porosities which reduced the water penetration to the tablet core.

To great extent, the degree of disintegration and diffusion rate of EFB compost pellets are expected to be dependent on the processing compaction pressure, moisture content, particle sizes and their distribution, pellet geometry and sizes. Hence, this thesis will investigate the causative effect of these parameters on the nutrient release profile of the pellets by the measurement of rate of change in water conductivity when the pellets are exposed to solute (Mesnier et al. 2013).

2.5.3.1 *Nutrient release kinetics of compost pellets*

Despite the fact that pelleted biomass compost was commonly used in agricultural field, little has been published on their release kinetics and mechanism. The only result which has been reported involving the effect of pelleting on composted manure is that it releases nutrient several weeks later than unprocessed compost (Hara 2001). Although the nutrient release kinetic has been widely studied on controlled release fertiliser, no known data have appeared in the public domain for lignocellulosic compost material. Furthermore, studies that evaluate the effect of processing conditions and material characteristics on the nutrient release patterns of the compost pellets are scarce.

Several studies have conducted on the nutrient release patterns from the biomass compost based on the field experiments (Yan et al. 2002, 2001; Hara 2001; Jakobsen 1996). However, there is lack of studies in laboratory method that allows quick estimation of nutrient release patterns of biomass compost. Field experiments requires long duration of studies, i.e. 180 sampling days (Yan et al. 2001). In addition, consideration of complex variables such as time, temperature, soil, moisture, biological and other conditions may cause difficulties in correlation studies (Sartain et al. 2004). Although, laboratory methods may not be able to predict the actual field release, the laboratory method can be used for quick comparison of nutrient release pattern between the compost pellets (Carson and Ozores-Hampton 2012).

The empty fruit bunch compost is largely insoluble in water due to high cellulose content and likely to release nutrient based on infusion. Therefore, studies on the kinetic release of tea infusion can be adopted to describe the nutrient release characteristic of the empty fruit bunch compost pellets.

Jaganyi and Mdletshe (2000) demonstrated that the kinetic of tea infusion follows the first order kinetic equation as:

$$\ln\left(\frac{c_\infty}{c_\infty - c}\right) = k_{obs}t + \alpha \qquad (2.14)$$

Where c is the concentration at time t, c_∞ is the equilibrium concentration, k_{obs} is the observed rate constant and α is the small intercepts.

2.6 Factors affecting densification behaviour

The extents of the effects of the biomass characteristics and process variables on the compaction behaviour are primary studied to answer the fundamental question of whether the given material can be compacted effectively. Both the characteristics of the biomass materials such as moisture content and particle size, and process variables such as compaction pressure have been found to affect the compaction behaviour of the biomass and the resulting mechanical behaviour of pellets. Understanding the effect of these variables will help to evaluate the overall effectiveness of the pelleting processes and develop strategies to further improve the quality of the pellets (Tumuluru, Wright, Kenney, et al. 2010; N.Kaliyan and Morey 2009).

Densification studies are conducted in either laboratory scale with closed-end dies or open-end dies, or pilot scale which involve small scale pellet mill unit. A closed-end die are usually used to study on the compaction behaviour with prescribed compaction pressures, while open-end die used to study compaction behaviour with attempt to simulate the pelleting or the extrusion process. In both systems, mechanical pressure was delivered with a hydraulic press or universal testing machine. Although pilot scale studies would reflect in better end results, the cost of the pellet mill unit can be substantial.

2.6.1 Effects of compaction pressure

In general, the application of compaction pressure has significant effect on physical characteristics on biomass pellets. Due to the application of high compaction pressure, the particles were brought close together encouraging inter-particulate attraction force between the particles, while the natural binders were squeezed out from the biomass cells and forms solid bridges between the particles (Kaliyan and Morey 2010). The effect of compaction pressure is typically studied in laboratory using a closed end die with a piston pressing downward unto the powder bed.

Mani et al. (2006a) found that the increase of compaction force improved the pellet density made with wheat straw, barley straw, corn stover and switchgrass. A study conducted by Carone et al. (2011) saw an increase of the pellet density and its elastic modulus with the increased compaction force. The author explained the particles rearrange and maintain their original physical properties at low pressures and deforms at higher pressures which cause the particles to fill in the gap spaces and increase the contact area between particles.

Lai et al. (2013) examined the effect of compaction pressure on oil palm kernel shell pellets and concluded that the increased compaction pressure improved the compressive strength of the pellets but to a plateau when the pellets density achieved close to the particle densities. A similar observation noted by Adapa et al. (2009) indicated the increase in pellet density was significant for an increase in compaction pressure for barley, canola, oat and wheat straw compact. However, no significant effect was observed with any further increase in compaction pressure as the compacts approached to their respective particle densities. Thus, applying compaction pressure beyond the limit of particle density may be deemed unnecessary.

2.6.2 Effects of die channel dimension

The dimension of a cylindrical die is defined by the ratio between the height and diameter of the die channel as $\frac{H}{D}$. It is the most important factor that influence the pressure built up in the die channel of a pellet mill (Holm et al. 2006). Holm et al. (2006) demonstrated an exponential correlation between the die channel length and the pelleting pressure. The effect of die geometry is usually studied with an open-end die or with a pilot-scale pelleting unit with different die plate thickness.

Munoz-Hernandez et al. (2006) studied the effect of die channel dimension on the compaction behaviour by extruding biomass mixture through a various die channel length and found that the increasing die channel length increased the extrusion pressure and pellet density. Similarly, the work of Zafari and Kianmehr (2013) demonstrated that the use of thicker die was found to enhance the compressive strength of the biomass pellets made from compost.

Tabil and Sokhansanj (1996) reported that pilot-scale pellet mill with die channel height to diameter ratio $\frac{H}{D}$ of 4.10 and 7.31 resulted in alfafa pellet durability of 49.8% and 65.8%. The durability is a measurement on the amount of fines produced when the pellet is subjected to shearing and abrasion(Stewart 1948). Čolović et al. (2010) found that the increase in $\frac{H}{D}$ resulted in increased pellet hardness and energy consumption when pelleting cattle feed with a pellet mill.

2.6.3 Effects of moisture content

The effect of moisture content of feed material on the pelletising behaviour and product quality has been the subject of several studies (Zafari and Kianmehr 2013; Carone et al. 2011; Serrano et al. 2011; Bernhart et al. 2010; Kaliyan and Morey 2009; Nielsen, Gardner, et al. 2009; Fasina 2008; Mani et al. 2006a; Rehkugler and Buchele 1969). In these studies, different type of biomass was pelletised at different levels of moisture content, whereby the impact of the moisture content on the quality of the pellet is analysed. Bernhart et al. (2010) found that at the time of compaction, the moisture content significantly affects the density of the poultry litter compact. After two months of storage, the moisture content has no significant effect on the pellet density but significantly increase the force required to rupture the samples. The author postulate that the moisture in the biomass acts as natural binder which facilitates formation of liquid bridges between the particles forming agglomerate (Pietsch 2008). A study conducted by Zafari and Kianmehr (2013) has shown that the moisture content significantly affected the compressive strength of municipal solid waste compost pellet produced with an open-end die. Highest hardness and durability of municipal solid waste compost pellet is observed with moisture content ranging from 40% to 43% (*w.b.*).

Rehkugler and Buchele (1969) demonstrated the compaction of different forages with a close-end die at increased level of moisture content increased the gross densities of the wafer compact however decreased in dry-matter densities beyond 15% (*w.b.*) moisture content. The author theorised that adequate moisture is necessary to reduce interparticle friction in order to eliminate pore space. However, any addition of moisture beyond the requirement for reduction of interparticle friction will occupy volume that would otherwise occupied by dry matter. Regardless the type of forages, the increase in moisture content from 6% to 25% decreases the final wafer densities significantly after wafer expansion for 30 minutes. A similar observation was made by Mani, Tabil and Sokhansanj (2006), Kaliyan and Morey (2009a), Carone, Pantaleo, and Pellerano (2011) and, Andrejko and Grochowicz (2007) where moisture content of biomass significantly affected the pellet density in the same manner.

Increase in moisture contents does have its positive influence on the durability of the pellets in contrast to the pellet's density as observed in the study by Kaliyan and Morey (2009) and Andrejko and Grochowicz (2007). Addition of moisture is necessary for gelatinisation of the starch in biomass to facilitate binding between particles resulting in improved physical pellet quality (Thomas et al. 1997). The presence of higher amount of water-soluble carbohydrates in corn stover than in switchgrass resulted in higher pellet durability at higher moisture contents (Kaliyan and Morey 2009). Moisture content may have adverse effect on the pellet strength made from binder-less material such as sawdust as demonstrated by Nielsen, Gardner, et al. (2009). The author deduced that primary bonding mechanism of sawdust relies on the combination of particle entanglement and auto-adhesive surface bond. Presence of moisture occupies the sites of inter-particle bonding and may therefore decrease the pellet strength (Nielsen, Gardner, et al. 2009).

Apart from the physical quality of the pellet, the pelleting process itself is influenced by the presence of moisture content. Andrejko and Grochowicz (2007) found that the energy necessary to compact ground lupine seeds to a constant volume is decreased up to 54% with the moisture content increased from 9.5% to 15.0%. Nielsen, Gardner, et al. (2009) have reported that an increase of moisture content for both pine and beech sawdust reduces the energy required to produce pellets. The increased moisture content decreases the stiffness of the wood and related to the softening of lignin thus reducing the energy requirement to compact (Nielsen, Gardner, et al. 2009).

The former studies found in the literature perform their tests with laboratory presses consist of closed-end die and a plunger to simulate the compaction of a pellet mill. The conditions are easily manipulated and experiments are cheaper with laboratory presses however did not take into account the additional factors such as pellet die channel length and its friction occurring in real pellet mills. Serrano et al. (2011) used a pilot scale pellet mill with die length to channel diameter ratio of 2.83 to study the effect of moisture content on the durability of the straw pellets. Moisture content of straw below 8% is inadequate for compaction to occur and no pellets are produced. Moisture content from 9% to 17% produced scarce and fragile pellets but an undesirable amount of powders. Moisture content between 19% and 23% produced pellets with the best durability and lowest fines. Alfafa grinds were pelletised by Tabil and Sokhansanj (1996) in pilot-scale ring die pellet mill and reported that too much moisture added from the steam conditioning may cause near choking condition in the die. In this condition, grind particles are well compacted and produced durable pellets. Moisture content above 9% would likely to choke using the 6.1mm die with ratio between the channel length and diameter *l/d* of 7.31, while bigger die 7.8mm with l/d ratio of 4.10 could tolerate higher grind moisture content up to 12.0%. In a separate study conducted by Stelte et al. (2011b) examined the effect of moisture content on the pelleting pressure, a pressure derived from the force required to extrude the pellet out of the die. The influence of moisture content is dependent on the type of biomass as the pelleting pressure dropped with the increase of moisture content in woody samples, while the pelleting pressure increased for wheat straw. This further suggests that the influence of moisture content is not limited to the facilitated inter-particulate bonds but also the adhesion between the pellet and the die wall.

2.6.4 Effects of particle size

Particle size of feed material plays an important role in the production of biomass pellets. In general, finer grind particle size produces higher quality of pellets due to the increased surface area of contact that facilitate inter-particulate bonding or solid bridges during compaction (Tabil et al. 2011). Similarly, the increased contact surface area between the pellet and the wall results in greater pelleting pressure in the study conducted by Stelte et al. (2011b). Finer particles also readily absorb moisture as compared to the larger particles and thus undergo a higher degree of conditioning (N.Kaliyan and Morey 2009). Large particles provide fissure points and have the propensity to cause cracks and fractures thus resulting in lower pellet durability (MacBain 1966).

The effect of particle size on the quality of the pellets is evident in the study conducted by Lai et al. (2013) as the pellet made with the largest particle size had a coarse surface and have the tendency to chip whereas smallest particle size produced finer surface appearance and no chipping was observed. Kaliyan and Morey (2009) studied the effect of particle size on the quality of the pellets made with corn stover and switchgrass. The study reported an increased pellet density and durability by decreasing the corn stover particle size however the effect of particle size is insignificant in switchgrass pellet density. Mani et al. (2006a) also reported a similar trend where pellet density of biomass samples increased slightly as the particle size decreases.

The influence of particle size on the pellet durability is rather ambiguous and dependent on the type of biomass. Adapa et al. (2010) reported an increased pellet durability produced with larger straw particles at 10% moisture content and further reasoned that it is primarily due to mechanical interlocking of relatively long fibres. On the contrary, several studies indicated the use of different particle sizes does not produce significant difference in the durability of the pellets (Serrano et al. 2011; Carone et al. 2011; Mani et al. 2006a; Tabil and Sokhansanj 1996). A study conducted by Zafari and Kianmehr (2013) observed the use of fine particle size produced municipal solid waste pellets with highest compression strength. Similarly, a study conducted by Lai et al. (2013) shows the highest compression and diametrical compressive strength is achieved with the finer oil palm kernel shell powder material.

2.6.5 Effects of storage time and conditions

The effect of storage time and the surrounding condition has been the subject of many studies as it is known affect the mechanical properties of the produced biomass pellets (Liu et al. 2014; Lai et al. 2013; Tabil 1996; Rehkugler and Buchele 1969). The mechanical strength of the pellets usually differs when measured immediately after production, which is known as "green strength", of after some curing time, which is known as "cure strength" (N.Kaliyan and Morey 2009).

Lai et al. (2013) observed that during the storage period, the volume of the palm kernel shell pellets expanded and resulted a decrease but to a plateau in pellet strength. The rate of expansion is further amplified when the pellet is stored in higher humidity conditions. Singh (2004) demonstrated that the biomass briquettes readily absorb moisture when stored in higher relative humidity conditions. Mollan and Celik (1995) theorised the rapid expansion of volume was probably due to the viscoelastic expansion of the material. The absorbed moisture may dissolve some bond and further weaken the inter-particulate bonding thus led to weakened pellet strength. Tabil (1996) also studied the effect of high humidity storage (90% relative humidity) on the mechanical strength of alfalfa pellet. The author found significant reduction in pellet hardness when the pellet moisture content increases from 5.2% (w.b.) to 8% (w.b.), but however did not affect the pellet durability. Further increase the pellet moisture content beyond 12% (w.b.) to 14% (w.b.) reduced the durability of the pellets. Tabil (1996) concluded that the pellet hardness was more sensitive to the moisture uptake than the pellet durability.

On the contrary, fluctuation in humidity may also lead to crystallisation of dissolved material and forming inter-particulate bond either by solid bridge or intermolecular forces result in greater pellet strength. The work of Eriksson and Alderborn (1994) demonstrated this behaviour as some of the sodium chloride compacts experienced an increase in crushing strength when stored various relative humidity condition over a period of time.

2.7 Conclusions

From the literature on the densification of biomass, it can be concluded that the characteristics of the biomass materials such as moisture content and particle size, and process variables such as compaction found to affect the densification behaviour of the biomass material. It is possible that by controlling the moisture content and particle size of the EFB compost and the applied compaction pressure, the resulting mechanical strength and the nutrient release profile of the EFB compost pellets can be optimised. In addition, the strength of the pellets may degrade or improve from storage dependent on the chemical content of the biomass. In the pellet mill compaction process, the applied compaction pressure is largely dependent on the friction build-up in the die channel and is in a function of die geometry and physical characteristics of the biomass material. In the current literature, the following areas are lacking:

1) Lack of a robust theoretical model and methodology that can describe the pellet mill compaction process. Current model requires methodology that is dependent on existing literature data and requires curve fitting of additional experimental data which can be time consuming. The independent effect of each variable from the current pellet mill compaction model is undiscernible as of result.
2) The compactability and compressibility of EFB compost have not been studied yet. Previous literature on biomass densification was not conclusive due to the difference in physical property and chemical composition.
3) Limited laboratory studies that allow quick testing of nutrient release profile of EFB compost pellets. In addition, studies of nutrient release profile lignocellulose based compost pellets such as EFB compost is limited.

CHAPTER 3:
COMPACTION BEHAVIOUR OF GROUND EFB COMPOST

3.1 Introduction

Densification of empty fruit bunch compost into solid pellets is an effective solution to the problem of storage and handling associated with the heavy and bulky characteristics of compost in its original form. Densification is capable of increasing the bulk density of the biomass by up to three-fold (Kaliyan 2008). However, the degree of densification may depend on the processing conditions and the input material characteristics such as the moisture content and the particle sizes. To understand and optimise the pelleting process, it is necessary to investigate the influence of the processing conditions and the input material properties such as the compaction pressure, moisture content and particle sizes on the resulting pellet quality. However, optimising the pelleting process based on trial-and-error method can be time consuming and expensive.

Laboratory studies using a single pellet press allows for fast and cheap tests in smaller scale which has been primarily used in biomass densification studies. Experimental data obtained from the single pellet press such as the compaction pressure-porosity relationships can provide useful interpretation of the densification behaviour of the biomass powder. Compaction model such as the Heckel model and Kawakita model has been used to estimate the pressure-porosity relationship which deriving physical constants which was used as a basis for comparison between biomass materials (Shaw 2008; Mani et al. 2004a).

Generally, two methods were used to collect the data for the compaction analysis. The first method is to measure the volume during the compaction process, termed as “in-die” or “at-pressure” method (Sun and Grant 2001; Paronen 1986). With the “in-die” method, the top punch displacement and position acquired from the testing machine were utilised to calculate the volume of the compact. This method requires lesser amount of work and time as the "in-die" compaction profile can be determined in a single compaction (Ilić et al. 2013). The second method is to measure the volume of the compact after ejected out from the die, commonly termed as "out-of-die" or "zero-pressure" method. The "out-of-die" method requires production of dozens of pellets to compile a compaction profile. As the data collection is discrete in nature, it provides less information on the shape of the compaction profile and requires significant amount of time and resources compared to the "in-die" method (Ilić et al. 2013). Nevertheless, the "out-of-die" method is said to provide reliable analysis as elastic deformation of powder during compaction does not play a role at high compaction pressure (Sun and Grant 2001). To date, it is yet established that the "in-die" method or the "out-of-die" is applicable for biomass lignocellulosic material. Quantitative comparison between these two method is not available. Here, these two methods were compared quantitatively while investigating the applicability of some of the existing the empirical compaction models on the compaction behaviour of EFB composts. The use of instrumented die also introduced in this chapter.

3.2 Material preparation

Oil palm empty fruit bunch compost fibre used for the study was obtained from a palm oil mill in Bintulu, Sarawak operated by Wawasan Sedar Sdn. Bhd., Malaysia. The moisture content of the obtained EFB compost fibre was measured using an infrared moisture analyser (MA35, Sartorius, Germany) and the average moisture content was found to be 40.8% (wet base). The EFB compost fibres were oven dried at 70°C for 5 days to avoid clogging problems during the milling process. The dried EFB compost fibres were ground in a hammer mill with screen size of 2.0 mm (Disk Mill FFC-45A, Qingdao Dahua Double Circle Machinery, China). The hammer mill had a 1.5 kW motor with a capability of 2800 rpm rotational speed.

The ground EFB compost powders were then sieved using a sieve shaker (Sieve Shaker EFL2000, Endecotts, UK) with woven wire mesh of nominal sieve openings 150 µm, 300 µm, 600 µm and 1.12 mm. The EFB compost powders with particle sizes of 150 μm – 300 μm and 300 μm – 600 μm were used for the experimental studies.

3.2.1 Measurement of moisture content and water activity

The moisture content of the EFB compost powder was measured using an infrared moisture analyser (MA35, Sartorius, Germany). The infrared moisture analyser was capable to measure the change of mass when heating with the resolution of 1mg. 2g of EFB compost powder was spread evenly on the dish and dried at 70°C. Finally, the water activity level of the EFB compost powders were analysed using a water activity meter (Aqualab Lite, Decagon, US).

3.2.2 Moisture adjustment

To adjust the moisture content of the EFB compost powders, glass desiccators with relative humidity of 11% and 73% were used to condition the moisture level of the compost powders to nominal values of 5% (wet basis) and 10% (wet basis). This was achieved by using saturated lithium chloride solution and sodium chloride solution.

To achieve EFB compost powders with higher moisture content of 15% (wet basis) and 25% (wet basis), the powders were thoroughly mixed with predetermined amount of distilled water and stored in a sealed container at 4°C for a minimum of 24 hours. The proportion of powder and water was according to:

$$m_w = \frac{m_i(M_f - M_i)}{1 - M_f} \tag{3.15}$$

where m_w is the mass of distilled water added to the compost powder, m_i is the initial mass of the compost powder, M_f is the final adjusted moisture content of the compost powder in fraction and M_i is the initial moisture content of the compost powder in fraction.

3.2.3 Measurement of true density of powder

The true density of each powder particle sizes were determined using a 100 cm^3 calibrated liquid pycnometer (Blaubrand, Germany) based on modified ASTM D864-14 method (ASTM 2014) . Preliminary measurement with water as the working liquid was found to be unsuitable because the EFB compost powders tended to swell and diffuse in water. Instead, kerosene was used in place of water to minimize the swelling tendency of the EFB compost powders (Mantanis et al. 1994). The EFB compost powder was added into the pycnometer and its mass was recorded. The pycnometer was then filled with kerosene to a level slightly above the powder. The entrapped air from the powder was removed by placing the pycnometer in a vacuum chamber for at least 1 hour. The pycnometer was then carefully filled to the calibration mark with kerosene and the volume of occupied by the powder was calculated. Finally, the true density of the EFB powder was calculated. The moisture content of the EFB compost was determined prior to the density measurement.

3.3 Experimental setup

The compaction experiments were carried out using a cylindrical die with 8 mm diameter cross-section instrumented with additional die wall measurement. The die-wall instrumentation was primary used in pharmaceutical research to investigate the friction phenomena during the compaction process (Michrafy et al. 2004; Michrafy et al. 2003) and to evaluate the compaction property of powders related to tableting problem such as capping, lamination and tool wear (Abdel-Hamid and Betz 2011b; Takeuchi et al. 2004; Cunningham et al. 2004). Several instrumented die design have been developed which are discussed in detail by Doelker and Massuelle (2004).

The measurements may either be in direct contact with the powder compact using split-dies or pistons connected to transducer or load cell (Crawford and Paul 1981; Nelson 1955), or indirect by measuring the elastic expansion of the die by attaching strain gauges or piezoelectric transducer onto the outside of a cut die (Sun 2015; Cocolas and Lordi 1993; Huckle and Summers 1985; Hölzer and Sjögren 1979; Leigh et al. 1967). Although the latter principle has minimal interference with the powder compact formation, it requires careful calibration to convert the expansion measurement into force values by applying known axial forces on a hydraulic material. Natural or synthetic rubber plugs were generally used as the calibration material due to their hydraulic fluid behaviour as it transmits pressures equally in all directions. However, hysteresis (non-linear output signal) may be expected due to excessive straining in the thin wall section of the instrumented die (Huckle and Summers 1985). Thicker die wall may improve the yield strength of the die but result in a transducer with poor sensitivity.

Arrangement with piston in direct contact with the powder compact may avoid the calibration procedure with rubber plugs as the connected load cells were calibrated with known load prior to compaction (Nelson 1955). However, the particulates may have frequently inserted in the gap clearance during the compaction cycle and grip the piston and may introduce hysteresis to the measurements. Regardless, this approach may have greater sensitivity, higher upper limit load measurement and in situ measurement of radial load. For this reason, instrumentation with piston arrangement was used in this study.

3.3.1 Design of instrumented die

The compaction tests were performed using a custom made instrumented die with the ability to measure top, bottom and radial pressure as shown in Figure 3.1. The cylindrical die was machined from an aluminium alloy 6061 rod and a diameter of 8mm die channel in the centre was produced with a precision reamer (Sherwood, UK) to provide consistent channel diameter and surface finish. To measure the bottom pressure, a brass backstop was placed underneath the die bore and was attached to a load cell with 10 kN capacity (UMA, Dacell Korea). To measure the radial pressure during the compaction process, a diameter of 2.4mm hole was drilled through perpendicularly to the die channel. A brass pin sized to closely fit into the 2.4mm hole was attached to the load cell with rated capacity of 500 N (ZNLBM, JnSensor, China). The pin-load cell assembly was attached to a spring loaded mounting bracket which allowed the end face of the pin to be closely aligned to the surface of the die bore. The end face of the pin was machined to match the curvature of the die bore to minimize disturbance to the compact. All of the load cells were calibrated with known load before assembly.

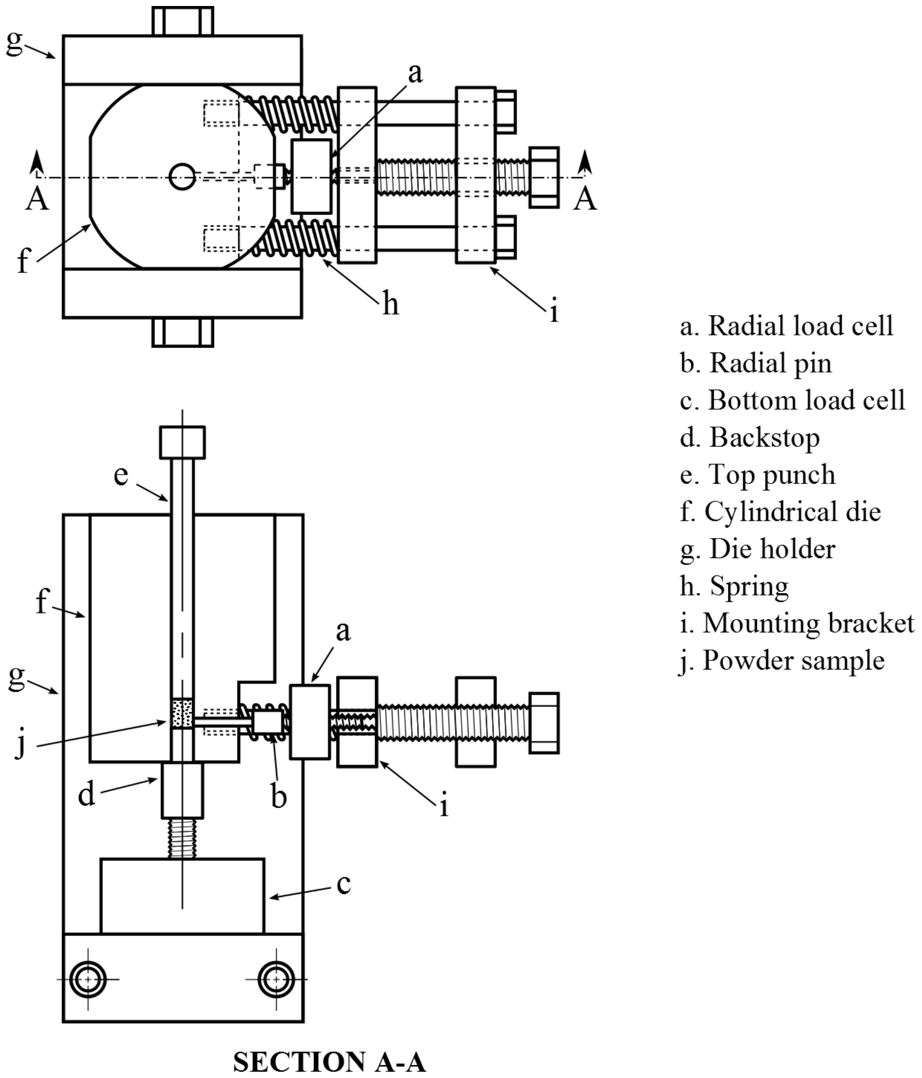

Figure 3.1: Schematic diagram of the instrumented die (i) Top view (ii) Sectional side view

The assembled instrumented die was placed between the steel platens of universal tensile compression testing machine (Lloyd LR10K, UK) as shown in Figure 3.2. The compaction load was applied through the downward movement of the upper crosshead of the testing machine with maximum load up to 9,500 N. The load cell attached on the crosshead of the machine was used to measure the applied load to the top punch.

Figure 3.2: The assembled instrumented die on a universal tensile compression testing machine. A separate LVDT was attached to the crosshead to synchronise data between separate data loggers.

A linear variable displacement transducer (LVDT) was used to determine the position of the crosshead and to measure the distance between the top punch and backstop. The height of the compact was calculated from this difference and corrected for the elastic deformation of the machine parts and die assembly according to Kalidindi et al. (1997). This was accomplished by determining the machine force-displacement compaction curve without any sample and subtracting the machine displacement from the sample height. Measurements obtained from the universal tensile compression testing machine coupled with a computer were collected using the software package NEXYGEN Plus (Lloyd Instruments Ltd, UK, Version 2.1).

The outputs of the bottom load cell and radial load cell from the instrumented die were collected separately with the multi-channel data acquisition system (DI-718B, DATAQ Instruments, US) connected to the computer with installed software package WinDaq (DATAQ Instruments Inc, US, version 3.92). Data are sampled at 10 samples per second per channel and recorded in Microsoft Excel. To synchronise with the data collected with NEXYGEN Plus, a secondary LVDT (DT-50A, Kyowa, Japan) was attached to the machine crosshead. The data collected with the WinDaq and the NEXYGEN Plus were synchronised in time by matching the peak displacement of the crosshead.

To verify the accuracy of the instrumented die, a lubricated nitrile butadiene rubber (NBR) with a known Poisson's ratio of approximate 0.50 (Fujimoto and Togo 1986) was compacted inside the instrumented die. Due to the hydraulic property of the rubber material, axial pressure loading would transmit an equal radial pressure. The responses from the load cells of the instrumented die are shown in Figure 3.3. Results shows that ratio between radial and axial pressure is close to unity with good linearity (R^2>0.999) and with minimal hysteresis curve. This suggests that the instrumented die is able to provide accurate reading of radial pressure.

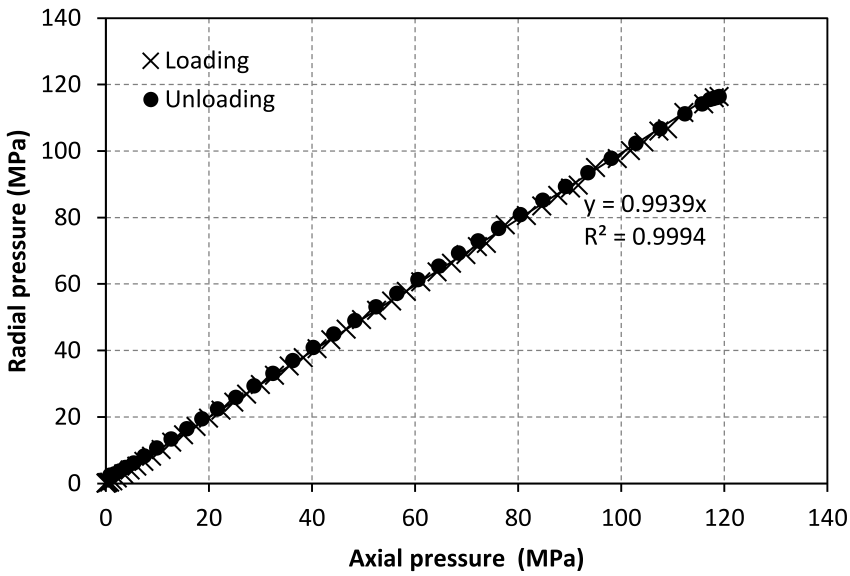

Figure 3.3: Radial pressure calibration of the instrumented die with NBR elastomer.

3.3.2 Powder compaction procedure

All compaction experiments were conducted under uniaxial compaction using the Lloyd compression-tension testing machine controlled. The compaction procedure was conducted in three stages: loading, de-loading, and ejection. The two EFB compost powder size ranges of 150-300 μm and 300-600 μm with nominal moisture content of 5%, 10%, 15% and 25% were used in this compaction studies.

The backstop was placed beneath the die and remained stationary during loading. Sample powder with nominal weight of 0.35g was manually added to the instrumented die and the top piston was inserted into the die from above. The machine crosshead was actuated downward to compact the sample powder to a specified maximum force ranging from 2000 N to 8000 N at a constant speed of 30mm/min. The load on the top punch is released immediately thereafter with the crosshead moving upward at a constant speed of 30mm/min (Kaliyan 2008). After un-loading, the backstop was removed from the base of the instrumented die. The crosshead-piston was programmed to move downward to push the powder compact out from the die. A constant crosshead speed of 30mm/min was used during the ejection.

During the compaction process, the top axial force F_{top}, the transmitted radial die wall force F_{rad}, the bottom axial force F_{bot}, and the distance travelled by the crosshead was recorded.

The pressure at the top, bottom and radial were calculated by dividing the respective forces to cross-sectional of the die as follows:

$$\sigma_{top} = \frac{F_{top}}{\frac{\pi D_{top}^2}{4}}, \qquad \sigma_{bottom} = \frac{F_{bottom}}{\frac{\pi D_{bottom}^2}{4}}, \qquad \sigma_{rad} = \frac{F_{rad}}{\frac{\pi D_{rad}^2}{4}} \qquad (3.16)$$

where D_{top}, D_{bottom}, and D_{rad} is the cross-section diameter of the respective pressure sensors.

During the compaction process, the "in-die" height of the powder compact was determined according to the difference in distance between the top punch and the bottom backstop (Figure 3.4). For "out-of-die" measurement the mass, height and diameter of the ejected compact were measured (a) immediately after ejection, and (b) after a week of storage. To investigate the influence of storage, pellets were stored in a controlled environment with fixed relative humidity 43% and room temperature of 25 °C. Three replicates were made for each compact samples.

The pellet density is calculated as:

$$\rho_c = \frac{m}{\frac{\pi D_{die}^2 H_c}{4}}, \qquad \rho_e = \frac{m_e}{\frac{\pi D_e^2 H_e}{4}}, \qquad \rho_f = \frac{m_f}{\frac{\pi D_f^2 H_f}{4}} \tag{3.17}$$

where ρ is the pellet density, m is the weight of the pellet, D and H is the diameter and height of the pellet. The subscript c, e, and f in the equation indicates when the measurement was taken during compaction, immediately after ejection, and after storage respectively.

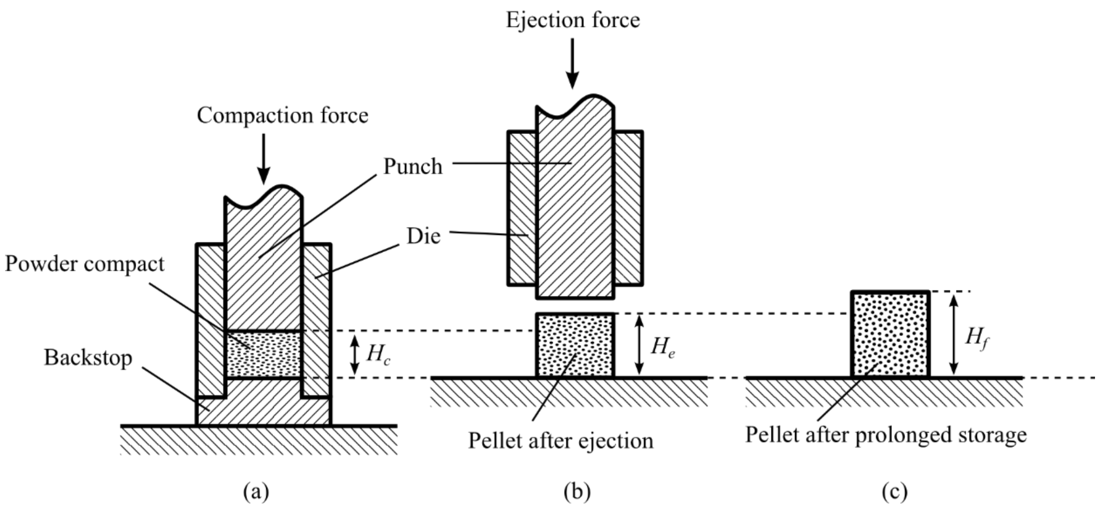

Figure 3.4: Measurement of pellet height (a) during compaction process, (b) after ejection, and (c) after prolonged storage

The porosity of the pellet ε is computed as:

$$\varepsilon_c = 1 - \frac{\rho_c}{\rho_a}, \qquad \varepsilon_e = 1 - \frac{\rho_e}{\rho_a}, \qquad \varepsilon_f = 1 - \frac{\rho_f}{\rho_a} \tag{3.18}$$

where ρ_a is the apparent density of the powder particle. The apparent density ρ_a at any moisture was calculated from:

$$\rho_a = \rho_p(1 - x_w) + \rho_w x_w \quad (3.19)$$

where ρ_p is the dry particle density, ρ_w is the density of water, and x_w is the moisture fraction.

3.4 Property of ground EFB Compost

3.4.1 Microscopy and Particle Size Analysis

Figure 3.5 shows the particle size distribution of the dry EFB compost ground with a 2.00mm screen hammer mill. Particle size of 300-600 µm showed the highest mass fraction followed by 150-300 µm and 0-150 µm. The shape of the EFB compost powder particles was found to be fibrous and slightly granular as shown in Figure 3.6. The granule particles could possibly be the residual shells left after the fruits were removed from the bunch during the stripping process.

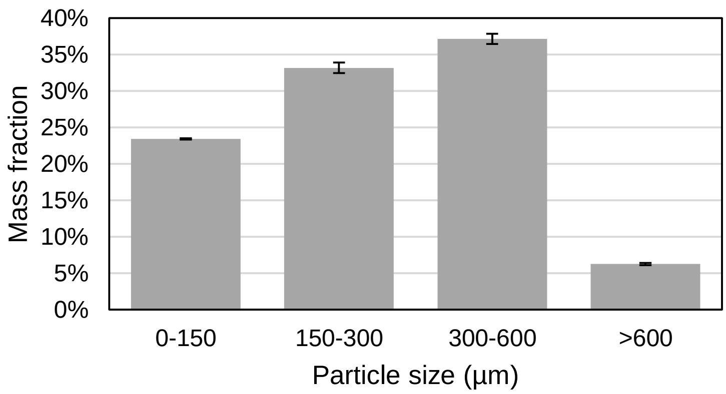

Figure 3.5: Particle size distribution of ground EFB compost

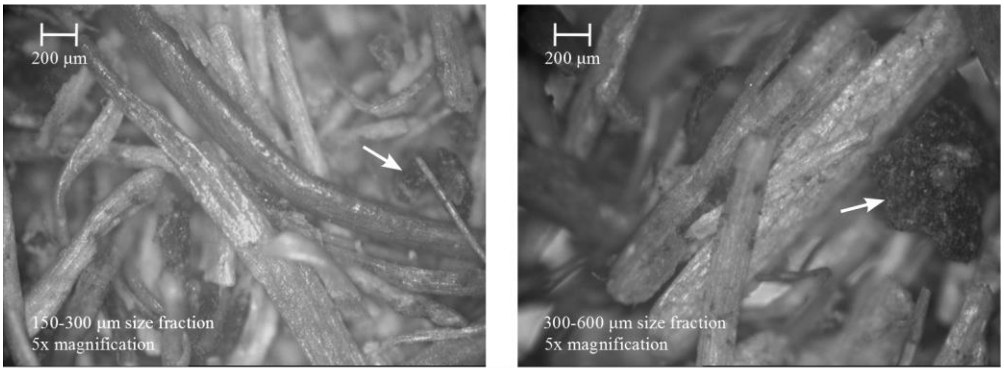

Figure 3.6: Micrograph of the compost powder with particle sizes of 150-300 µm (left) and 300-600 µm (right). Granular particles as indicated by the arrow.

3.4.2 Particle density, moisture content and water activity

Table 3.1 shows the particle density of the ground EFB compost powder in relation to the particle sizes as well as the relation between the moisture content and water activity of the compost powder. The value of particle density ρ_T is reported in reference to the dry mass and was calculated according to the following equation (Steendam et al. 2001):

$$\rho_p = \frac{\rho_a - \rho_w x_w}{1 - x_w} \qquad (3.20)$$

where ρ_a is the apprent particle density, ρ_w is the density of water and x_w is the moisture content in fraction.

The particle density of the EFB compost powder appeared higher than the untreated EFB reported in literature (Mohammed et al. 2012). The disparity of density between the EFB compost and untreated EFB could probably due to the degradation of low density component lignin during the composting process (García-Gómez et al. 2005). The particle density values were used to calculate the relative density and porosity of the compact.

Table 3.1: Properties of ground EFB compost powder

Grind moisture content (% wet basis) ± S.D.	Water activity (a_w) ± S.D.
Particle size 150-300 µm (*Dry particle density = 1.586 g/cm^3 ± 0.004)	
5%	0.211 ± 0.017
10%	0.733 ± 0.020
15%	0.804 ± 0.011
25%	0.901 ± 0.006
Particle size 300-600 µm (*Dry particle density = 1.569 g/cm^3 ± 0.004)	
5%	0.213 ± 0.012
10%	0.747 ± 0.013
15%	0.799 ± 0.014
25%	0.906 ± 0.006

3.5 Results and discussions

3.5.1 Loading and unloading

Four levels of moisture content (5%, 10%, 15% and 25% wet basis) of ground EFB compost powder with two different particle sizes (150-300 µm and 300-600 µm) were used in this experiment. A nominal weight of 0.35g of EFB compost powder were compacted in the instrumented die and the top and bottom axial force, radial die wall force and compact height were recorded during the compaction process. The results obtained were used to determine the pelleting parameter of radial-axial transmission ratio, residual die wall pressure and coefficient of friction.

Figure 3.7 shows a typical pressure data obtained from the instrumented die plotted with respect to time during the compaction process. In the initial stage of the compaction process, particle rearrangement occurred and the particles came into close proximity with each other indicated by the gradual slope. As the compaction progressed, the slope increased rapidly. Both radial pressure and bottom pressure increased in similar manner with the applied top pressure. The value for the bottom pressure was lower than the top pressure was due to the effect friction during compaction. Once the applied top pressure reached the pre-set value, the compaction pressure is released. Both the top and bottom axial pressure were reduced to zero during the release while the compact remained under a residual radial pressure when the axial pressure is completely removed.

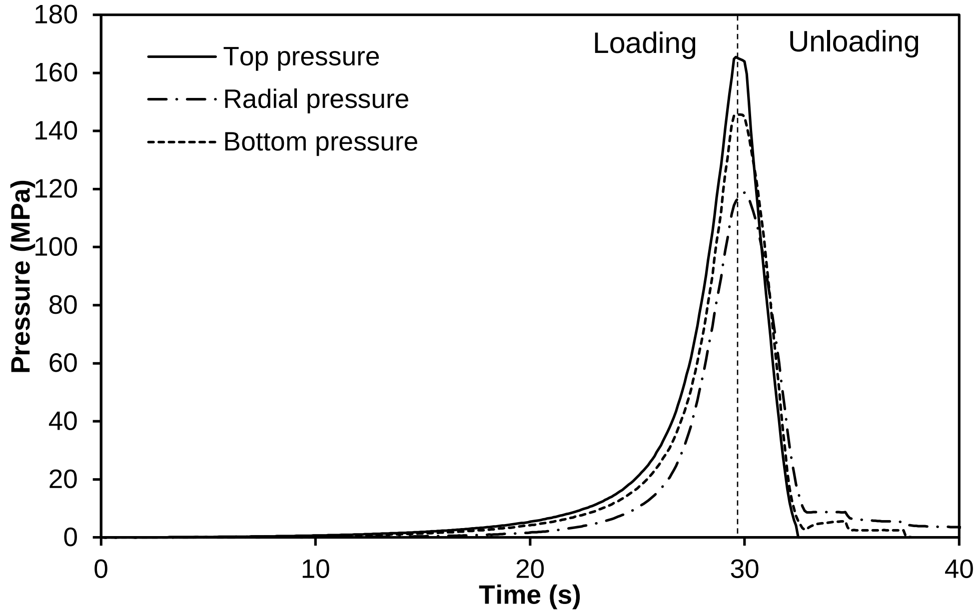

Figure 3.7: Typical compaction data from the instrumented die during loading and unloading. Pre-set compaction load of 8000 N with ground EFB compost particle size of 150-300 μm and 15% (w.b.) moisture content.

Figure 3.8 shows a typical radial-axial compaction curve of ground EFB compost powder obtained from the instrumented die. The radial-axial compaction curve illustrates the relationship between the change of radial die wall pressure and axial pressure corrected to the position of the radial pressure sensor. The radial pressure appeared to be increased with the axial pressure during loading and decreased during unloading. Residual radial pressure was observed when the axial pressure reached zero. The EFB compost powder with 15% (wet basis) moisture content shows a slight increase in slope in the radial-axial compaction curve during loading cycle. The change of slope occurs when the powder bed was compacted at a pressure beyond the elastic limit of the material where plastic deformation occurs (Doelker and Massuelle 2004). However, the change in slope for drier EFB compost powder with 5% (wet basis) moisture content was absent which is possibly attributed by the poor compactability of dry material correspond to the increased elastic limit of the material.

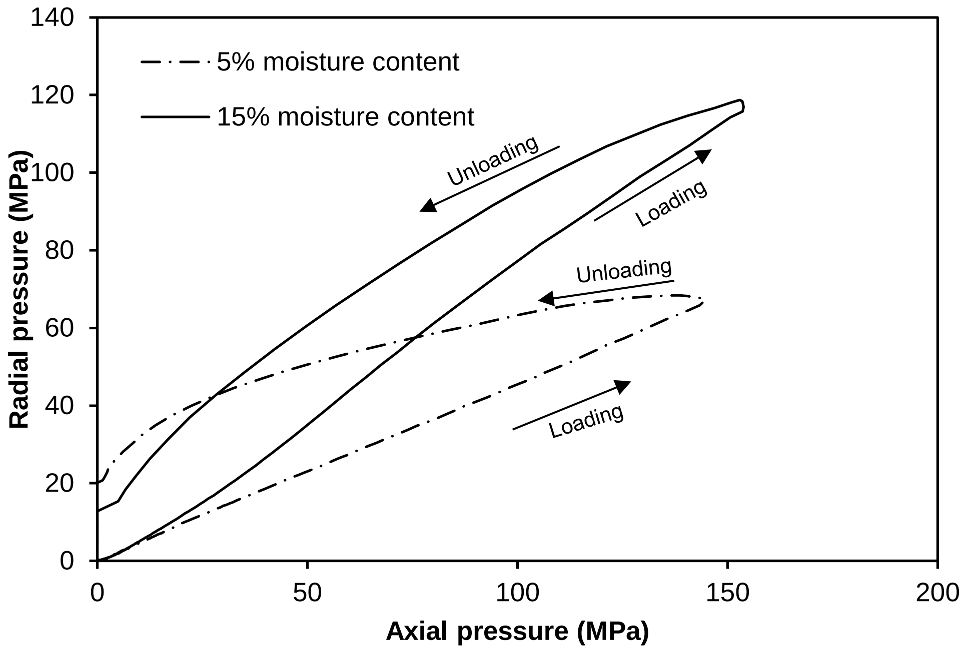

Figure 3.8: Typical radial-axial compaction curve of ground EFB compost in the instrumented die. Pre-set compaction load of 8000 N with EFB compost particle size of 150-300 μm.

Figure 3.9 shows the relationship between the compaction load and the “in-die” compact height for particle size of 150-300 μm and 300-600 μm respectively. EFB compost powders with moisture content of 25% (wet basis) were compacted to a maximum force of 6000 N to avoid clogging of the die. The height of the compact varied by the compaction pressure applied and the moisture content of EFB compost. The height of the compact after the compaction load was released was found to be slightly higher than the compact height at maximum load. This indicated that the compact had expanded slightly after the release of the compaction load.

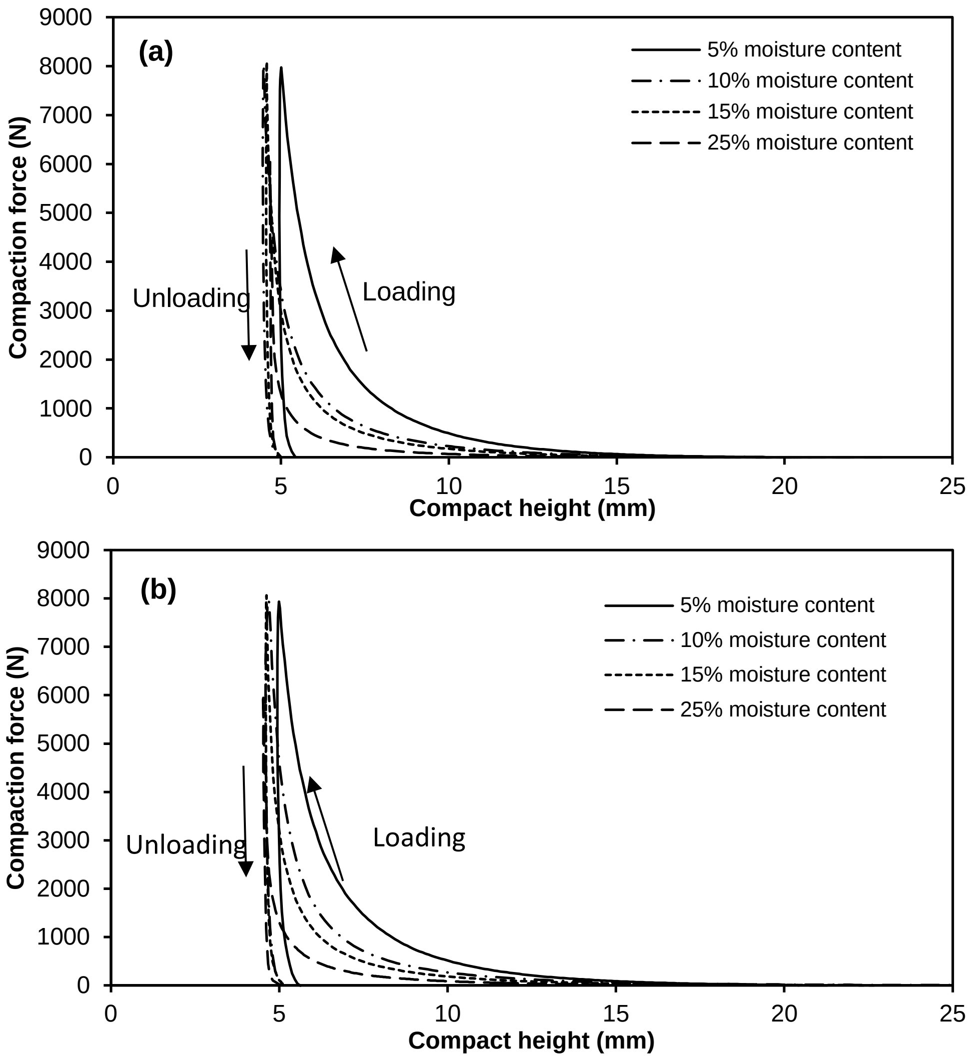

Figure 3.9: Compaction curve during loading and unloading obtained from Lloyd testing machine for the particle size of (a) 150-300 µm and (b) 300-600 µm with different moisture content tested at the highest pre-set load. The displacement data has been corrected for machine elasticity.

3.5.1.1 *Specific energy of compaction*

To further demonstrate the influence of the moisture content and particle size on the compaction behaviour, specific energy consumption was calculated by estimating the area under the force-displacement curve using trapezoidal rule (Cheney and Kincaid 2012). Figure 3.10 illustrate the specific energy required to compact the EFB compost powder with different moisture contents and particle sizes up to 8000 N of compaction force. Force difference between the top punch and the bottom backstop was used to calculate the specific energy loss due to friction.

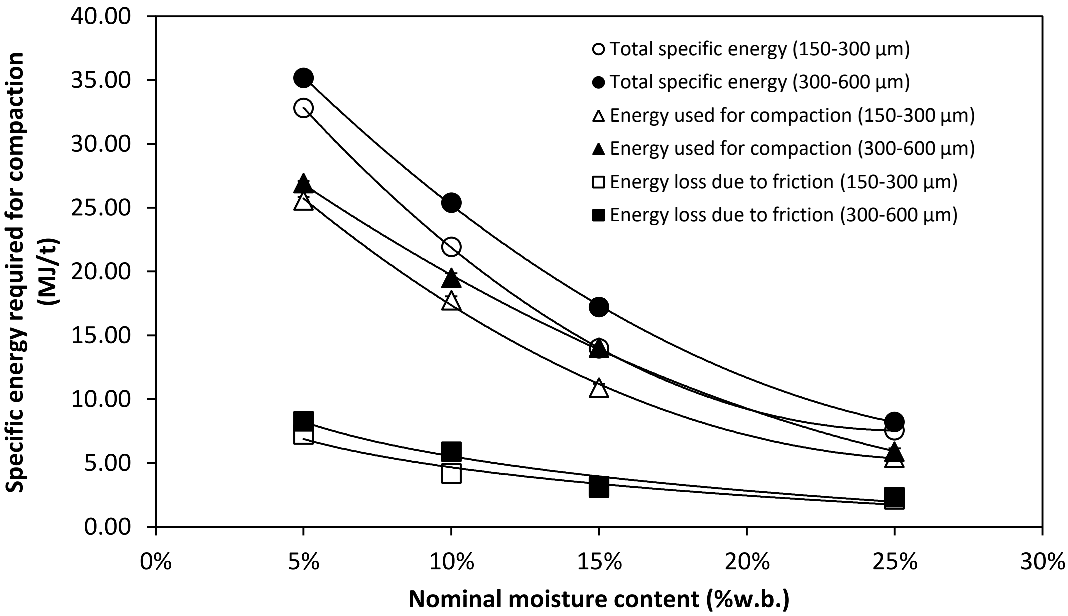

Figure 3.10: Specific energy requirement of compaction for EFB compost powder with different moisture content and particle size.

It appears that the increased moisture content of the compost powder significantly reduced the specific energy requirement for both particle sizes of EFB compost powder. Similarly, Mani et al. (2006b) reported that the energy required for compacting corn stover was reduced with the increase of moisture content. The addition of moisture presumably acts as a plasticiser which softens the powder particles and thereby facilitates the compactability of the powder. Only a minor decrease in specific energy was observed with the decrease of particle size from 300-600 μm to 150-300 μm. The specific energy loss due to friction also reduced with increasing moisture content, possibly due to lubricating effect of moisture which reduced the contact friction on the die wall during compaction. Friction during the compaction process may exist due to the friction between powder particles and the resulting contact between the powder and the die wall (Michrafy et al. 2003).

3.5.2 Porosity

The relationship between the porosity measured at different conditions and the applied compaction pressure is shown in Figure 3.11 and Figure 3.12. It was found that porosity of the powder compact varied widely depending on the conditions being measured, powder particle sizes, moisture content and the applied compaction pressure. In general, the porosity of the powder compact decreased and approached toward zero with the increase of applied compaction pressure.

The compaction pressure needed to achieve zero compact porosity ε_c increased with larger particle size and lower moisture content. The EFB compost powder with 5% moisture content, however, did not achieve zero porosity within the range of applied compaction pressure. Some negative porosity values were also observed and this could probably due to mechanical dewatering of the compact at high compaction pressure. The expulsion of moisture from the compact could lead to an increase in the apparent particle density and therefore resulted in negative porosity value. The porosity of the compact appeared to increase for all samples after the release of compaction pressure with "out-of-die" measurement.

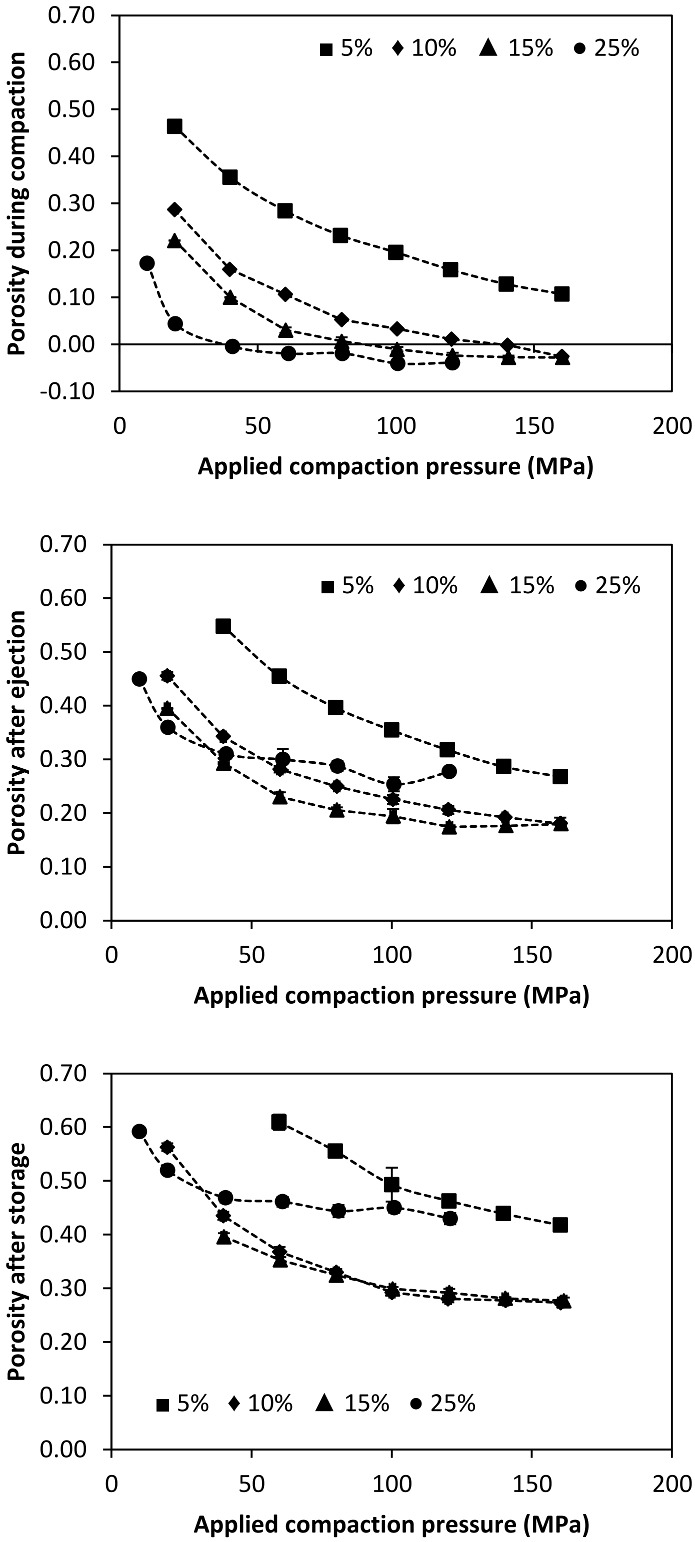

Figure 3.11: Relationship between porosity at different conditions and the applied compaction pressure for EFB compost powder with particle size of 150-300 µm and moisture content ■ 5%, ♦ 10%, ▲ 15%, ● 25%

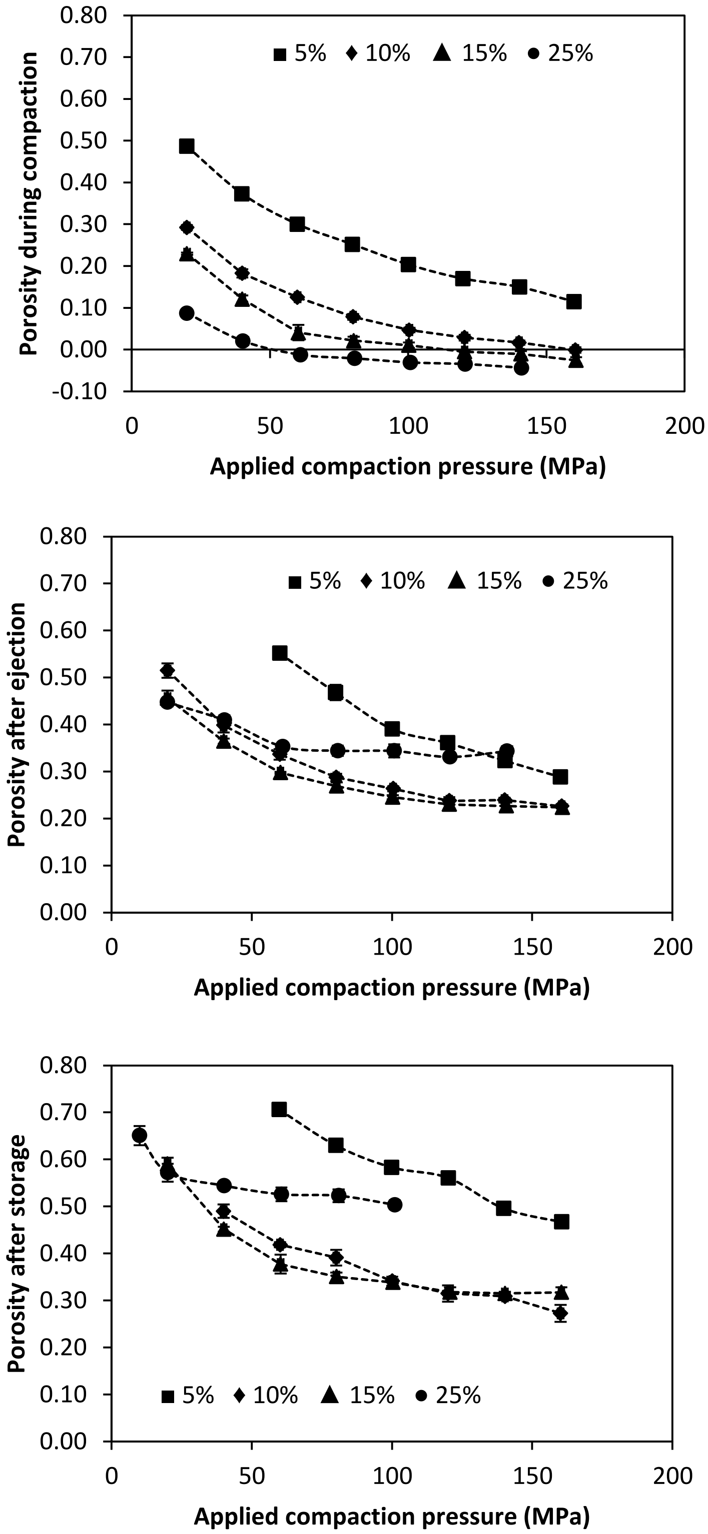

Figure 3.12: Relationship between porosity at different conditions and the applied compaction pressure for EFB compost powder with particle size of 300-600 µm and moisture content ■ 5%, ♦ 10%, ▲ 15%, ● 25%

3.5.2.1 *Negative porosity during compaction*

To demonstrate the cause of negative porosity measurement due to mechanical dewatering of the compact, the coefficient of friction during compaction was measured. The effect of friction during the compaction process was determined by evaluating the axial pressure from the top punch and bottom backstop and the radial pressure. The Janssen-Walker analytical model for compaction based on the "method of differential slices" in Equation (3.21) was used to determine the coefficient of friction during compaction μ_c (Nedderman 2005; Cunningham et al. 2004).

$$\mu_c = \frac{D}{4H}\frac{\sigma_B}{\sigma_{rad}}\left(\frac{\sigma_T}{\sigma_B}\right)^{\frac{z}{H}}\ln\frac{\sigma_T}{\sigma_B} \tag{3.21}$$

Where D and H is the diameter and height of the compact, σ_B, σ_T and σ_{rad} is the pressure measured at the bottom, top and radial direction of the compact, and z is the position of the radial sensor from the bottom of the compact (Figure 3.13).

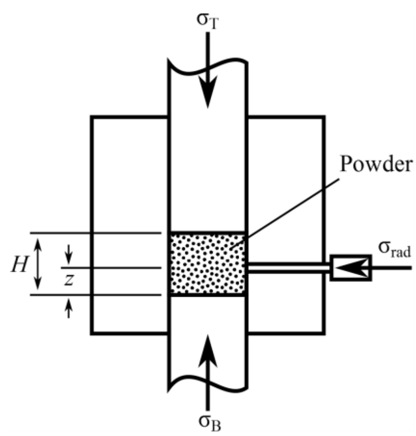

Figure 3.13: Schematic diagram of powder compaction in an instrumented die

The resulting coefficient of friction during compaction with the EFB compost powder was plotted against the compact porosity in Figure 3.14 and Figure 3.15. For EFB compost with the particle size of 150-300 μm, the coefficient of friction for 5% moisture content initially decreased, but gradually increased from 0.15 to 0.19 thereafter. In contrast, for EFB compost with 10% moisture content, the coefficient of friction decreased in the initial stage of compact (porosity > 0.5) and converged towards value of 0.12. However, the friction behaviour in compost powder with 15% moisture content appears to be slightly different that the friction coefficient initially decreases towards a constant value of 0.18 and abruptly decreased to 0.08 when the compact porosity was in negative value. The sudden drop in friction coefficient occurred at zero porosity and could probably related to the expulsion of water towards the die wall when compacted at high pressure. The lubricating effect of moisture was more pronounce in compost powder with 25% moisture content where the coefficient of friction continuously decreased with the compact porosity without a tendency to converge towards a constant value. A similar trend was also observed in EFB compost powder with 300-600 μm particle size, but with a slight increase in overall coefficient of friction.

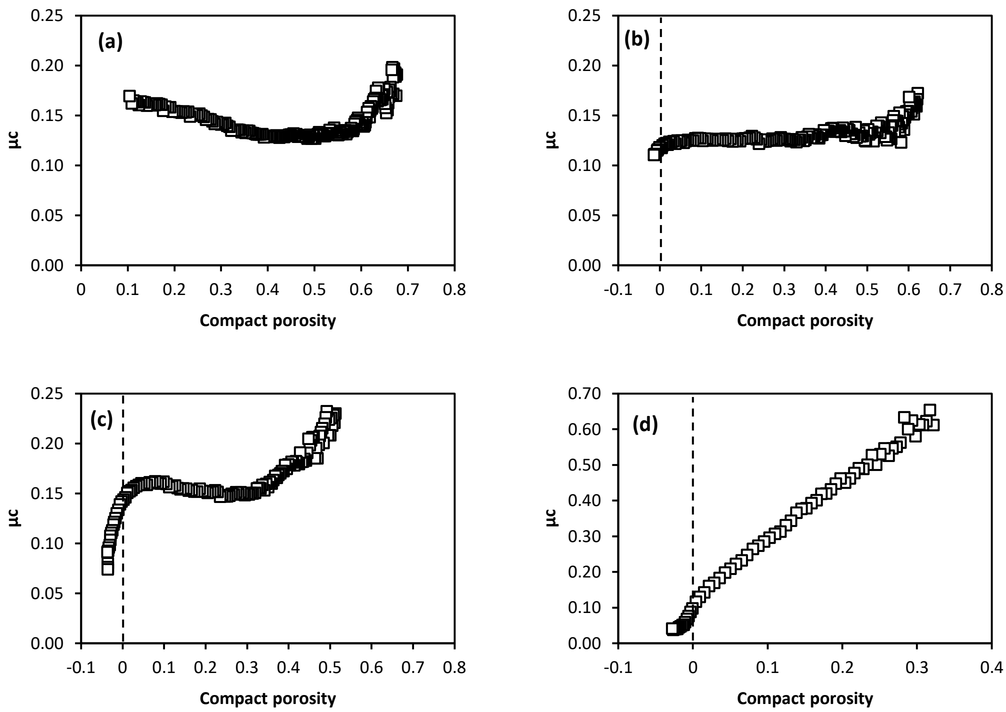

Figure 3.14: Relationship between coefficient of friction during compaction and compact porosity with particle size of 150-300 μm and moisture content of (a) 5%, (b) 10%, (c) 15% and (d) 25%

Although the results indicate that the increased moisture led to the higher coefficient of friction in the initial stage of compaction process, the friction coefficient was significantly lower with increased moisture content only when the compaction occurred below zero porosity. This further supports that the negative porosity was due to mechanical dewatering at high compaction pressure which led to the increased lubricating effect on the die wall.

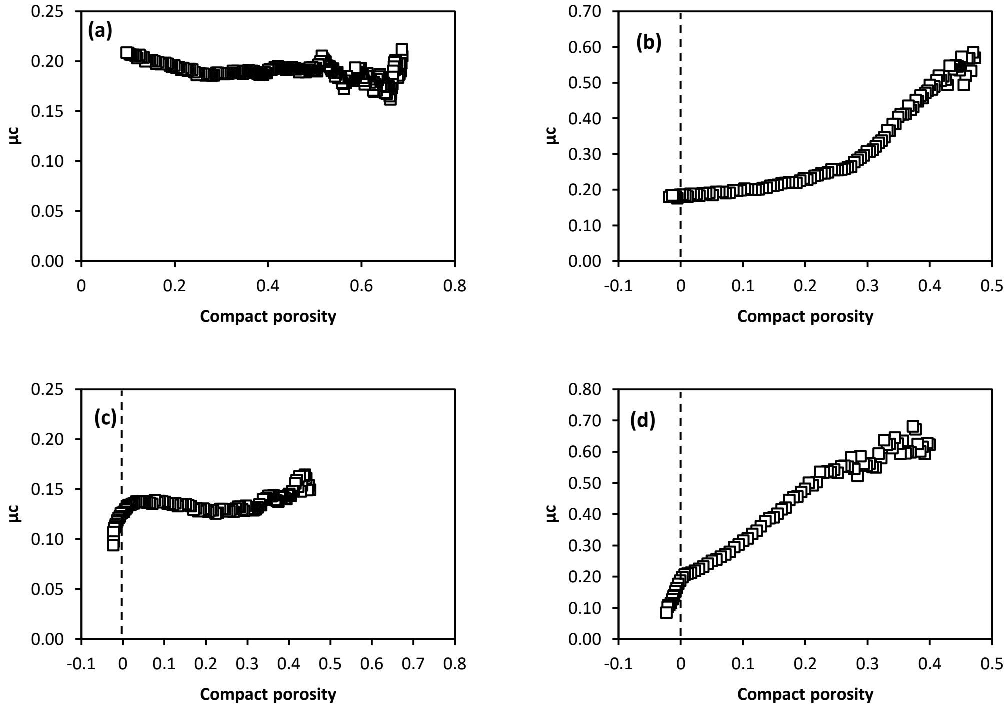

Figure 3.15: Relationship between coefficient of friction during compaction and compact porosity with particle size of 300-600 μm and moisture content of (a) 5%, (b) 10%, (c) 15% and (d) 25%

3.5.3 Compaction models

3.5.3.1 *Heckel model*

The Heckel model relates the relative density changes with the applied compaction pressure as (Heckel 1961):

$$\ln\frac{1}{\varepsilon} = kP_a + A \tag{3.22}$$

where P_a is the applied compaction pressure, ε is the porosity of the powder compact, k and A is the Heckel model constant.

"In-die" Heckel model results

In-die Heckel plots for some selected pellet compacts with particle size of 150-300 µm and 300-600 µm are presented in Figure 3.16. The slope of the linear regression represented by the solid lines is the Heckel coefficient k and its reciprocal value which is known as yield pressure P_y is the measure of the powder compactibility (Ilić et al. 2013). Higher value of k or lower value of P_y indicates better compactability and vice versa. Fit of the compaction data was excellent for all samples as indicated by the high R^2 (>0.999) of the linear regions.

However, an upward curvature was observed towards the end of compaction pressure for EFB compost powder with moisture content of 10%, 15% and 25% (Figure 3.16). Sun and Grant (2001) suggested the upward deviation from the linear region of the "in-die" Heckel analysis is due to the elastic deformation of the powder. The author further explained that materials with greater elastic modulus develop lower strain under similar pressure and therefore exert smaller deviation from linearity (Sun and Grant 2001). From Figure 3.16, the deviation from linearity was observed at lower compaction pressure as the moisture content increases.

The average yield pressure P_y of the EFB compost powder appears to decrease with increasing moisture content as highlighted in

Table 3.2. This suggest that the EFB compost powder with particle size of 150-300 µm and 5% moisture content was harder and less plastic, and requires a higher compaction pressure correspond to the yield pressure of 88.33 MPa to deform. Whereas at 25% moisture for 150-300 µm particle size, the lower yield pressure of 11.83 MPa indicates the EFB compost powder is soft, plastic and easier to be compact at lower pressure.

For EFB compost with the particle size of 300-600 µm, the yield pressure P_y decreased from 95.85 MPa to 13.15 MPa with the increase of moisture from 5% to 25%. When compared to smaller particle size, EFB compost powder with larger particle size exhibited an overall slight increase in the yield pressure.

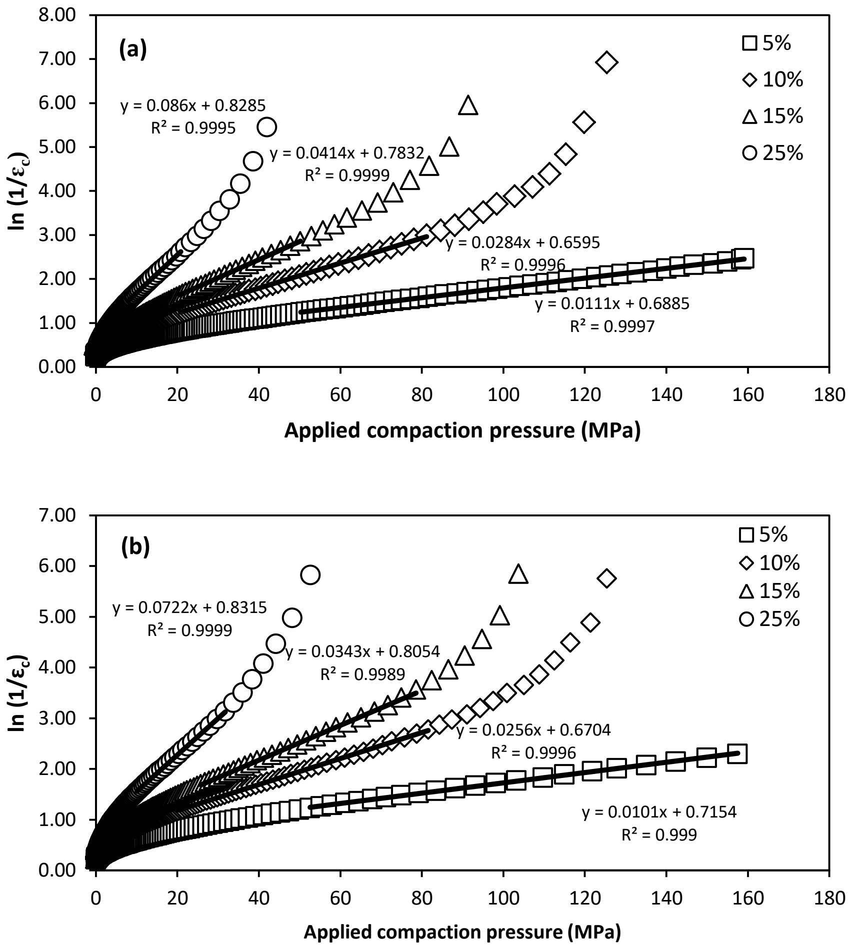

Figure 3.16: In-die Heckel plot for EFB compost powder with particle size of (a) 150-300 µm and (b) 300-600 µm. Values in legend indicates the initial moisture content of the pellet.

Table 3.2: Calculated "in-die" Heckel model physical constants for EFB compost

Particle size (µm)	Moisture content (% w.b)	k ($\times 10^{-3}$)	A	P_y (MPa)	R^2
150-300	5%	11.36 ± 0.67	0.720 ± 0.024	88.33 ± 5.07	0.9996
	10%	27.40 ± 0.73	0.664 ± 0.015	36.52 ± 0.95	0.9996
	15%	41.87 ± 2.47	0.776 ± 0.035	23.97 ± 1.40	0.9998
	25%	84.54 ± 1.80	0.815 ± 0.015	11.83 ± 0.26	0.9996
300-600	5%	10.43 ± 0.09	0.699 ± 0.006	95.85 ± 0.87	0.9992
	10%	25.33 ± 0.33	0.669 ± 0.002	39.48 ± 0.51	0.9994
	15%	32.27 ± 2.47	0.836 ± 0.028	31.23 ± 2.82	0.9995
	25%	76.17 ± 1.80	0.837 ± 0.018	13.15 ± 0.52	0.9998

"Out of die" Heckel model results

The EFB compost powders were compacted at eight different compaction pressures (20, 40, 60, 80, 100, 120, 140, and 160 MPa) and the pellets were evaluated immediately after the ejection and 7 days after the being stored in a constant relative humidity chamber of 43%. In the case of compost powder high moisture content, production at below 20 MPa did not produce pellets with sufficient mechanical strength that allows handling and measurements of dimension. In addition, negative porosities were observed at high pressure region which could probably due to the expulsion of moisture from the compact and result in increased particle density. Although positive porosity was observed after the ejection and prolonged storage, result from the "out-of-die" Heckel plot can be counterintuitive due the negative deviation from the linear plot which would substantially increase the yield pressure. For this reason, the "out of die" method was taken into consideration within pressure ranges before mechanical dewatering occurred. To allow better comparison between "in die" and "out of die" results, the same pressure range was used to calculate the slopes of the Heckel plots.

Table 3.2 shows the fit of "out of die" was reasonable for most materials studied (R^2 > 0.95) within the pressure range studied. Yield pressure for EFB compost powder at 25% moisture content however, was not calculated due to insufficient data points. A slight curvature was observed for moisture content of 10% and 15%, which reduces the R^2 values. EFB compost powder with 5% moisture content still exhibit excellent fit with R^2 of over 0.99. This result shows that a reasonable fit for "out of die" Heckel plot can be obtained within the selected pressure ranges before mechanical dewatering, which contrast with the findings obtained in the study by Mani et al. (2006a). Compaction data of biomass grinds obtained by Mani et al. (2006a) did not fit well with the Heckel plot, however it is not known if the data was inclusive of mechanical dewatering that causes deviation from the linear regression fit.

Table 3.3: "Out of die" Heckel model physical constants for EFB compost with particle size of 150-300 μm

Measurement method	Moisture content (% w.b)	k ($\times 10^{-3}$)	A	P_y (MPa)	R^2
After ejection	5%	5.25	0.543	190.48	0.9927
	10%	6.21	0.877	161.03	0.9769
	15%	7.03	0.970	142.25	0.9720
	25%	-	-	-	-
After storage	5%	2.90	0.4512	344.83	0.9982
	10%	5.10	0.7551	196.08	0.9677
	15%	5.02	0.7784	199.20	0.9933
	25%	-	-	-	-

Table 3.4: "Out of die" Heckel model physical constants for EFB compost with particle size of 300-600 μm

Measurement method	Moisture content (% w.b)	k ($\times 10^{-3}$)	A	P_y (MPa)	R^2
After ejection	5%	4.83	0.4374	207.04	0.9945
	10%	5.60	0.7715	178.57	0.9827
	15%	6.43	0.7839	155.52	0.9601
	25%	-	-	-	-
After storage	5%	3.98	0.1542	251.26	0.9772
	10%	5.36	0.5763	186.57	0.9839
	15%	4.68	0.6476	213.68	0.8884
	25%	-	-	-	-

Figure 3.17 and Figure 3.18 shows the "out of die" Heckel plot for EFB compost powder with particle size of 150-300 μm and 300-600 μm respectively. The results show similar behaviour with the "in die" Heckel plot, where the yield pressure decreased with the increase in the moisture content. However, the yield pressure values were elevated when measured immediately after ejection and elevated further after prolonged storage. The extent of elevation differed significantly between the moisture contents and particle sizes investigated.

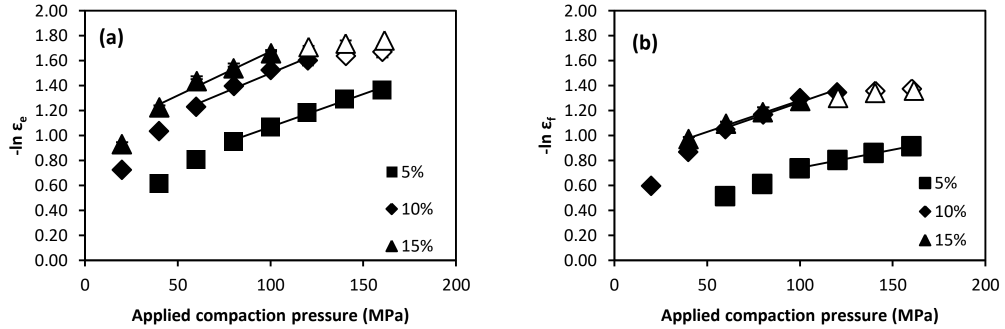

Figure 3.17: Heckel plot for EFB compost powder with particle size of 150-300 µm and various moisture contents measured at different condition (a) after ejection, and (b) after prolonged storage. Values in legend indicate the initial moisture content of the pellet.

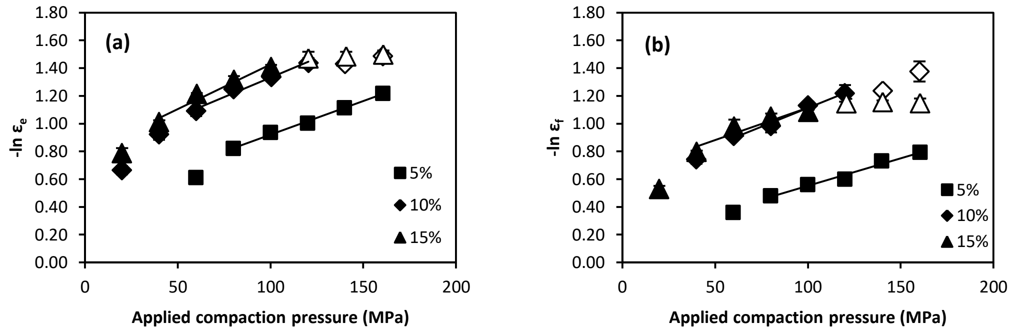

Figure 3.18: Heckel plot for EFB compost powder with particle size of 300-600 µm and various moisture contents measured at different condition (a) after ejection, and (b) after prolonged storage. Values in legend indicate the initial moisture content of the pellet.

A similar phenomenon was observed in the studies of Sun and Grant (2001) and Ilić et al. (2013). Ilić et al. (2013) postulated that the main difference between the "in die" and "out of die" methods is the exclusion or inclusion of the elasticity of the material studied. The "in die" method is inclusive of the elastic deformation because the compact dimensions were obtained under pressure during the compaction process. On the other hand, the "out of die" method is exclusive of this elastic deformation, making it more representative of actual condition. The elastic recovery occurred during storage decreased the pellet density and increased its porosity. The increase in porosity is further compounded by the changes in moisture content during the storage period.

Sun and Grant (2001) proposed that the differences between the "in die" and "out of die" Heckel plots become greater for the materials with smaller elastic moduli. To test this assumption, the elasticity of the EFB compost powder was determined using the elastic recovery index (Ilić et al. 2013). The elastic recovery was calculated as:

$$\mathrm{ER} = \frac{H_f - H_0}{H_0} \tag{3.23}$$

where H_f is the height of the pellet after storage and H_0 is the minimum height of the compact during compaction. Figure 3.19 shows the relationship between the elastic recovery and the applied compaction pressure. The elastic recovery appears to decrease with increasing moisture content from 5% - 15%.

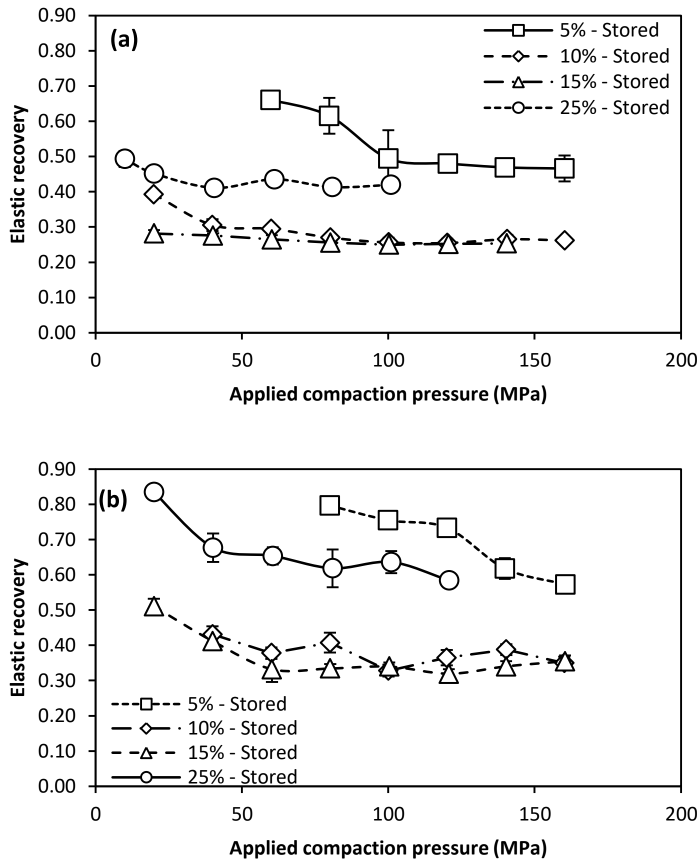

Figure 3.19: Elastic recovery of pellet after storage particle size of (a) 150-300 μm (b) 300-600 μm at different moisture content.

The differences between the "in die" and "out of die" after prolonged storage Heckel coefficients observed in this study were compared using the average elastic recovery obtained from Figure 3.19 and this is shown in Figure 3.20. Interestingly, a negative correlation was found where the difference between the "in die" and "out of die"

Heckel coefficient k decreased with increasing elastic recovery. These results are in contrast with the studies of Sun and Grant (2001) and Ilić et al. (2013), however, it is important to note that their results were compared among different pharmaceutical materials with different elasticity. Here, the elasticity of the compost powder decreases with increase in moisture content. Despite the EFB compost powder with 15% moisture content exhibited the lowest mean elastic recovery; it produced the largest shift in the Heckel coefficient. The differences in Heckel coefficient appears to be decreased with decreasing moisture content. This could probably due to the significant change of pellet porosity after storage. The pellet porosity is calculated taking into account of the loss of moisture during storage which increases the apparent particle density. As of result, the pellet porosity significantly increased despite low elastic recovery. Corresponding to the increase in porosity, the measured yield pressure may be flawed for “out of die” measurement in particular for EFB compost powder with high moisture content.

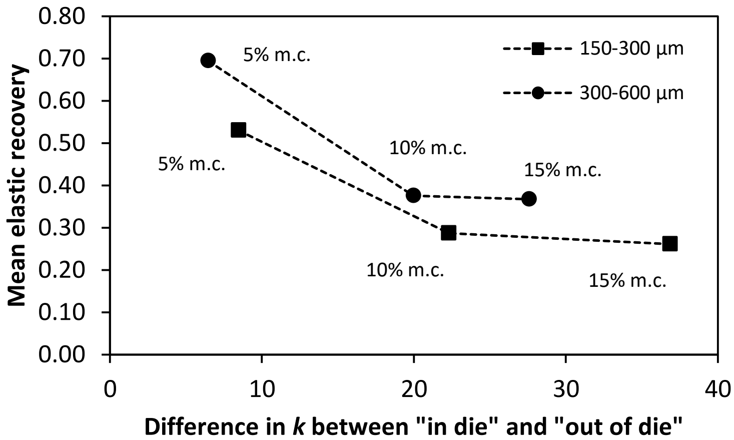

Figure 3.20: Relationship between the mean elastic recovery and the difference in Heckel constant *k* between “in die” and “out of die” after storage result.

3.5.3.2 *Kawakita model*

The Kawakita model equation assumes that the particles subjected to compaction load in a confined spaced are viewed as a system and in equilibrium at all compaction stages, therefore the product of pressure term and volume terms is constant (Kawakita and Lüdde 1971). The model equation is expressed as:

$$\frac{P_a}{C} = \frac{1}{ab} + \frac{P_a}{a} \quad (3.24)$$

And

$$C = \frac{V_0 - V}{V_0} \quad (3.25)$$

where P_a is the applied compaction pressure, C is the degree of volume reduction, and a is the value of initial porosity which correspond to the value of C at infinitely large pressure P_a. Mathematically, the reciprocal of b is the pressure needed to reduce the powder bed volume by 50% (Shivanand and Sprockel 1992). The constant b is also proposed to be inversely related to the yield strength of particles (Nicklasson and Alderborn 2000). Similar to the Heckel model analysis, the "in die" and "out of die" method was used for the Kawakita model analysis.

"In die" Kawakita model results

Figure 3.21 shows part of the "in die" Kawakita plot for EFB compost powder with various moisture content and particle sizes of 150 – 300 μm and 300 – 600 μm respectively. The Kawakita constants a and $\frac{1}{b}$ were obtained from linear regression of the Kawakita plot and the results are described in Table 3.5. It appears that the fit of data was excellent for all materials as indicated by the high R^2. A slight curvature was observed for EFB compost powder at 5% moisture content in the initial region (<20 MPa) of the Kawakita plot and the curvature progressively absent as the moisture content increases. It is also interesting to note that the Kawakita plot maintained excellent linearity over the full pressure range investigated, in contrast with the Heckel plot where linear region is limited within the pressure before the mechanical dewatering occurs.

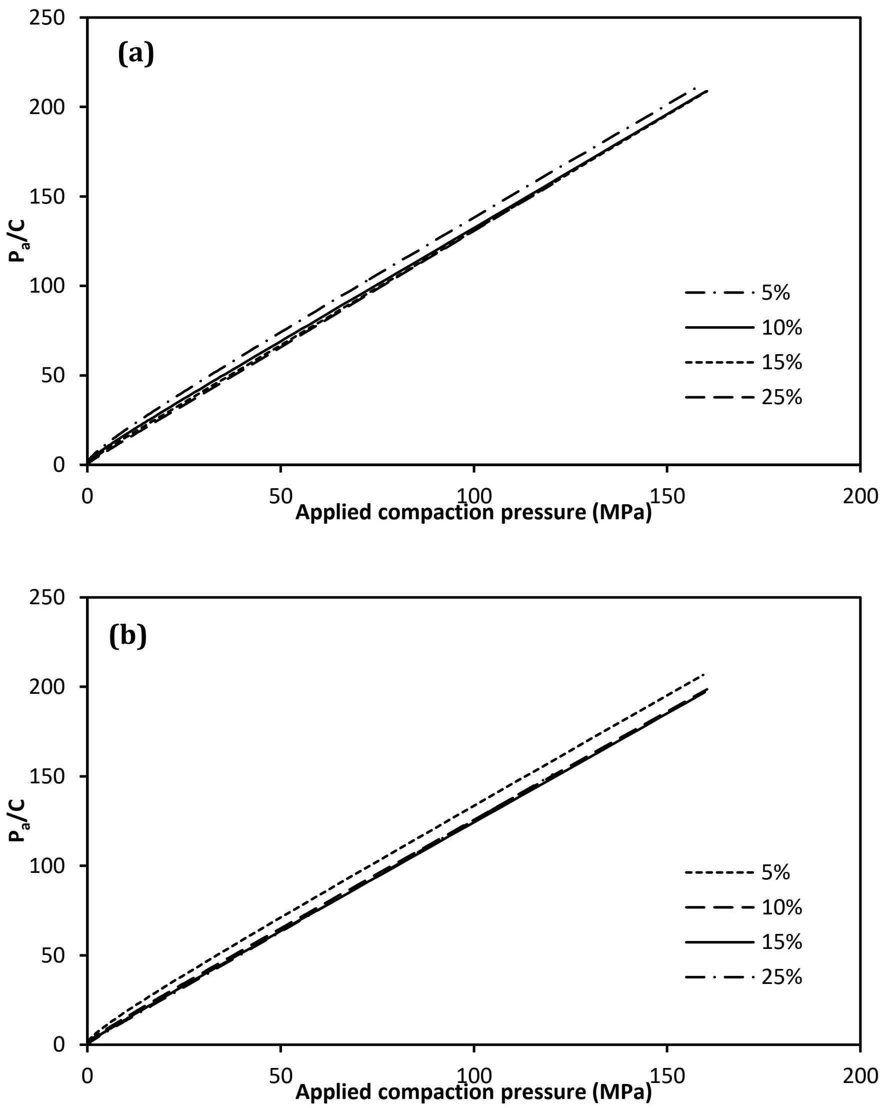

Figure 3.21: "In die" Kawakita plot for EFB compost powder with the particle size of (a) 150-300 µm and, (b) 300-600 µm at various moisture contents. Values in legend indicate the initial moisture content of the pellet.

The "in die" Kawakita results show the constant a exhibits reasonable agreement with the measured initial porosity for the EFB compost powder with the moisture content of 5%. However, increasing the moisture content above 5% resulted in slight overestimation of the initial porosity value, despite the excellent fit in the Kawakita plot. This overestimation has also been reported in the study of Shaw (2008) with the compaction of biomass feedstock with moisture content of 9% and 15%.

The reciprocal of the constant b appears to decrease with the increase of moisture content. The results suggest that the compactability of the EFB compost powder increases with the moisture content which is consistent with the definition of yield pressure value obtained from the Heckel model. However, this is not the case with the change in particle size as it appears that the constant $\frac{1}{b}$ consistently decreased slightly with the increase in particle size from 150-300 µm to 300-600 µm regardless of the moisture content. The values for yield pressure P_y from the Heckel model are also much larger when compared to the values for $\frac{1}{b}$ (

Table 3.2 and Table 3.5). Shivanand and Sprockel (1992) suggested that at pressures of $\frac{1}{b}$, the volume reduction occurs primarily by particle arrangement and elastic deformation, since the pressures needed to plastically deform the powder bed are higher than the pressure requirement for the elastic deformation.

Table 3.5: Calculated "in-die" Kawakita model parameter for EFB compost

Particle size (µm)	Moisture content (% w.b)	a	$1/b$	Initial porosity[1]	R^2
150-300	5%	0.7768 ± 0.0036	6.143 ± 0.233	0.7731	0.9996
	10%	0.7834 ± 0.0030	3.732 ± 0.130	0.7615	1.0000
	15%	0.7702 ± 0.0130	2.185 ± 0.110	0.7560	1.0000
	25%	0.7678 ± 0.0055	0.926 ± 0.025	0.7558	1.0000
300-600	5%	0.8000 ± 0.0051	5.419 ± 0.209	0.7996	0.9998
	10%	0.8226 ± 0.0036	2.967 ± 0.075	0.8079	1.0000
	15%	0.8170 ± 0.0031	1.912 ± 0.052	0.8040	1.0000
	25%	0.8011 ± 0.0085	0.837 ± 0.023	0.7927	1.0000

[1]Initial porosity measured with the height of the powder bed obtained on the onset of compaction process from the NEXYGEN Plus software

"Out of die" Kawakita model results

Figure 3.22 and Figure 3.23 shows the "out of die" Kawakita plot with the dimension of the EFB compost compact pellets measured immediately after the ejection and after prolonged storage. Excellent fit was obtained for the "out of die" results, demonstrated by the high value of R^2 from the linear regression fit within the full pressure range studied (Table 3.6 and Table 3.7). Comparison between the "in die" and "out of die" Kawakita showed similar trend for these two methods, where the constant $\frac{1}{b}$ decreased with the increase moisture content. However, the "out of die" method produced elevated values of $\frac{1}{b}$ when measured after ejection and elevated further with prolonged storage.

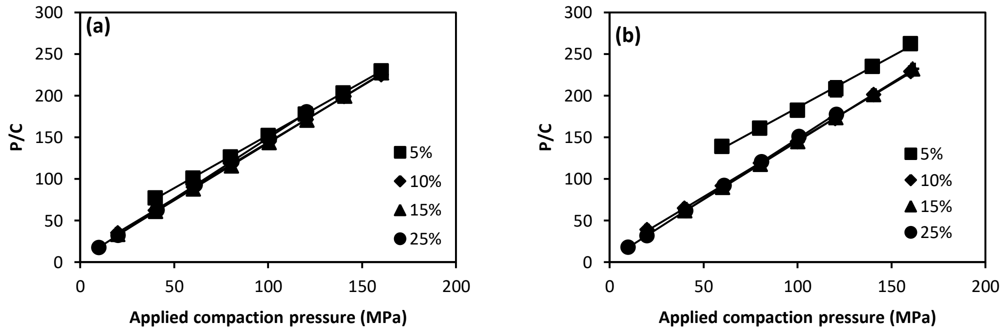

Figure 3.22: "Out of die" Kawakita plot for EFB compost powder with particle size of 150-300 µm and various moisture contents measured (a) after ejection, and (b) after prolonged storage. Values in legend indicate the initial moisture content of the pellet.

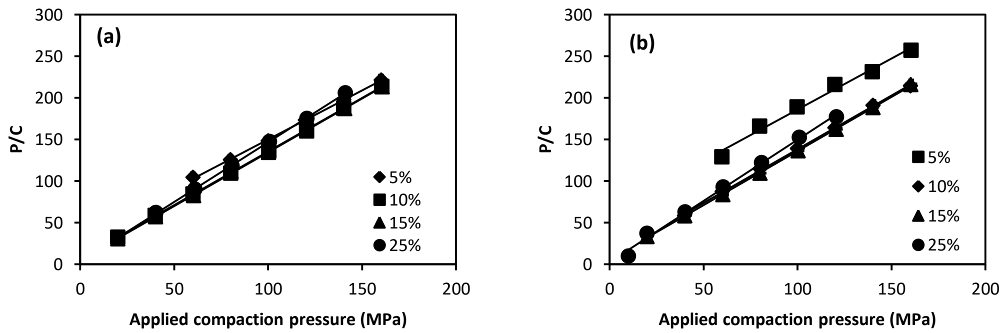

Figure 3.23: "Out of die" Kawakita plot for EFB compost powder with particle size of 300-600 µm and various moisture contents measured (a) after ejection, and (b) after prolonged storage. Values in legend indicate the initial moisture content of the pellet.

Table 3.6: Calculated "out of die" Kawakita model parameter for EFB compost with particle size of 150-300 μm

Measurement method	Moisture content (% w.b)	*a*	*1/b*	Initial porosity	R^2
After ejection	5%	0.7862	19.883	0.7731	0.9998
	10%	0.7379	6.197	0.7615	1.0000
	15%	0.7252	3.817	0.7560	0.9998
	25%	0.6840	2.028	0.7558	0.9999
After storage	5%	0.8136	51.082	0.7731	0.9997
	10%	0.7390	8.011	0.7615	0.9998
	15%	0.7146	3.772	0.7560	0.9998
	25%	0.6887	2.183	0.7558	0.9998

Table 3.7: Calculated "out of die" Kawakita model parameter for EFB compost with particle size of 300-600 μm

Measurement method	Moisture content (% w.b)	*a*	*1/b*	Initial porosity	R^2
After ejection	5%	0.8495	27.408	0.7996	0.9992
	10%	0.7770	5.331	0.8079	0.9999
	15%	0.7738	4.175	0.8040	0.9997
	25%	0.6994	2.433	0.7927	0.9999
After storage	5%	0.8159	51.614	0.7996	0.9870
	10%	0.7752	7.229	0.8079	0.9992
	15%	0.7690	4.608	0.8040	0.9997
	25%	0.6798	1.680	0.7927	0.9957

A comparison between the "out of die" and "in die" Kawakita plot is illustrated in Figure 3.24 which is based on the example of EFB compost powder with 5% moisture content and 150-300 μm particle size. The "out-of-die" data points were shifted toward a higher value of $\frac{P}{C}$ when compared to the "in die" plot. This could probably due to the increased pellet compact volume due to the elastic recovery of the compact. The shift was noticeably greater for dry EFB compost than for highly moisturised EFB compost powder. In addition, the "out of die" method showed significant discrepancy between the value constant a and the measured initial porosity for the EFB compost powder. In contrast with the "in die" method, the constant a obtained from the "out of die" method underestimated the measured initial porosity of the EFB compost powder. Comparisons based on this constant therefore must be approached with caution.

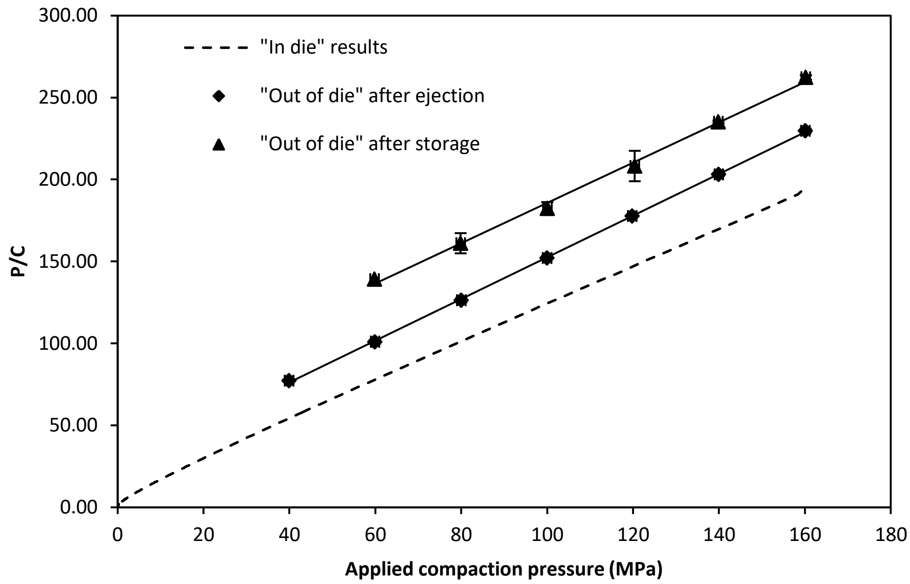

Figure 3.24: Comparison of the "in die" and "out of die" Kawakita plot for EFB compost powder with 5% moisture content and 150-300 μm particle size

3.6 Conclusions

This study shows that the physical property of the EFB compost powder such as particle size and moisture content could affect the compaction behaviour of the powder. The porosity of the EFB compost pellet decreased with the increase of applied compaction pressure, and the degree of compaction was found to be influenced by the moisture content and particle size. Negative porosity was observed during the compaction process and was due to the mechanical dewatering of the compact at high compaction pressure. This led to the sudden decrease of coefficient of friction during compaction. The porosity was found to be increased when the pellet compact was ejected out from the die and increased further with prolonged storage. The degree of change in porosity corresponded to the elastic recovery which was found to be affected by the applied compaction pressure, the moisture content and the particle size of the EFB compost powder.

The Heckel model and the Kawakita model was used to study the compactability of the EFB compost powder. Both “in die” and “out of die” results of the Heckel and Kawakita models were compared. Among the two compaction models, the Kawakita model provided the best fit with the compaction data of all material studied. Reasonable fit was obtained for both “in die” and “out of die” Heckel model, however the linear fit was limited within pressure range before mechanical dewatering occurred at high compaction pressure. In contrast, the Kawakita model seems more robust and less sensitive towards the effect of mechanical dewatering at high moisture content. Both models suggest that the compactability of the EFB compost powder increased with the increase in moisture content. However, no conclusive remark can be drawn for the change in particle size due to conflicting result between Heckel and Kawakita model. Nonetheless, the yield pressure P_y from the Heckel model was consistently higher than the Kawakita constant $\frac{1}{b}$ which suggest the compaction behaviour of the EFB compost powder was primary due to the particle arrangement and elastic deformation. The difference in between the “in die” and “out of die” result was observed and corresponds to the material elasticity.

CHAPTER 4:
PROPERTIES OF EFB COMPOST PELLETS

4.1 Introduction

Composting is one of the most effective way to reduce palm oil industrial biomass wastes where the palm oil empty fruit bunches are converted into organic fertilisers that are beneficial for the plant growth (Mohammad et al. 2012). However, the empty fruit bunch composts are heavily moisturised and inherently bulky, therefore unsuited to be utilised in its original form. The empty fruit bunch composts can be further processed into pellets through the densification process by means of applying mechanical pressure. Densification decreases the bulk volume of the empty fruit bunches compost while maintaining the net nutrient content. Because of its reduced shape and sizes, pelleted compost can be easily handled and requires lesser amount of storage.

Mechanical strength is one of the important criteria in determining the quality of the biomass compost pellets. Weak pellets may breakdown easily during storage and handling causing inefficiency in transportation. Organic fine dust may constitute a health risk for those who handle the pellets. The strength properties of the pellets can be identified by two distinct parameters, such as hardness, defined by the force necessary to crush the pellet, and durability, which defined by the amount of fines produced by the pellets after being subjected to external agitation (Thomas and van der Poel 1996).

The mechanical strength of the biomass pellets may vary depending on the processing conditions and the input material characteristics. These variables can be adjusted for optimal production efficiency and to improve the quality of pellets. To date, various author have studied the effect of processing parameters and material properties on the mechanical strength of biomass pellets produced with crop residues (Lai et al. 2013; Carone et al. 2011; Kaliyan and Morey 2009; Shaw 2008; Andrejko and Grochowicz 2007; Mani et al. 2006a), wood residues (Nielsen, Gardner, et al. 2009; Rhén et al. 2005), or municipal solid wastes (Zafari and Kianmehr 2013).

Studies have found that the increased applied compaction pressure and the use of material with smaller particle size reduces porosity and consequently increases the mechanical strength of the biomass pellets (Lai et al. 2013; Zafari and Kianmehr 2013). Other studies have found that the increased moisture content improves the physical quality of herbaceous biomass pellets (Kaliyan and Morey 2009; Andrejko and Grochowicz 2007); but detrimental to the strength of the pellet produced with wood residues (Nielsen, Gardner, et al. 2009; Rhén et al. 2005). However, research in the densification of composted empty fruit bunches is very limited. Previous studies on the densification of palm oil wastes conducted by Lai et al. (2013) and Husain et al. (2002) may differ due to difference in chemical composition which may affect the densification process (Tumuluru, Wright, Kenny, et al. 2010). Presence of soluble salt content in the empty fruit bunch compost (Agnew and Leonard 2003) may recrystallise in the event of dehydration and potentially promotes bonding between particles and subsequently giving strength to the compost pellets (Pietsch 2008).

Another aspect of compost pellet quality is the capability to maintain constant supply of nutrients within the plant root zone for a desired period of time (Friedman and Mualem 1994). Pelletisation may allow steady release of nutrient as the compost pellets disintegrate and release nutrient slower than the ordinary compost (Hara 2001). Hara (2001) reported that crops that receive pelleted manure compost generally have better yield when compared with ordinary unprocessed compost. The nutrient content in the composts and the release patterns of the organic nutrient vary with the material used for composting. For example, nutrient release rate of the dairy cattle wastes is reportedly slower than the poultry and swine waste due to high fibre content of dairy cattle wastes (Yan et al. 2001).

There was, however, limited study on the nutrient release patterns of pelleted compost derived from lignocellulosic material such as the palm oil empty fruit bunch. Studies that evaluate the effect of pellet processing conditions and material characteristics on the nutrient release patterns of the compost pellets have not been reported. However, it is known that the compaction pressure, particle size and moisture content can affect the release behaviour of the tablets as reflected in the various pharmaceutical studies (Chu et al. 2012; Sun 2012; Chowhan et al. 1982;

Khan and Rhodes 1972). Therefore, the nutrient release patterns of the compost pellets may behave similarly to the conditions involved in the processing the pharmaceutical tablets.

Several studies have conducted on the nutrient release patterns from the biomass compost based on the field experiments (Yan et al. 2002, 2001; Hara 2001; Jakobsen 1996). However, there is lack of studies in laboratory method that allows quick estimation of nutrient release patterns of biomass compost. Field experiments requires long duration of studies, i.e. 180 sampling days (Yan et al. 2001). In addition, consideration of complex variables such as time, temperature, soil, moisture, biological and other conditions may cause difficulties in correlation studies (Sartain et al. 2004). Although, laboratory methods may not be able to predict the actual field release, the laboratory method can be used for quick comparison of nutrient release pattern between the compost pellets (Carson and Ozores-Hampton 2012).

In this chapter, the effect the applied compaction pressure, moisture content, particle size and also the influence of storage on the physical strength of EFB compost pellets was investigated. In addition, the nutrient release behaviour of the EFB compost pellets was studied based on a rapid laboratory methodology using temperature-controlled incubation method (TCIM).

4.2 Materials and Methods

4.2.1 Pellet preparation

A universal tensile-compression testing machine (Lloyd LR10K, UK) with a load cell of 10 kN was used to produce pellets for compression testing. An instrumented die comprising an aluminium alloy 6061 cylindrical body, a detachable brass backstop, and a brass top piston that was in contact with the testing machine crosshead was used to make the pellets. The die channel was cylindrical with a diameter of 8 mm.

To produce the pellets, a nominal weight of 0.35 g of the empty fruit bunch compost powder was manually added into the die cavity with the backstop placed beneath the die. The machine crosshead was actuated downward to displace the top piston and compact the compost powder. The load on the top punch was released immediately after the maximum compaction was achieved. The backstop was removed immediately thereafter, and the crosshead-piston actuated downward to eject the pellet out from the die.

The compaction forces were varied from 1 kN to 10 kN, which corresponds to the compaction pressures of 10 MPa to 160 MPa. A crosshead speed of 30 mm/min was used during the compaction and ejection of the pellets.

4.2.2 Mechanical strength test

The physical characteristics of the produced pellets were tested in two separate conditions: green condition where the pellet was tested immediately after ejection, and cured condition where the pellet was tested after a week of storage in a glass desiccator with constant relative humidity of 43% in room temperature. This was achieved by using saturated potassium carbonate solution.

The weight of each pellet was measured before the strength test using an analytical balance (Mettler Toledo, Switzerland) with the resolution of 0.1 mg. The dimension of the pellets was measured using a digital vernier calliper (Mitutoyo, Japan) with the precision of 0.01 mm. In addition, the water activity level of the pellets was analysed using a water activity meter (Aqualab Lite, Decagon, US).

Axial compressive strength test was not conducted as preliminary experiments have established that the pellets showed no cracking behaviour when compressed axially, and instead it squeezed in between the platens like a paste. This tended to produce high scatter predominantly for pellets with high moisture content. Also, it has been established that the biomass pellets are more likely to fail in diametrical compression (Lai et al. 2013). For this reason, the mechanical strength tests were conducted by crushing the pellet diametrically in between two polished steel platens of the same universal tensile-compression testing machine (Lloyd LR10K, UK). The pellet to be tested was placed on the fixed base of steel platen with the diametrical axis parallel to the direction of the crushing force (see Figure 4.1). The top steel platen which is affixed to the crosshead was gradually lowered at a compression speed of 10 mm/min until the pellet was fractured.

The diametrical compressive strength was calculated by the following equation (Fell and Newton 1970):

$$\sigma_T = \frac{2F}{\pi D_p L} \tag{4.1}$$

where F is the crushing force when the pellet breaks.

The pellet strain ϵ was calculated as:

$$\epsilon = \frac{\Delta D}{D_p} \tag{4.2}$$

where ΔD is displacement of the crosshead relative to the pellet original diameter D_p.

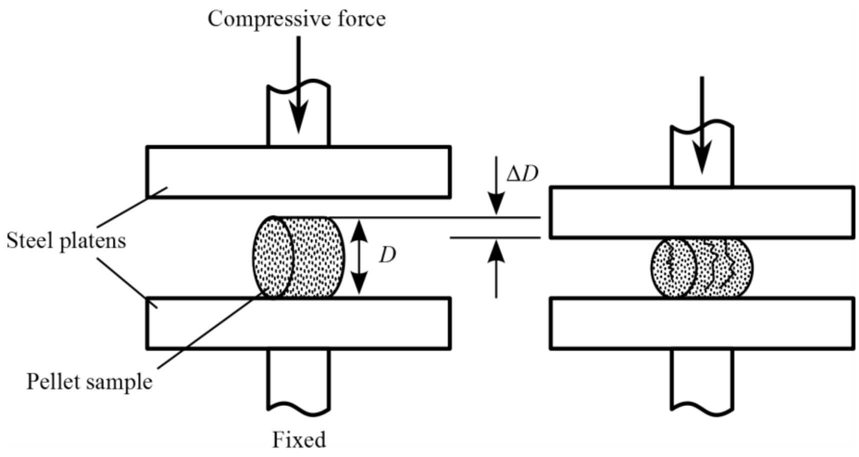

Figure 4.1: Schematic diagram for crushing of pellet in diametrical direction

4.2.3 Nutrient release tests

Nutrient release tests were performed in laboratory using temperature-controlled incubation method (TCIM) by submerging a beaker containing the compost pellets and 100 ml of distilled water at constant temperature (Carson and Ozores-Hampton 2012). The beaker with a magnetic stirrer bar was placed on top of a magnetic stirrer (IKA RET basic, Germany), which was set to give a temperature of 30°C inside the beaker with temperature fluctuation of ±1°C and agitation speed at 150 rpm.

Schematic diagram of the experimental setup is depicted in Figure 4.2. Preliminary experiment had established that simply dropping the pellet into the water tend to give irreproducible results, presumably because some of the pellets tend to float and disintegrated immediately due to trapped air inside the pellets. Therefore, a polyethylene and polypropylene filter bag was used to contain the compost pellet and was carefully submerged into the water to ensure that no air was trapped inside.

The released nutrient from the pellets was measured using a conductivity meter (Mettler Toledo SevenMulti, Switzerland) as measured conductivity provides an indication of total dissolved salt or electrolyte content released from the compost (Agnew and Leonard 2003). The conductivity meter was coupled with a computer, with the corresponding software package LabX direct pH (Mettler Toledo, Switzerland, version 3.3), measuring at the 3 second sampling interval for a minimum period of 10 minutes. The nutrient release test was conducted in three replicates for each parameter.

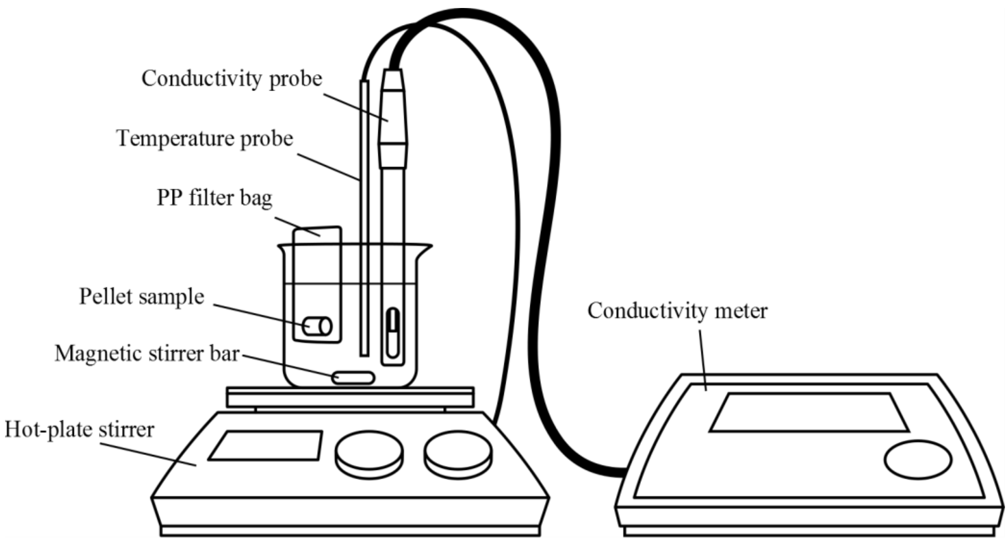

Figure 4.2: Schematic diagram of the kinetic release experimental setup

4.2.4 Analysis of kinetic release data

In this study, the kinetic release model developed by Spiro and Siddique (1981) was used to investigate the release pattern of the EFB compost pellets. This model was originally expressed for the kinetic studies of tea and coffee infusion, which was used to predict first order behaviour and analyse the concentration data. The kinetic model is expressed as:

$$\ln\left(\frac{c_\infty}{c_\infty - c}\right) = k_{obs}t + \alpha \tag{4.3}$$

Where c_∞ is concentration at equilibrium, c is concentration at time t, k_{obs} is the observed rate constant and α is the model constant. The experimental data obtained from the conductivity meter was used to fit into the kinetic model from Equation (4.3) to estimate k_{obs} using least square fitting with Microsoft Excel.

4.2.4.1 *Determination of concentration equilibrium constant c_∞*

Due to large variation in the final weight of the pellets, the concentration equilibrium constant c_∞ was separately determined prior to the nutrient release test. Compost powder of various weights ranging from 0.1 g to 0.4 g diluted with 100 ml distilled water, and allowed to equilibrate in a period of 5 days in a sealed glass container. The concentration equilibrium constant was reported in terms of electrical conductivity, measured using the same conductivity meter. The measured conductivity at equilibrium was plotted against the sample weight to water volume ratio, and a linear equation was obtained after regression analysis of the obtained data. The concentration equilibrium released by the pellets is calculated using this linear equation.

4.3 Results and discussion

4.3.1 Mechanical properties

The EFB compost powders were compacted at eight different compaction pressures (20, 40, 60, 80, 100, 120, 140, and 160 MPa) and the pellets were evaluated immediately after the ejection and 7 days after the being stored in a constant relative humidity chamber of 43%. Table 4.1 shows the physical changes of the EFB compost pellets before and after a week of curing in a constant relative humidity of 43%. Large deviation in measurements were observed for pellets with 5% and 10% moisture content due to formation of unstable pellets made with low compaction pressure, therefore omitted from the results. It appears that all of the pellets with different moisture content achieved an average constant water activity of 0.556 after a week of equilibration. EFB compost pellets with initial moisture content of 25%

exhibited the highest weight loss after equilibration, followed by 15% and 10%. Pellets with 5% initial moisture content however, increased in weight. It has been observed that moisture content of biomass material is dependent on the material, relative humidity, and temperature of surrounding atmosphere (Singh 2004). There was no observable difference between two particle sizes in terms of weight changes.

The mean volume change after storage varied widely depending on the initial moisture content and particle sizes. The mean volume change after storage was found to decrease with the increase of initial moisture content for EFB compost pellets with 150-300 μm. The EFB compost pellets with larger particle size 300-600 μm exhibited larger change in volume after storage probably due to the weaker bonding strength resulted from the smaller surface area for bond formation.

Table 4.1: Physical changes of EFB compost pellets after a week storage

Particle size (μm)	Initial moisture content	Initial water activity (a_w)	Final water activity (a_w)	Mean volume change after storage (%)	Mean weight change after storage (%)	Mean porosity change after storage (%)
150 - 300	5%	0.211 ± 0.017	0.556 ± 0.005	32.48 ± 6.10	2.09 ± 0.76	47.62 ± 7.12
	10%	0.733 ± 0.020	0.555 ± 0.004	3.72 ± 1.63	-3.93 ± 0.66	27.16 ± 6.58
	15%	0.804 ± 0.011	0.557 ± 0.011	2.82 ± 1.09	-5.99 ± 0.94	45.53 ± 7.91
	25%	0.901 ± 0.006	0.547 ± 0.015	0.48 ± 2.10	-16.49 ± 0.68	48.01 ± 12.04
300 - 600	5%	0.213 ± 0.012	0.559 ± 0.009	40.13 ± 7.25	0.44 ± 1.19	47.55 ± 8.28
	10%	0.747 ± 0.013	0.546 ± 0.006	8.801 ± 2.81	-4.07 ± 1.68	21.72 ± 5.20
	15%	0.799 ± 0.014	0.571 ± 0.011	3.87 ± 1.82	-6.59 ± 0.47	33.41 ± 6.16
	25%	0.906 ± 0.006	0.558 ± 0.006	7.55 ± 3.46	-16.03 ± 0.60	46.12 ± 4.66

4.3.1.1 *Stress strain curve*

Figure 4.3 to Figure 4.6 shows the stress-strain curve of pellets measured from the diametrical compression tests. The stress-strain curves correspond to the pellets produced with different compaction pressure compressed immediately after ejection and after a week of storage is shown. The pellets exhibited a gradual increase in stress at low strains, followed by a small region of linear increase in the stress-strain curve and gradually plateauing before the pellets fractured.

The pellets had different initial modulus and peak strength depending on the initial moisture content, particle size, compaction pressure, and storage. The initial modulus as indicated by the slope of the linear region of the stress-strain curve slope appears to increase with the increase of compaction pressure. However, the slopes seem to coincide after a certain compaction pressure, evidently for pellets with higher moisture content. The behaviour on the stress-strain curves suggests that the initial modulus of the pellets plateaued at high compaction pressure and which appears to correspond to the plateau in pellet porosity during the compaction process.

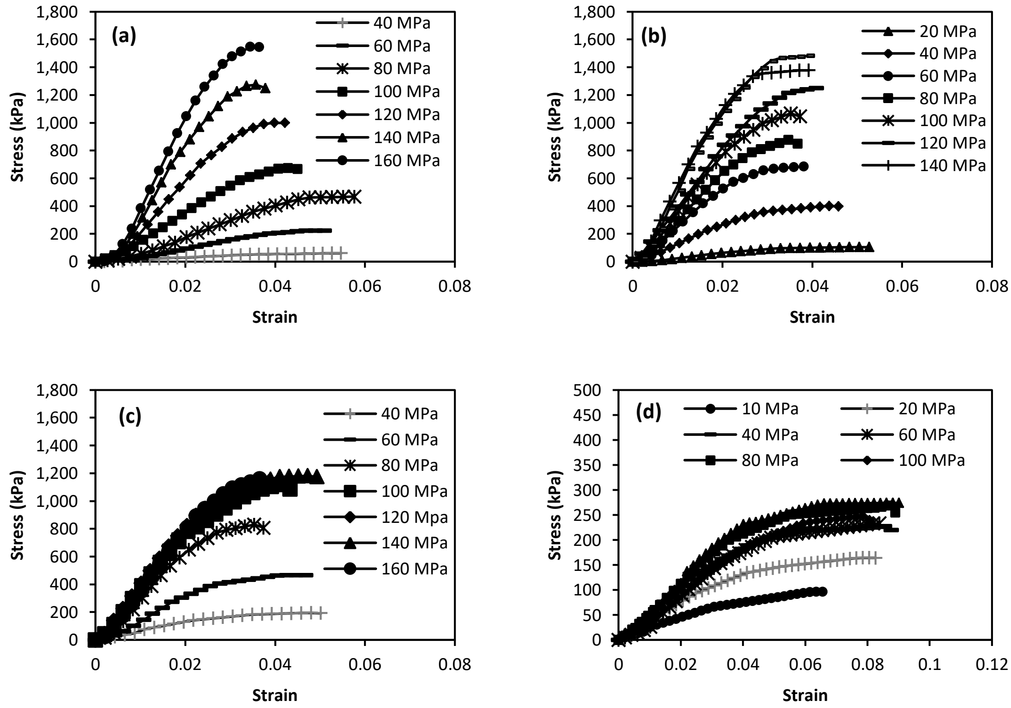

Figure 4.3: Stress-strain curve for EFB compost pellets with 150-300 µm particle size and moisture content of (a) 5% (b) 10% (c) 15% and, (d) 25% tested immediately after ejection. The numbers in legend indicate the applied compaction pressure.

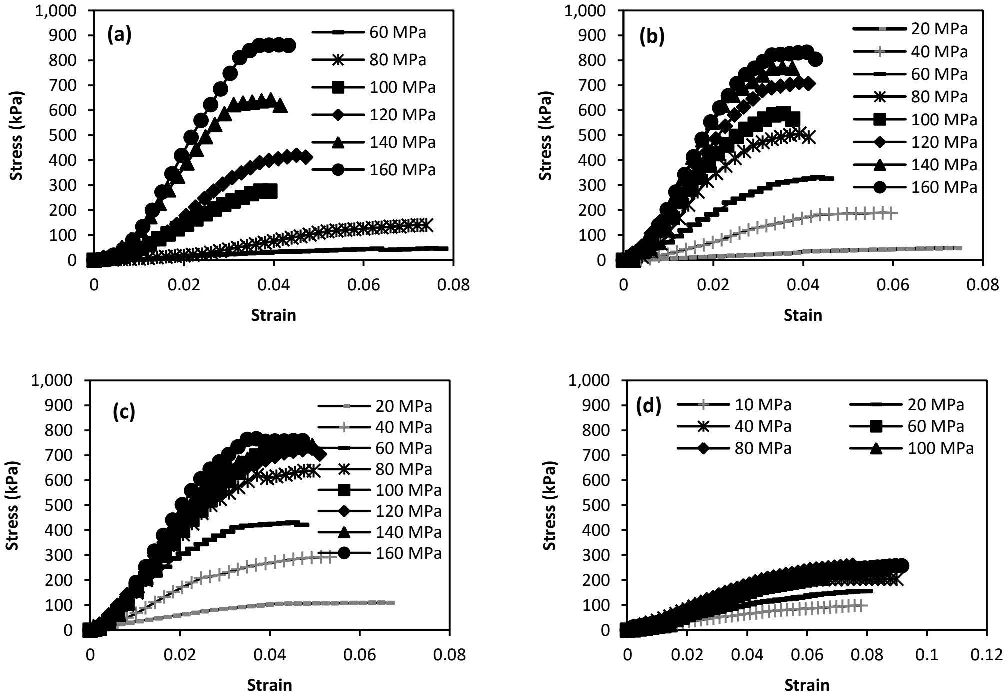

Figure 4.4: Stress-strain curve for EFB compost pellets with 300-600 µm particle size and moisture content of (a) 5% (b) 10% (c) 15% and, (d) 25% tested immediately after ejection. The numbers in legend indicate the applied compaction pressure.

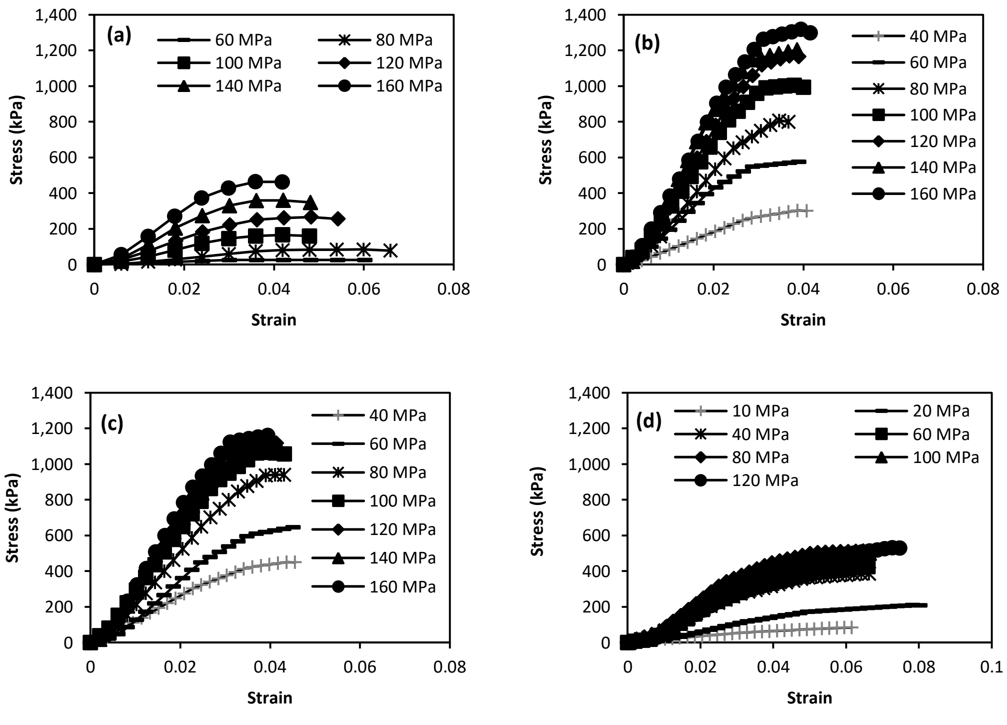

Figure 4.5: Stress-strain curve for EFB compost pellets with 150-300 µm particle size and moisture content of (a) 5% (b) 10% (c) 15% and, (d) 25% tested after 1 week storage. The numbers in legend indicate the applied compaction pressure.

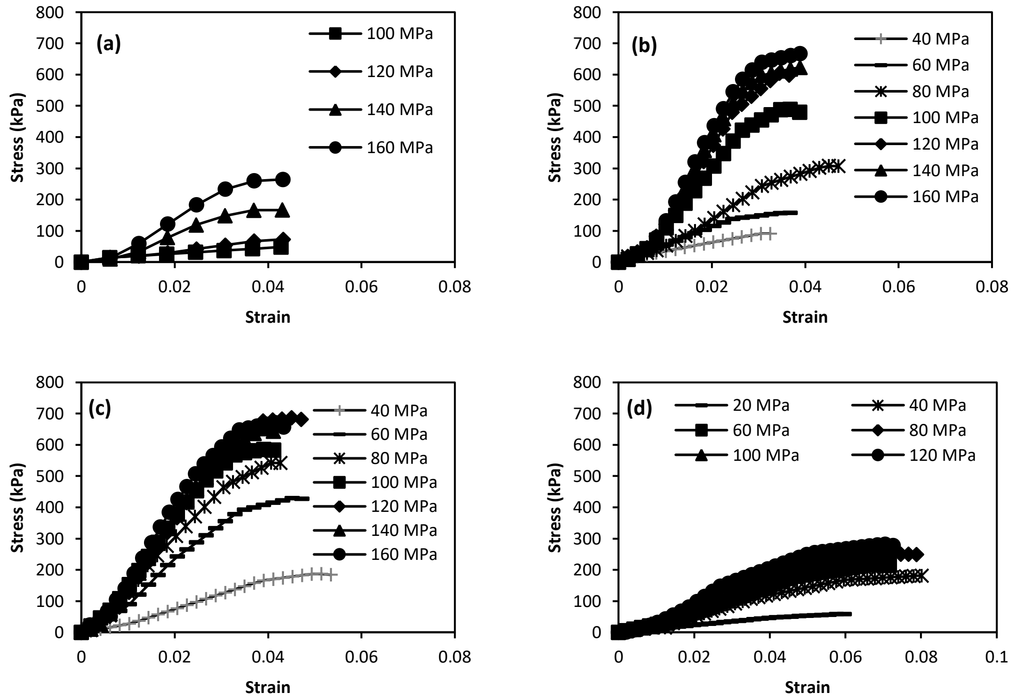

Figure 4.6: Stress-strain curve for EFB compost pellets with 300-600 μm particle size and moisture content of (a) 5% (b) 10% (c) 15% and, (d) 25% tested after 1 week storage. The numbers in legend indicate the applied compaction pressure.

4.3.1.2 *Diametrical compressive strength*

Figure 4.7 shows the relationship between the diametrical compressive strength and compaction pressure with different moisture content and particle size, corresponding to the condition of the pellets tested. Similar to the behaviour of initial modulus, an increase in diametrical compressive strength with increasing compaction pressure may be seen, but appears to reach a plateau after a certain compaction pressure. The maximum diametrical compressive strength was largely affected by the initial moisture content of the pellets. Increasing the initial moisture content resulted in pellets with higher strength at lower compaction pressures but a lower maximum strength. Pellets with larger particle size exhibited comparatively lower diametrical compressive strength than the smaller particle size (Figure 4.8). Similar behaviour also has been observed in the study of Steendam et al. (2001) with pharmaceutical tablets.

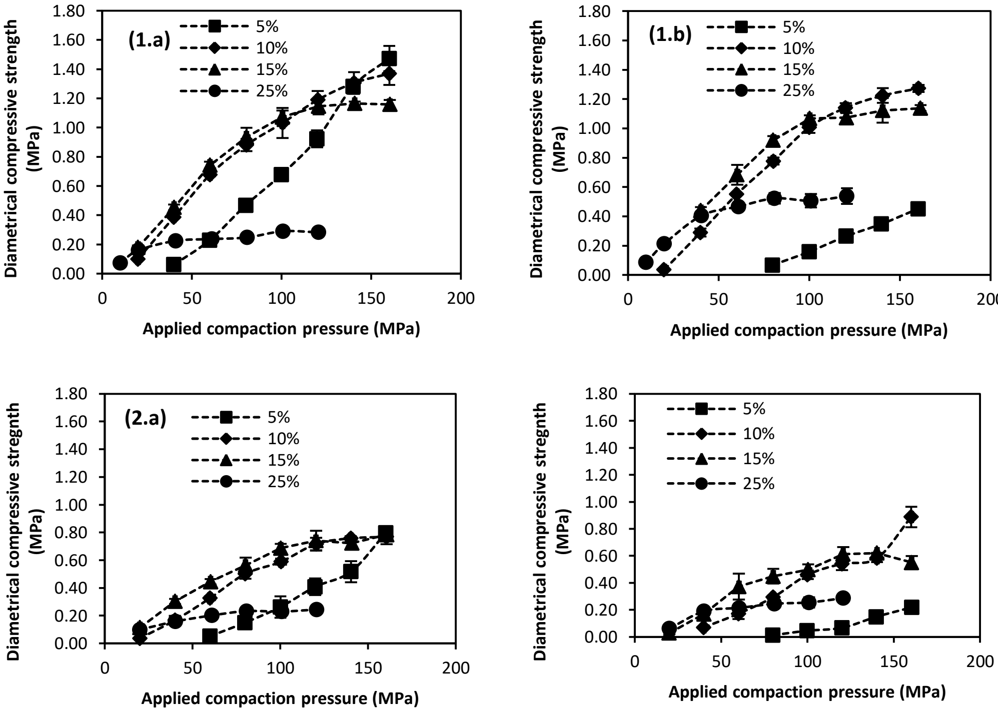

Figure 4.7: Relationship between the diametrical compressive strength pellets and the applied compaction pressure with different moisture content. Top row shows particle size of 150-300 µm measured (1.a) after ejection, and (1.b) after storage. Bottom row shows particle size of 300-600 µm measured (2.a)) after ejection, and (2.b) after storage. The numbers in legend indicate the initial moisture content of the pellets.

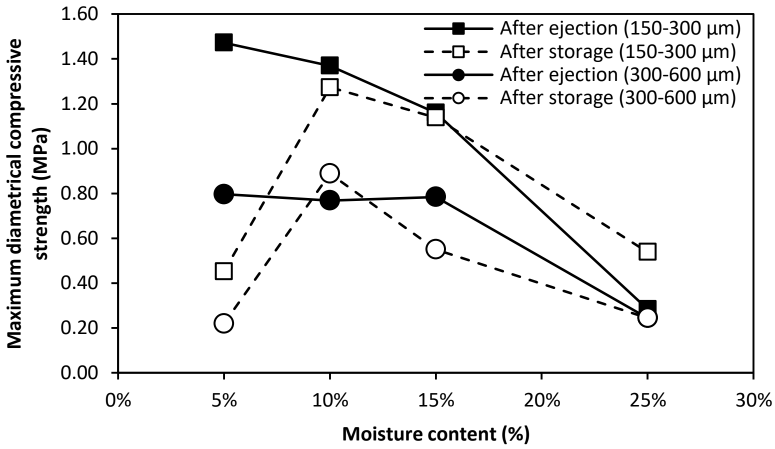

Figure 4.8: Relationship between maximum compressive strength and the initial moisture content of the compost pellets corresponding to the particle size and storage

The diametrical compressive strenght of the pellets also appears to be affected by storage and behaved differently with the initial moisture content and particle sizes. Figure 4.9 shows the relationship between the changes in the diametrical compressive strength after storage reported in percentage and the applied compaction pressure correspond to the initial moisture content. The pellets were stored in a constant relative humidity of 43%. The change in the diametrical compressive strength is calculated in reference to the initial compressive strength after ejection. A negative change in compressive strength was observed and the value is reduced with increasing compaction pressure and increasing moisture content for both particle sizes. Pellets with coarser particle size exhibited significant change in compressive strength in comparison with pellets with smaller particle size.

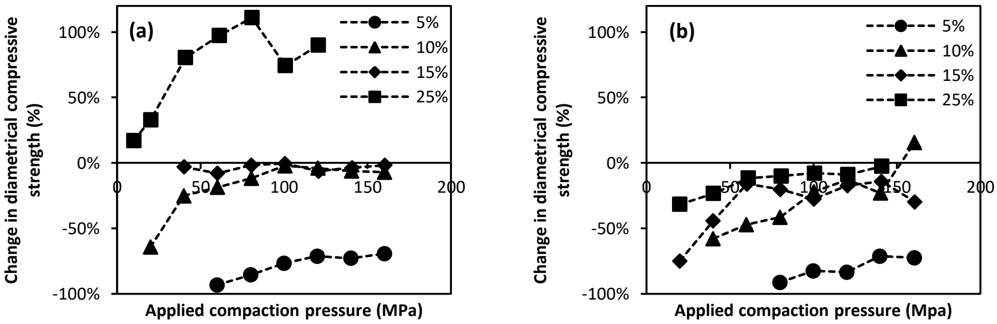

Figure 4.9: Change in diametrical compressive strength after storage for particle size of (a) 150-300 µm, and (b) 300-600 µm. The numbers in legend indicate the initial moisture content of the pellets.

Despite the increase in pellet porosity after storage (Table 4.1), some pellets exhibited no significant changes in strength. Pellets with initial moisture content of 25% for the particle size of 150-300 however, showed a significant increase in compressive strength after storage. Therefore, it is possible that there is new bond formation resulted from the prolonged storage dependent on the initial moisture content and particle sizes.

To further demonstrate the possibility of new bond formation after prolonged storage, the relationship between diametrical compressive strength and the pellet porosity corresponding to the storage was compared and this is shown in Figure 4.10 and Figure 4.11. It appears that the compressive strength increased after storage with consideration to the pellet porosity and appears to be dependent on the initial moisture content of the pellets. Pellets with 5% initial moisture content shows no significant difference in strength (Figure 4.10(a) and Figure 4.11(a)) which possibly indicates no new formation of inter-particulate bond. The bonding strength of the dry pellets largely depends on the inter-particulate attraction force such as the hydrogen bond, Van der Waals' force and mechanical interlocking bond (Kong et al. 2012). Such bond are too weak to resist the disruptive forces caused by the elastic recovery

(Kong et al. 2012) which resulted in increased porosity and consequently reduced pellet strength as no new bond was formed to strengthen the pellet.

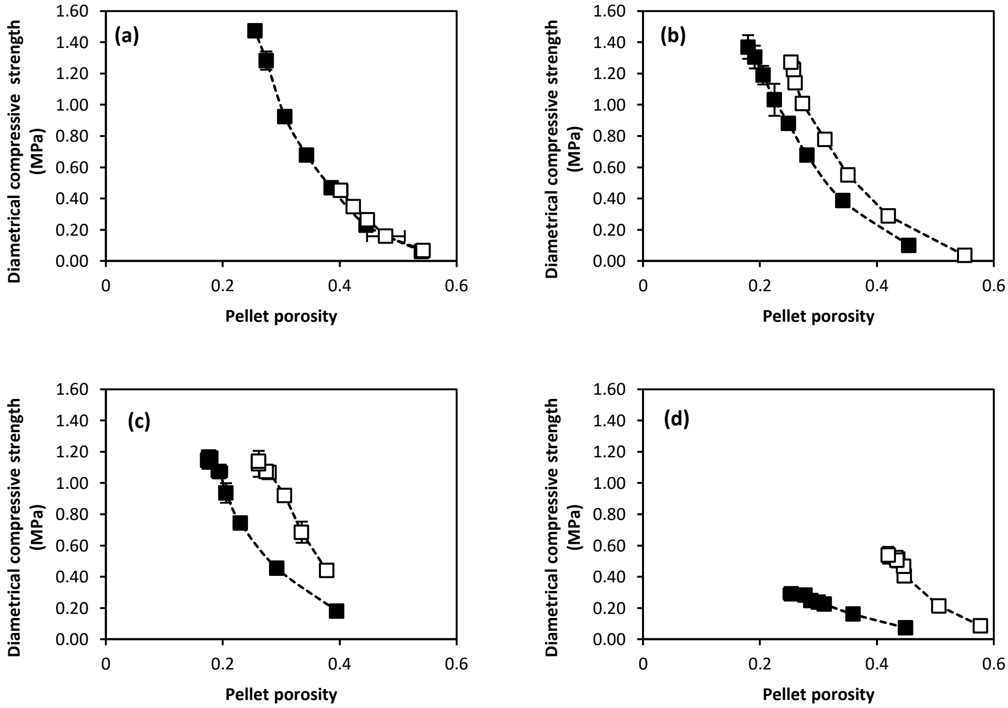

Figure 4.10: Comparison of diametrical compressive strength between pellets measured before storage (■), and after storage (□) against the pellet porosity with the moisture content of (a) 5%, (b) 10%, (c) 15% and, (d) 25% for particle size of 150-300 µm

Pellets with higher initial moisture content, however, showed a greater increase in diametrical compressive strength after storage, possibly due to the formation of solid bridges. The addition of moisture may dissolve some of the ingredient in the EFB compost such as palm oil mill effluent (POME) which contains high amount of soluble salt (Igwe and Onyegbado 2007). When pellets were stored in an environment with low relative humidity, the moisture evaporates and the dissolved salt may recrystallise and form solid bridges which strengthen the bond between particulates. The solid bridge bonds are strong enough to partially resist the disruptive force caused by the elastic recovery and therefore resulted in increased strength. This is evident in pellets with higher initial moisture content as seen in Figure 4.10 and Figure 4.11.

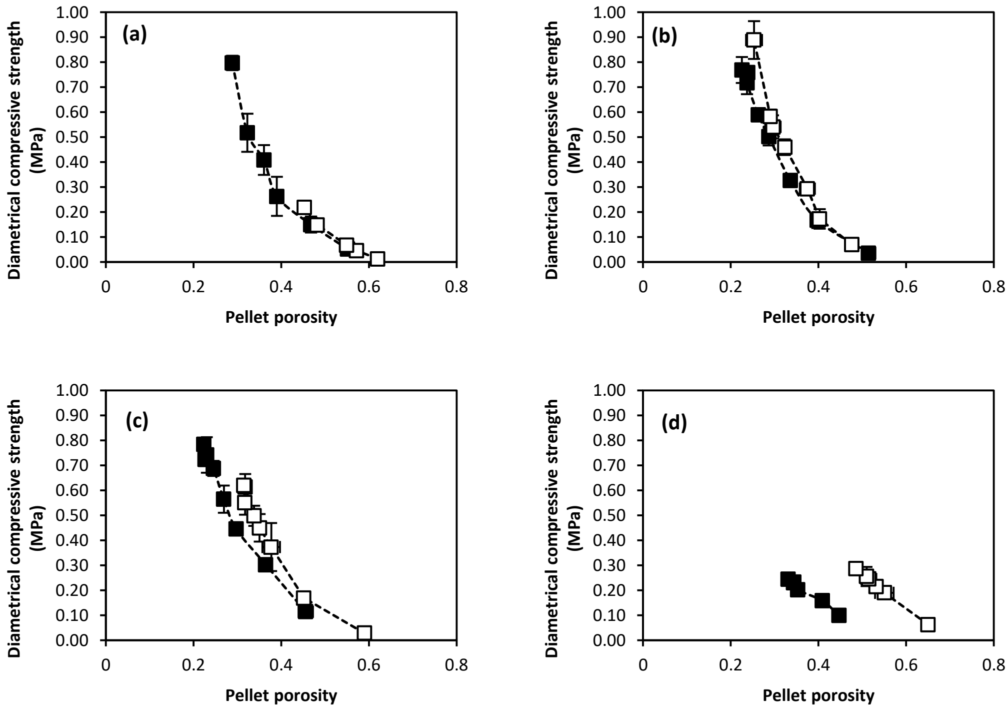

Figure 4.11: Comparison of diametrical compressive strength between pellets measured before storage (■), and after storage (□) against the pellet porosity with the moisture content of (a) 5%, (b) 10%, (c) 15% and, (d) 25% for particle size of 300-600 µm

The effect of solid bridge bond formation also appears to be dependent on the particle size of the pellets. Pellets that are produced with larger particle size exhibited minor increase in compressive strength with in consideration to the pellet porosity. This could be probably due to smaller contact area with large particle size that reduces the contact point available for the formation of solid bridges. Therefore, the limited bond site for solid bridge may lead to weaker bond formation which decreased the diametrical compressive strength of the pellets.

4.3.1.3 *Ryskewitch – Duckworth equation*

The diametrical compressive strength and porosity data of the pellets from Figure 4.10 and Figure 4.11 was fitted according to the Ryshkewitch – Duckworth equation (Duckworth 1953):

$$\ln \frac{\sigma_T}{\sigma_{T_0}} = -\eta\varepsilon \tag{4.4}$$

where σ_T is the diametrical compressive strength of the pellet, ${\sigma_T}_0$ is the diametrical compressive strength extrapolated at zero porosity, ε is the pellet porosity and η is a constant known as "bonding capacity". High values of η typically indicates strong bonding of particles (Van der Voort Maarschalk et al. 1996). This relationship was originally derived for "out-of-die" pellet porosity measured prior to the compression test. However, it can be seen that a plateau in compressive strength was attained despite the increase in applied compaction pressure, in which correspond to the zero or negative porosity during compaction as reflected in Figure 4.7. Goh et al. (2008) argues that comparing the pellets strength based on the final density or porosity can be misleading due to the differences in the degree of elastic recovery of pellets with different material property. The predicted value of ${\sigma_T}_0$ would have been overestimated when compared to the maximum compressive strength measured in the experiments. Therefore, Goh et al. (2008) proposed that comparison should be made using compacted density or the "in-die" porosity measurement which disregards the effect of elastic recovery of the pellets. This model has also been applied to the biomass material with palm oil kernel shell powders by Lai et al. (2013).

The values of η and ${\sigma_T}_0$ with the "in-die" porosity measurement were obtained by means of regression fit of linear region in $\ln \sigma_T$ *vs.* "in-die" porosity plot and were shown in Table 4.2 and Table 4.3. Some deviation of the data from the predicted linearity of Ryshkewitch – Duckworth equation is observed when the "in-die" compact porosity is above 0.2. In particular, pellets with 5% initial moisture content and 300-600 μm (Figure 4.12) exhibited deviation from the Ryshkewitch – Duckworth equation with the "in-die" compact porosity above 0.2 possible due to the rapid expansion of the pellets. The some of value of η and ${\sigma_T}_0$ could be overestimated as a result of the deviation. Similar deviations were reported for pharmaceutical compacts (Tye et al. 2005) and alumina compacts (Ryshkewitch 1953).

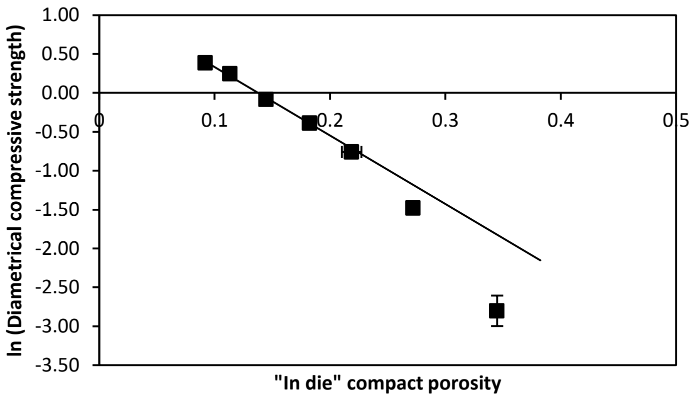

Figure 4.12: Example of deviation in Ryshkewitch – Duckworth plot. Solid line indicates the fitted Ryshkewitch – Duckworth to the linear region of the plot.

Table 4.2: Fit parameters of Ryshkewitch – Duckworth equation before storage

Particle sizes (µm)	**Initial moisture content (%)**	η	σ_{T_0}**(MPa)**	R^2
150-300	5	8.81	3.367	0.9947
	10	7.20	1.297	0.9834
	15	7.51	0.958	0.9955
	25	6.41	0.217	0.9976
300-600	5	13.97	4.145	0.9875
	10	7.07	0.823	0.9704
	15	6.94	0.673	0.9552
	25	7.29	0.187	0.9911

Table 4.3: Fit parameters of Ryshkewitch – Duckworth equation after storage

Particle sizes (µm)	**Initial moisture content (%)**	η	σ_{T_0}**(MPa)**	R^2
150-300	5	12.22	1.423	0.9827
	10	7.56	1.133	0.9987
	15	7.96	0.961	0.9924
	25	8.49	0.372	0.9898
300-600	5	18.55	1.567	0.9929
	10	9.24	0.524	0.9437
	15	8.25	0.502	0.9149
	25	10.27	0.180	0.9867

Results show that the bonding capacity and compressive strength at zero compact porosity decreased with increasing initial moisture content of the pellets for both particle sizes. Similar trend was observed in the study of Steendam et al. (2001) where the bonding capacity and tensile strength at zero porosity decreased with increasing moisture content. The compressive strength at zero compact porosity appeared to be decrease with larger particle size; however there were no discernible differences in bonding capacity between both particles sizes.

In addition, the effect of storage appears to have positive influence on the bonding capacity and the magnitude of increase is dependent on the initial moisture content of pellets. This further supports the assumption that solid bridge bonding may have formed with the recrystallization of dissolved salt resulted from the evaporation of moisture during storage. As a result, the compressive strength at zero compact porosity was seen to be increase with storage for pellets with higher moisture content.

4.3.2 Nutrient release

4.3.2.1 *Concentration equilibrium constant c_∞*

The EFB compost powders were placed in a distilled water with different weight to water ratio and the conductivity of the diffused nutrient were evaluated after incubation period of 5 days. For both compost powder with the particle size of 150-300 µm and 300-600 µm, plots of conductivity at equilibrium against the ratio of powder weight to water volume (Figure 4.13) were found to be in good linearity with the correlation coefficient R^2 greater than 0.995. It appears that the values c_∞ for particle sizes 150-300 µm was slightly higher than 300-600 µm. Slopes were calculated using least square method and were then used to determine the equilibrium conductivity of the pellets for the kinetic release analysis.

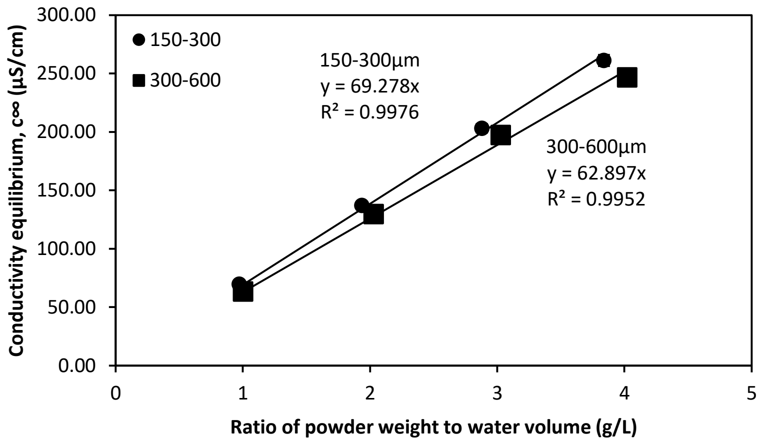

Figure 4.13: Conductivity at equilibrium for EFB compost powder with different particle sizes. Values in legend indicate the particle size range of the EFB compost powder.

4.3.2.2 *Nutrient release kinetic characteristics*

Figure 4.14 shows the changes in the size of an EFB compost pellets with time when soaked in water. First the water is quickly absorbed and followed by rapid expansion of the pellet. It can be seen from this image that the pellet expands in axial direction immediately when in contact with water. This suggests that the disintegration mechanism of EFB compost pellets is contributed mainly by the shape recovery of the deformed particles. During the compaction process, the shape of the powder particulate is permanently deformed, resulting in high-energy state of lignocellulosic natural polymer stabilised by the entangled polymer chains or local crystallisation (Quodbach et al. 2014). When the deformed particles come in contact with water, the water molecules enhanced the mobility of the natural polymer chains, and the particles return to their original shape. This would cause the pellets to expand in the opposite direction of the compaction force (Quodbach et al. 2014).

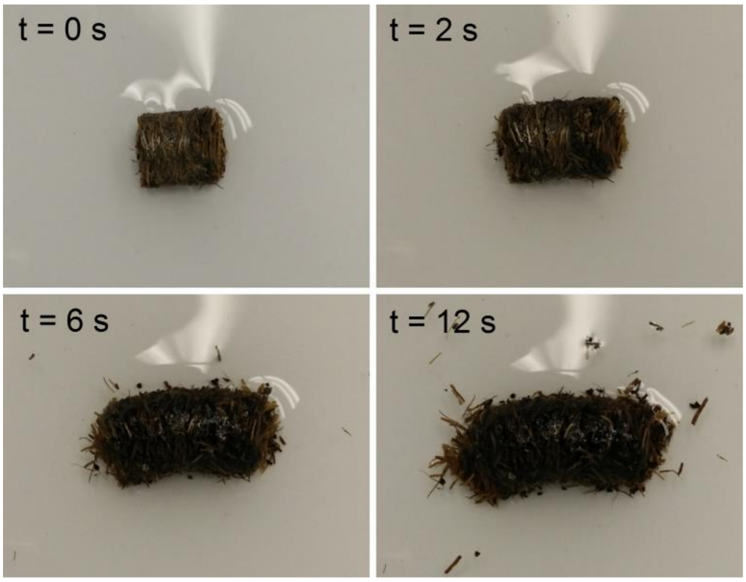

Figure 4.14: Changes in the size of an EFB compost pellets with time when soaked in water

For analytical evaluation of the EFB compost pellets nutrient release behaviour, the pellets with different initial moisture content, particle sizes and compaction pressure were prepared. The concentrations of the released nutrient were measured over time and the results are shown in Figure 4.15 and Figure 4.16. The curves represent the average of three repetitions and the error bars have been omitted for clarity. It appears that, for each of the nutrient release kinetic plots (Figure 4.15 and Figure 4.16), there is an initial time lag followed by a steep curve corresponding to high rate of diffusion. The disintegration of pellets possibly begins with wetting of surface and breaking of inter-particulate bonds, which correspond with slow diffusion rate in the initial stage. This may continue only for a relatively brief period of time until the pellets fully disintegrated from the shape recovery of particles, followed by rapid increase in conductivity with time. The nutrient release rate appeared to slow down as the conductivity reach toward the equilibrium value.

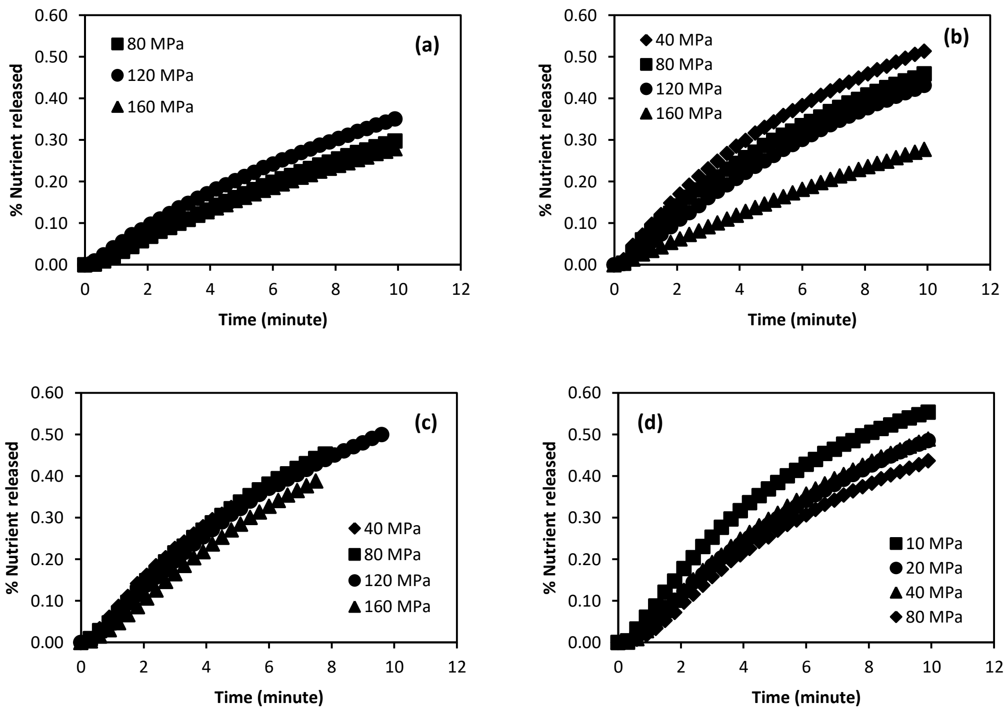

Figure 4.15: Kinetic release plot of EFB compost pellets with particle size of 150-300 µm and initial moisture content of (a) 5%, (b) 10%, (c) 15%, and (d) 25%. Values in legend indicate the applied compaction pressure.

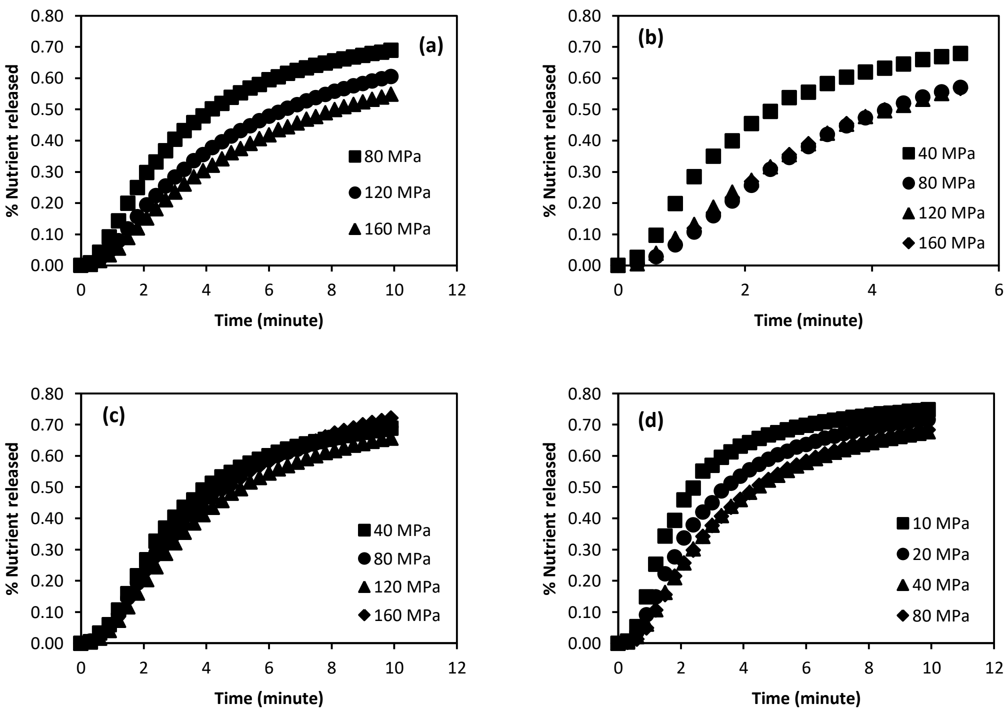

Figure 4.16: Kinetic release plot of EFB compost pellets with particle size of 300-600 µm and initial moisture content of (a) 5%, (b) 10%, (c) 15%, and (d) 25%. Values in legend indicate the applied compaction pressure.

4.3.2.3 *Nutrient release rate constant*

Further insight into the pellet diffusion process can be achieved by determining the rate constant from the first order kinetic plot with Equation (4.3). The nutrient release data of the EFB compost pellets from Figure 4.15 and Figure 4.16 were fitted into Equation (4.3). The plots of $\ln\left(\frac{c_\infty}{c_\infty - c}\right)$ against time appears to be in good linearity as can be seen in Figure 4.17 showing the least square plots, representing the diffusion of EFB compost pellets with different particle size and with initial moisture content of 25% compacted at 80 MPa. Similar plots were obtained for other initial moisture content, particle sizes and compaction pressure and the results are tabulated in Table 4.4.

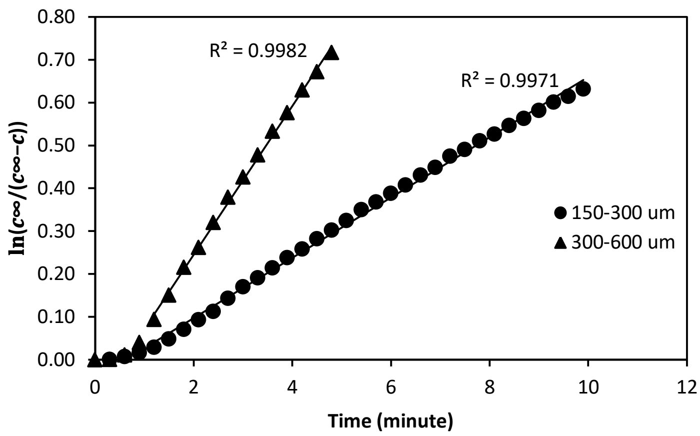

Figure 4.17: Typical plot of $\ln\left(\frac{c_\infty}{c_\infty - c}\right)$ against time for the diffusion of EFB compost pellets with initial moisture content of 25% compacted at 80 MPa.

Table 4.4: Rate constant for the diffusion of the EFB compost pellets

Particle size (µm)	Initial moisture content	Compaction pressure (MPa)	Stored porosity	Diametrical compressive strength (MPa)	Rate constant (min^{-1})
150 - 300	5%	80	0.543 ± 0.010	0.068 ± 0.010	0.034 ± 0.004
		120	0.448 ± 0.005	0.265 ± 0.013	0.040 ± 0.002
		160	0.401 ± 0.012	0.452 ± 0.022	0.032 ± 0.007
	10%	40	0.419 ± 0.008	0.289 ± 0.027	0.077 ± 0.003
		80	0.311 ± 0.002	0.777 ± 0.025	0.072 ± 0.034
		120	0.260 ± 0.007	1.142 ± 0.031	0.061 ± 0.016
		160	0.253 ± 0.004	1.273 ± 0.024	0.031 ± 0.003
	15%	40	0.379 ± 0.007	0.440 ± 0.023	0.077 ± 0.006
		80	0.306 ± 0.012	0.919 ± 0.028	0.082 ± 0.013
		120	0.272 ± 0.007	1.074 ± 0.032	0.076 ± 0.012
		160	0.257 ± 0.006	1.139 ± 0.021	0.067 ± 0.009
	25%	10	0.577 ± 0.005	0.086 ± 0.012	0.097 ± 0.031
		20	0.506 ± 0.005	0.213 ± 0.007	0.070 ± 0.004
		40	0.447 ± 0.006	0.406 ± 0.021	0.075 ± 0.019
		80	0.433 ± 0.014	0.523 ± 0.036	0.061 ± 0.011
300-600	5%	80	0.620 ±0.012	0.013 ± 0.002	0.191 ± 0.037
		120	0.549 ±0.006	0.068 ± 0.005	0.117 ± 0.012
		160	0.453 ±0.009	0.219 ± 0.035	0.097 ± 0.025
	10%	40	0.476 ±0.015	0.071 ± 0.004	0.324 ± 0.032
		80	0.375 ±0.017	0.294 ± 0.012	0.194 ± 0.009
		120	0.297 ±0.018	0.626 ± 0.125	0.189 ± 0.002
		160	0.253 ±0.018	0.888 ± 0.076	0.190 ± 0.013
	15%	40	0.452 ±0.005	0.169 ± 0.008	0.216 ± 0.059
		80	0.351 ±0.009	0.450 ± 0.055	0.192 ± 0.029
		120	0.318 ±0.010	0.613 ± 0.052	0.160 ± 0.029
		160	0.317 ±0.010	0.550 ± 0.048	0.170 ± 0.28
	25%	10	0.720 ±0.001	0.068 ± 0.002	0.359 ±0 .046
		20	0.641 ±0.021	0.121 ± 0.006	0.240 ±0. 018
		40	0.560 ±0.019	0.178 ± 0.012	0.185 ±0. 290
		80	0.513 ±0.015	0.212 ± 0.011	0.189 ±0. 027

Influence of compaction pressure and porosity

Figure 4.18 shows the plot of diffusion rate constant of EFB compost pellets against the applied compaction pressure. The diffusion rate constant appeared to be decreased with the increasing compaction pressure, however, plateaued at high compaction pressure. Lower diffusion rate constant indicates slower release of nutrient over time. With the increase in compaction pressure corresponding in the decrease of pellet porosity, more bonds were formed between the particles and the pellets strength are expected to be stronger. This can be clearly seen from Figure 4.19 where the decrease in pellet porosity resulted in the decrease of diffusion rate constant. High pellet porosity may have allowed greater water penetration such that the pellet may readily disintegrate when in contact with water. This is in accordance with previously published work on pharmaceutical tablet where that tablets with lower porosity showed slower disintegration time (Berry and Ridout 1950).

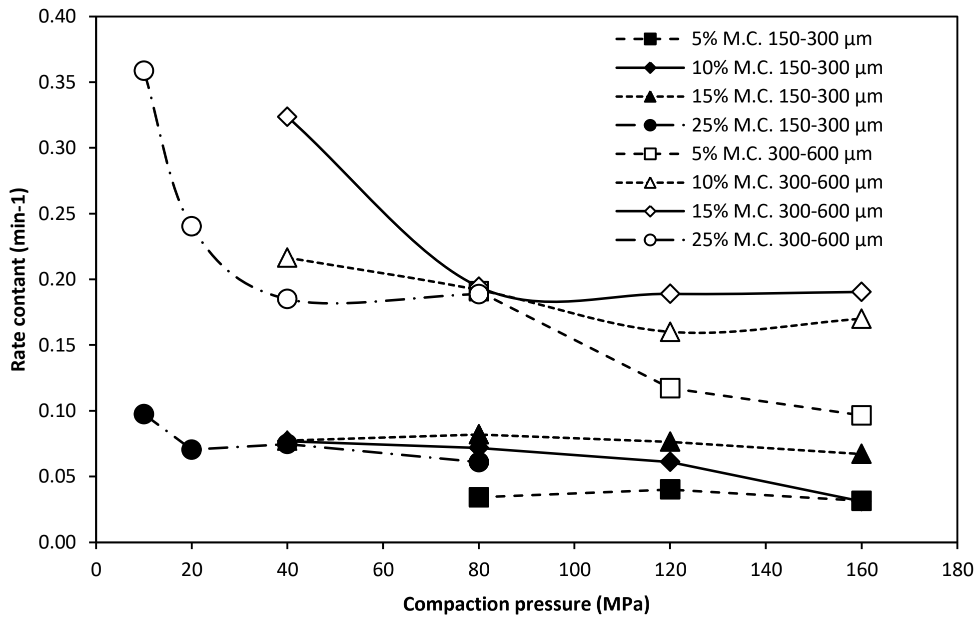

Figure 4.18: Effect of compaction pressure on the diffusion rate constant of EFB compost pellets

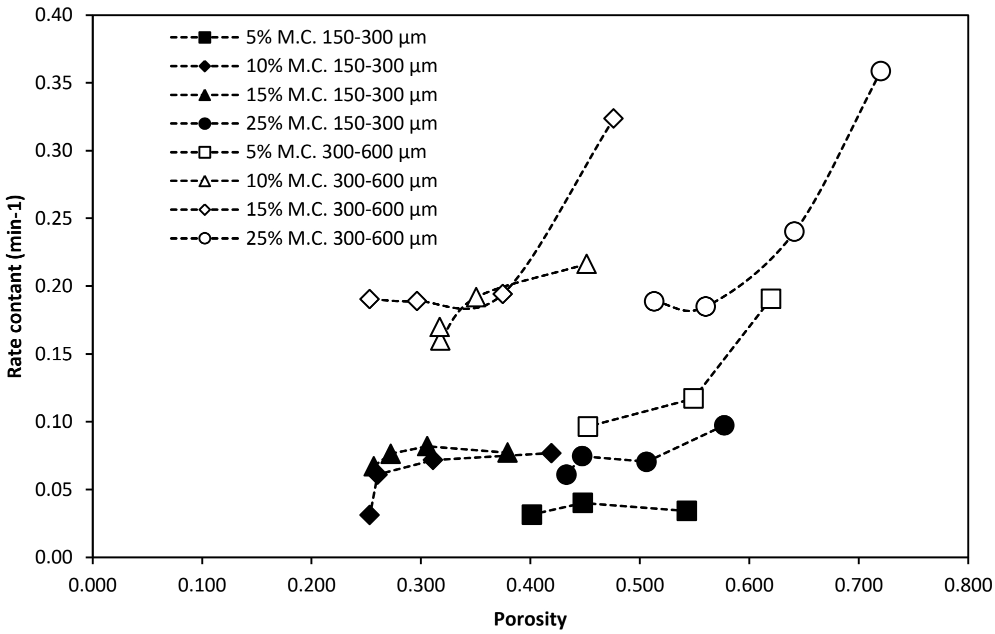

Figure 4.19 Effect of pellet porosity on the diffusion rate constant of EFB compost pellets

Influence of pellet strength

Interestingly, pellets with the higher porosity may not necessarily show a faster diffusion rate, evidently with pellets with particle size of 300-600 µm as illustrated in Figure 4.19. While the EFB compost pellets with 25% initial moisture content show a higher porosity value, the pellets diffused at a lower rate when compared to the pellets with initial moisture content of 15% with lower porosity value. It is apparent that the pellet porosity may not be the limiting factor for diffusion, but the bonding strength between particles that needs to be overcome for pellets to disintegrate. It is possible that formation of solid bridges, an inter-particulate bond within the pellets with higher initial moisture content contributed to the bonding strength of the pellets. The increased bonding strength limited the pellet disintegration and therefore lowers the diffusion rate. The bonding strength of the pellets can be described in terms of diametrical compressive strength and the values were obtained from the previous Chapter Section 4.3.1. Figure 4.20 shows a clear relationship between the pellet diametrical compressive strength and pellet diffusion rate constant. It appears that pellet diffusion rate constant decreased with the increased pellet diametrical compressive strength and reached a plateau at an approximate compressive strength above 0.2 MPa. There has been no significant difference observed in the diffusion rate constant with different moisture content in reference with their pellet strength. The combined counter effects of strong inter-particulate bond in opposition with the release of energy from the shape recovery of deformed particle may have limited the diffusion rate constant of the EFB compost pellets.

It is interesting to note that pellets with 5% initial moisture content showed significantly lower rate constant in comparison to the pellets with initial moisture content greater than 10%. It is possible that during the compaction process, some of the moisture may have expelled from the fibres, and then recrystallised on the fibre surface as the moisture evaporate. These expelled moistures may readily dissolve when in contact with water which therefore increases the diffusion rate of the nutrient. Pellets that are produced with low initial moisture content may diffuse slower as there could be no readily available moisture to dissolve on the fibre surface.

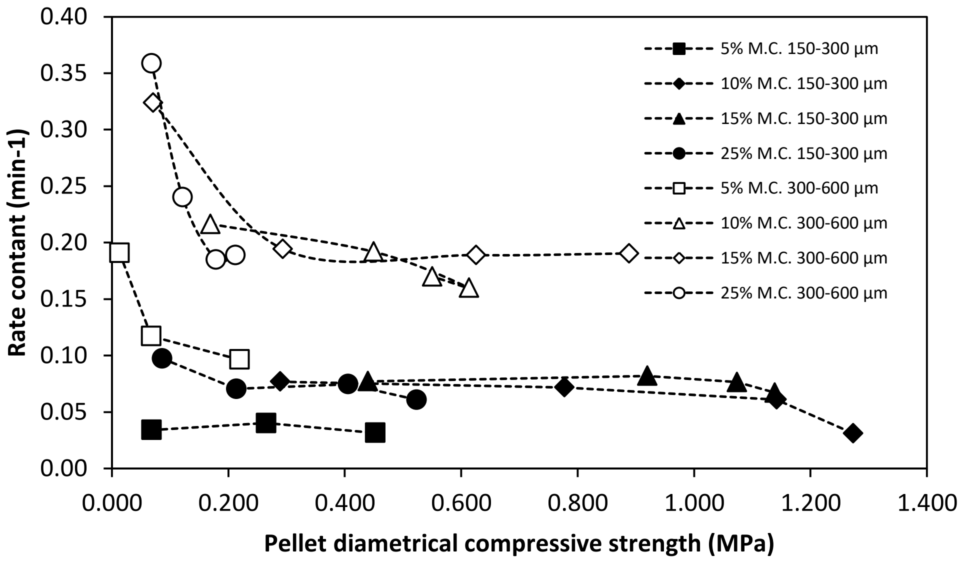

Figure 4.20: Effect of pellet tensile strength on the diffusion rate constant of EFB compost pellets

Influence of particle size

The pellet diffusion rate constant also appeared to be affected by the particle size of the pellets. In general, the diffusion rate constant was significantly lower with smaller particle size. Although smaller particle size may have larger surface area for diffusion, the higher bulk density with smaller particle size after recovery may have been the limiting factor for diffusion. Since the pellets were confined within the volume of the filter bag to avoid mechanical agitation from the stirrer, the pellets may able to retain in a smaller volume after disintegration. This reduced the effective pathway for diffusion, and therefore decreased in the rate constant.

4.4 Conclusions

The effect of storage, compaction pressure, moisture content, and particle size on the diametrical compressive strength of EFB compost pellets has been investigated. Results show that the decrease in pellet porosity increased the compressive strength of the pellets, in which corresponded to the applied compaction pressure, the pellet initial moisture content and particle size. The compressive strength of the pellets were found to be increased with storage assuming equal porosity due to formation of solid bridge bond with the recrystallization of dissolved salt during storage. This assumption was supported by the increase in bonding capacity and zero porosity compressive strength after storage with the Ryshkewitch – Duckworth equation.

The nutrient release pattern of the EFB compost pellets was studied using rapid laboratory methodology with temperature-controlled incubation method (TCIM) Process parameter which could affect the diffusion behaviour such as compaction pressure, moisture content and particle size are investigated. Spiro and Siddique kinetic model was used in the diffusion study and showed good agreement with the experimental results. The result shows that the increased strength of the pellets corresponding to the increased compaction pressure resulted in decreased diffusion rate constant of the EFB compost pellets. No noticeable difference was observed for pellet with tensile strength greater than 0.2 MPa. Pellets with smaller particle size significantly decreased the diffusion rate due to the decrease in effective pathway for diffusion.

CHAPTER 5:
MODELLING OF THE PELLET MILL COMPACTION MECHANISM

5.1 Introduction

Among the several commercially available densification equipment, pellet mill is one of the most commonly used equipment in the biomass densification process (Stelte et al. 2012). In the pelletising process, raw materials are drawn into the narrow gap between the roller and the die plate, and compacted when being extruded through the holes on the die plate to form pellets. Characteristics of the input material such as moisture content and particle size, and the process parameter of the pellet mill such as die channel length have been found to affect the quality of the produced pellets (Serrano et al. 2011; Čolović et al. 2010; Tabil and Sokhansanj 1996). Therefore, studying the pellet mill mechanism through experiments and modelling would help in designing optimal pelleting operations while producing high quality pellets.

Despite its popularity, it is surprising how little attention has been paid to the modelling of compaction mechanism of pellet mill. Only in recent years, approach in fundamental theoretical model for pellet mill compaction modelling has been published. Holm et al. (2006) proposed that the degree of compaction pressure is dependent friction force build-up in the die channel and derived an equation based on force balance on a differential control volume as shown in Equation (2.5). Equation (2.5) can be then fitted into experimental data obtained by measuring P_x at different value of $\frac{L}{D}$. However, due to mutual correlation of the variable parameters (P_{N0}, ν_{LR} and μ) in a single equation, it is not possible to fit all of the parameters in a single step (Holm et al. 2011). Application of this approach also assumes that an independent estimate of ν_{LR} is available. Holm et al. (2011) further simplified the model Equation (2.5) by combining the variable parameters as $U = \mu P_{N0}$ and $J = \mu \nu_{LR}$ allowed faster estimation with fewer experimental trials. However, efforts in discerning the independent effect of each variable still remained unresolved. To date, there has been no established methodology in biomass densification study which measures the variables independently. In addition, inclusion of Poisson's ratio ν_{LR} in Equation (2.5) is rather ambiguous because in practice, a body of powder under compaction rarely behave elastically under significant pressure. For these reasons, there is a need to re-examine the approach towards pellet mill compaction modelling from basic theoretical standpoint.

In this chapter, pellet mill compaction mechanism is investigated in reference with existing powder compaction model to predict pressure variation in powder compact. New methodology has been devised to facilitate a detailed analysis on the mechanism of pellet mill compaction. Independent experimental data generated by this method was used to verify the proposed model.

5.2 Theory

For the purpose of following derivation, the pellet mill compaction mechanism was modelled based on the force balance analysis of a plane element within a finite dimension in one direction known as differential slice method. This method was first suggested by Janssen (1895) to predict vertical wall pressure caused by the powder and granular materials in a bin. Here, the term "pressure", P and "stress", σ will be used interchangeably. Consider a cylindrical powder compact of diameter D and height H compacted in the axial direction, with elemental slice of dz located a distance z from the bottom of the compact (Figure 5.1).

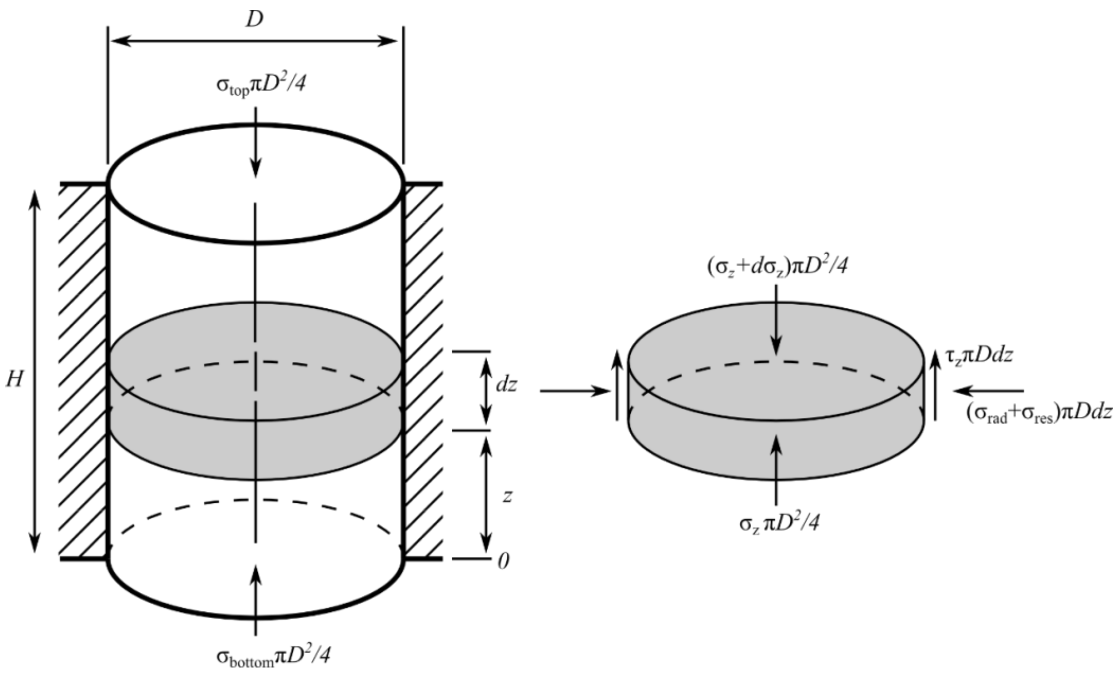

Figure 5.1: Force balance analysis of a plane element within a cylindrical compact

Assuming the weight of the compact is negligible and the axial force is uniform in any horizontal cross-section of the compact, the force balance equation within the elemental slice dz in axial direction is:

$$\frac{\pi D^2}{4} d\sigma_z = \tau_z \pi D dz \tag{5.1}$$

where $d\sigma_z$ is differential axial stress difference in elemental slice dz and τ_z is the shear stress at given height z.

The axial pressure σ_z transmits pressure on the radial direction σ_{rad_z} and its relationship at given height z can be written as:

$$\sigma_{rad_z} = K\sigma_z \tag{5.2}$$

where K is referred as radial-axial transmission ratio, stress ratio, or the Janssen constant. According to Coulomb's law of friction, the shear stress τ_z due to friction force acting on the elemental slice can be expressed as:

$$\tau_z = \mu_e(\sigma_{rad_z} + \sigma_{res}) \tag{5.3}$$

where μ_e is the coefficient of friction between the powder compact and the die wall during ejection, and σ_{res} is the residual stress due to irrecoverable radial stress after compaction. The radial stress σ_{rad_z} is superimposed on the residual stress σ_{res} caused by the transmission on axial loading. Combining Equation (5.2) and (5.3) the force balance in equation (5.1) can be rewritten as:

$$\frac{1}{K\sigma_z + \sigma_{res}}\mathrm{d}\sigma_z = \frac{4}{D}\mu_e \mathrm{d}z \tag{5.4}$$

Assuming K, μ_e and σ_{res} is independent of height position z, Equation (5.4) can be integrated by the appropriate boundary condition:

$$\int_{\sigma_{bottom}}^{\sigma_{top}} \frac{1}{K\sigma_z + \sigma_{res}}\mathrm{d}\sigma_z = \int_0^H \frac{4}{D}\mu_e \mathrm{d}z \tag{5.5}$$

With the solution:

$$\frac{K\sigma_{top} + \sigma_{res}}{K\sigma_{bottom} + \sigma_{res}} = e^{4\frac{H}{D}\mu_e K} \tag{5.6}$$

Since σ_{bottom} is 0 in pelleting process and σ_{top} is also the pelleting compaction pressure σ_P, equation (5.6) becomes:

$$\sigma_P = \frac{\sigma_{res}}{K}\left(e^{4\frac{H}{D}\mu_e K} - 1\right) \tag{5.7}$$

The derived equation (5.7) yields a differential equation similar to that of Holm's model equation (2.5) but with the omission of material Poisson's ratio ν_{LR} and replaced with radial-axial transmission ratio K of the control volume. Both equations describe an exponential increase of pelleting pressure with the increase of compact length or height. With the Equation (5.7), the pelleting pressure σ_P can be calculated according the die geometry $\frac{H}{D}$, coefficient of friction during ejection μ_e, radial-axial transmission ratio K and its residual stress σ_{res}.

5.3 Materials and methods

5.3.1 Materials

Raw oil palm empty fruit bunch compost obtained from a palm oil mill in Bintulu, Sarawak, operated by Wawasan Sedar Sdn. Bhd was used as a model powder in this study. The compost was ground and sieved into different size fraction of 150 – 300 µm and 300 – 600 µm for particle size analysis and conditioned into different moisture content of 5%, 10%, 15% and 25% (w.b.) Details of the material preparation is presented in previous chapter.

5.3.2 Compaction experiments

A nominal weight of 0.35 g of powder sample was manually added into the instrumented die and compacted with compaction force up to 8 kN corresponding to pressure of 160 MPa. The crosshead speed of the testing machine was set at 30 mm per minute. Immediately after the compaction, the compact was ejected out from the die at the same speed of 30 mm per minute. Details of compaction experiment is presented in previous chapter 3.

In this study, the instrumented die described in the previous was used to calculate σ_{res}, K and μ independently. The aim is to measure the radial and axial pressure during the compaction cycle and use the relevant measurements to calculate σ_{res}, K and μ (Figure 5.2).

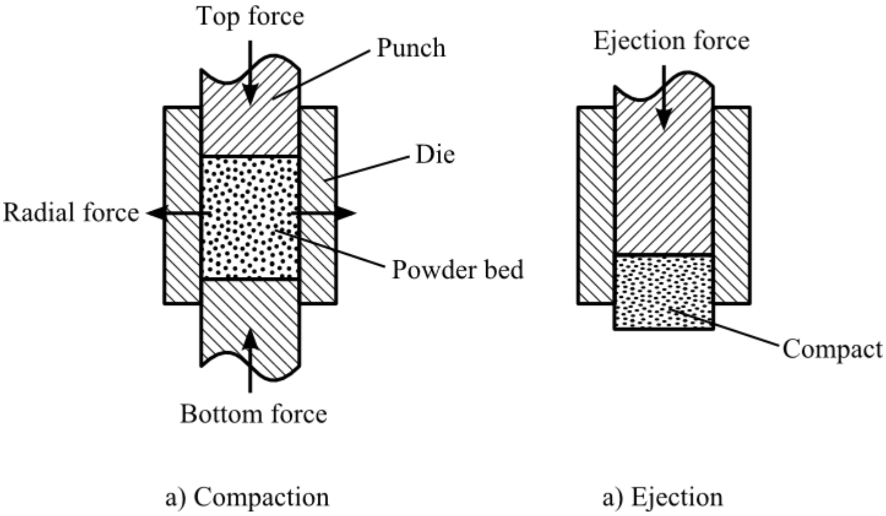

Figure 5.2: Schematic diagram of forces measured with die-wall instrumentation

5.3.2.1 *Radial-axial transmission ratio*

Radial-axial transmission ratio K is described as the ratio of applied axial pressure to the transmitted radial pressure on the die wall in a uniaxial die compaction. When the axial pressure is exerted on a hydraulic material inside the die channel, the pressure applied would be transmitted 1:1 radially as toward the die wall. When a powder is being compacted, the applied axial pressure is only partly transformed to radial pressure toward the die wall. Using the measured data from the instrumented die, K was calculated by the ratio of the radial pressure to the axial pressure as:

$$K = \frac{\sigma_{rad_z}}{\sigma_z} \tag{5.8}$$

where σ_{rad_z} and σ_z are the measured radial pressure and the axial pressure positioned at the height z of the radial sensor. Due to the effect of friction between the powder and the die wall during compaction, the pressure distribution in the compact is not uniform as the measured top axial pressure is typically higher than bottom axial pressure. Therefore, the axial pressure at a given height z at the position of the radial sensor was estimated as (Cunningham et al. 2004):

$$\sigma_z = \sigma_{top}^{\frac{z}{H_c}} \sigma_{bottom}^{(1-\frac{z}{H_c})} \tag{5.9}$$

Where σ_{top}, σ_{bot}, z and H are the top pressure, bottom pressure, position of the radial sensor from the backstop, and height of the powder respectively (Figure 3.13).

5.3.2.2 *Residual die wall stress*

The residual die wall stress σ_{res} occurs due to the irrecoverable radial stress that remained after applied compaction pressure is removed. The existence of residual die wall stress provides the necessary force to induce friction during ejection. The nature of residual die-wall stress was first investigated by Higuchi et al. (1965) and reported the die wall stress rapidly decreased after the applied pressure is removed. Part of the stress remains on the die wall as residual and was observed to decay over time. For this study, the residual die wall stress was obtained from the radial pressure sensor measured seconds before the ejection phase (Figure 5.3).

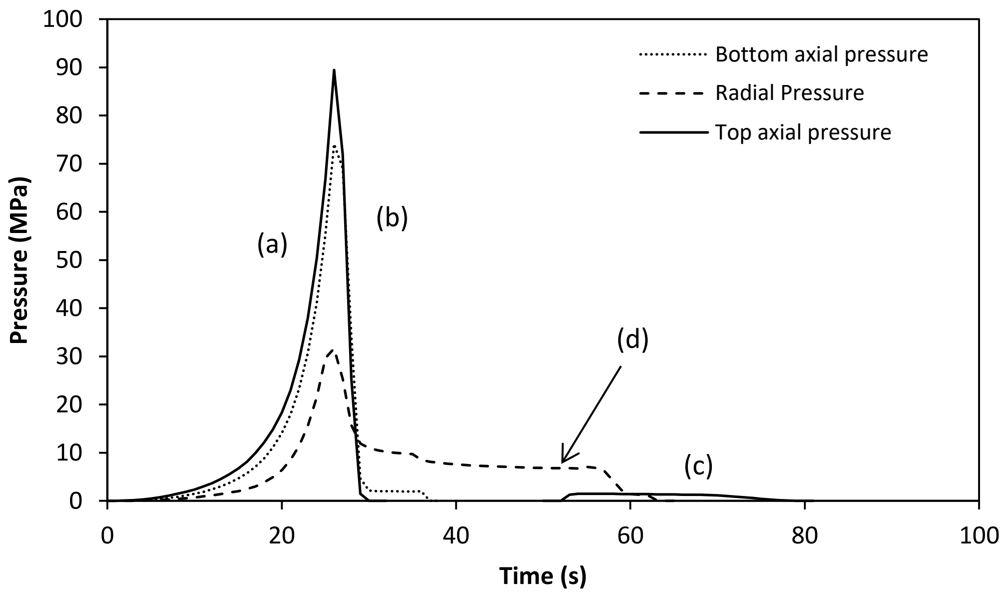

Figure 5.3: Typical measurement obtained using instrumented die during compaction cycle. Pressures were measured during (a) compaction, (b) unloading, and (c) ejection phase. Label (d) indicates the residual die wall pressure measured

5.3.2.3 *Coefficient of friction*

Friction phenomena occurs in all densification process: compaction, de-compaction, pre-ejection and ejection (Doelker and Massuelle 2004). It depends on the characteristics of the compact powder, surface morphology of the die and the die material and is described by the well-known Coulomb's equation as (Cunningham et al. 2004):

$$F = \mu N \tag{5.10}$$

where F is the total frictional force acting between two bodies, N is the normal force acting on the interface between the two bodies and μ is the coefficient of friction.

For powder densification in a cylindrical die, the friction coefficient may not be constant for powder compaction as the surface morphology of the compact varied with the applied compaction force. The values of friction coefficient may also varied depending on the phases of the compaction process (Hölzer and Sjögren 1981).

During the ejection phase, the coefficient of friction during ejection μ_e was estimated based on the rearranged Equation (5.7) in the form of:

$$\mu_e = \frac{D}{4H_r K} \ln \frac{\sigma_P K + \sigma_{res}}{\sigma_{res}} \tag{5.11}$$

where σ_P is the static friction pressure needed to eject the compact and K is the radial-axial transmission ratio of the compact.

5.4 Results and discussions

5.4.1 Radial axial transmission ratio, K

Figure 5.4 shows the relationship between the radial pressure and axial pressure for moisture content of 5%, 10%, 15% and 25% and particle size of 150-300 µm and 300-600 µm respectively. It appears that the radial pressure increased with the increase in axial pressure for all level of moisture content and particle size. The increased level of moisture content also appears to increase the slope in the radial-axial curve for the particle size of 150-300 µm and 300-600 µm.

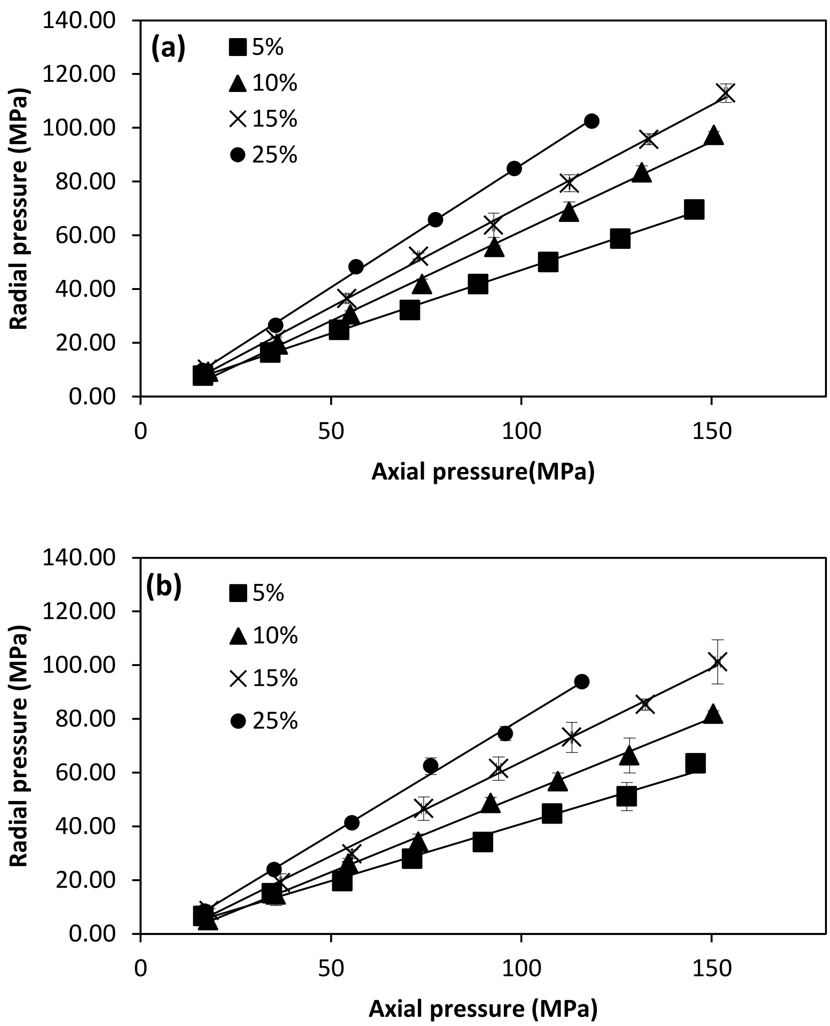

Figure 5.4: Relationship between the radial pressure on the die wall and the axial pressure at the position of the radial sensor with different moisture content and particle size of (a) 150-300 and, (b) 300-600 µm. Values in legend indicate the moisture content.

5.4.1.1 *Effects of porosity*

Figure 5.5 shows the plot of radial-axial transmission ratio against the porosity of the compact with particle size of 150-300 µm and 300-600 µm respectively. The radial-axial transmission ratio was calculated by dividing the radial pressure with the axial pressure at the position of the radial sensor. The relationship between the radial-axial transmission ratio K and compact porosity ε appeared to be linear and was modelled as:

$$K = n\varepsilon + K_0 \tag{5.12}$$

where n is the empirical model constant and K_0 is model intercept indicating the radial-axial transmission ratio when the compact porosity is zero. The model constants were estimated using linear regression fit and listed in Table 5.1. Results shows that compact with 5% moisture content appears to be independent with the compact porosity indicated by the value of m approaching towards zero. Increasing the moisture content however increased the value of n where the radial-axial transmission ratio increased rapidly with the decrease in compact porosity.

Table 5.1: Values of m and K_0 obtained from linear fitting of Equation (5.12)

Particle size (μm)	Moisture content (% w.b.)	n	K_0	R^2
150-300	5	0.0283	0.4652	0.1770
	10	-0.4118	0.6216	0.8188
	15	-0.7657	0.7037	0.8506
	25	-3.3187	0.8305	0.9386
300-600	5	-0.0158	0.4068	0.0065
	10	-0.7206	0.5394	0.9472
	15	-0.7882	0.6361	0.8470
	25	-2.5966	0.7641	0.9644

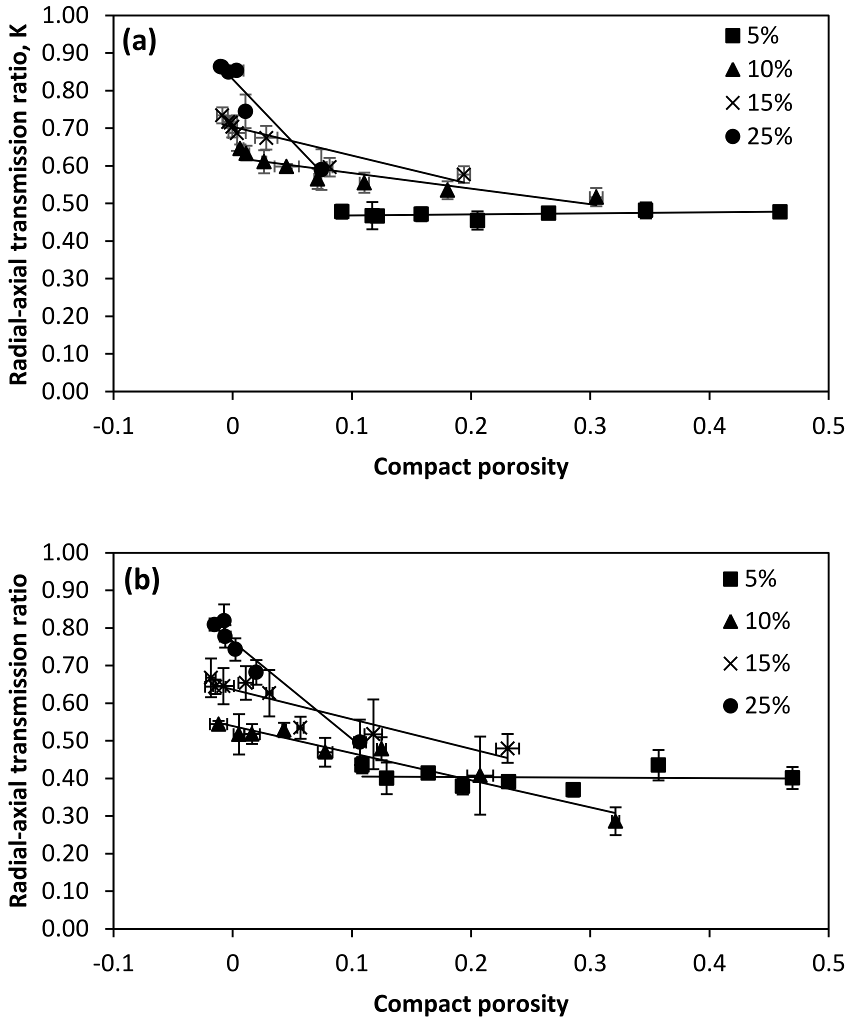

Figure 5.5: Relationship between the radial-axial transmission ratio and the compact porosity with different moisture content for particle size of (a) 150-300 µm and, (b) 300-600 µm. Values in legend indicate the moisture content.

5.4.1.2 *Effect of particle size*

Change in particle size of the EFB compost powder appears to have only a minor effect on the radial-axial transmission ratio. Decreasing the particle size from 300-600 µm to 150-300 µm was found to increase the radial-axial transmission ratio slightly for all level of moisture content. Higuchi et al. (1965) reported that radial-axial pressure curves were identical for sodium chloride powder with different particle size, while potassium bromide with smaller particles behaved slightly different from that of coarser particles. Although minor differences were observed, the increase in stress ratio was probably correlated to the improved compatibility of the biomass powder with smaller particle size as reported by Lai et al. (2013).

5.4.1.3 *Effect of moisture content*

The radial-axial transmission ratio also was also found to be affected by the moisture content. Similar trend was observed by Abdel-Hamid and Betz (2011a) where the stress ratio was significantly increased with the increased moisture content for pre-gelatinized starch. The radial-axial transmission ratio was reportedly increased as the material hardness decreases, of which probably due to the lower yield strength of the powder that increased the area of contact and thus stress transmission (Doelker and Massuelle 2004; Ridgway et al. 1969; Higuchi et al. 1965). The addition of moisture plasticises and lubricates the compact and thus facilitates the deformation of powder particles and therefore increases the radial-axial transmission ratio of the compact. The addition of moisture also probably introduced elements of incompressibility to the compact due to hydrostatic behaviour of water. As a result, the radial-axial transmission ratio will have the propensity to reach unity due to the addition of moisture.

5.4.2 Residual die wall pressure

Figure 5.6 shows the relationship between the residual pressure and the applied compaction axial pressure for moisture content of 5%, 10%, 15% and 25% and particle size of 150-300 µm and 300-600 µm respectively. It appears that the residual pressure increased linearly with the axial pressure (R^2 > 0.90) for all level of moisture content and particle sizes. Similar trend was also reported for pharmaceutical excipients as the residual die pressure increased with compaction pressure (Takeuchi et al. 2004; Leigh et al. 1967). The increased residual pressure was more pronounced as the moisture content of the EFB compost powder decreases.

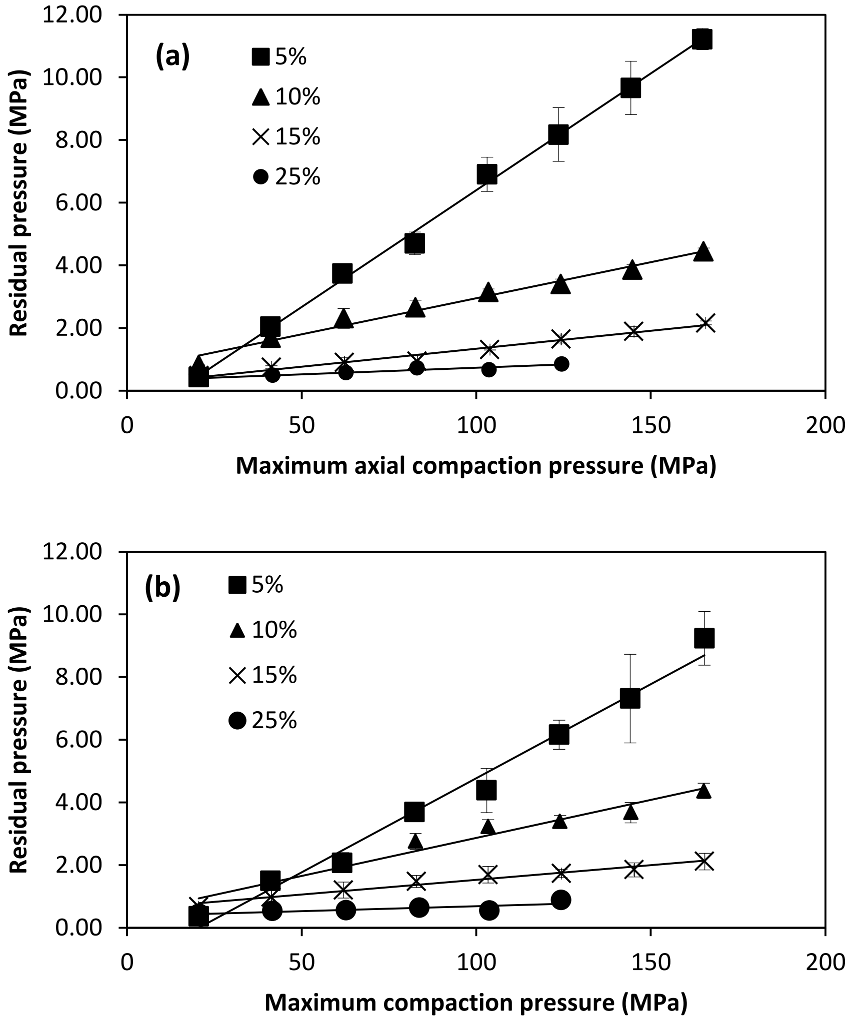

Figure 5.6: Relationship between residual pressure and the applied compaction pressure with different moisture contents for particle size of (a) 150-300 µm and, (b) 300-600 µm. Values in legend indicate the moisture content.

5.4.2.1 *Effect of porosity*

Figure 5.8 shows the plot of residual die wall pressure against the in-die relaxed porosity of the compact measured after the compaction load was released. It appears that the residual die wall pressure increased exponentially as the porosity approaches zero and was modelled as:

$$\sigma_{res} = \sigma_{res_0} e^{-\varphi \varepsilon_r} \quad (5.13)$$

where σ_{res_0} is the residual stress when the compact porosity is zero, φ is the model constant and ε_r is the in-die relaxed compact porosity corresponding to the height of the powder compact measured after the compaction load is fully released (Figure 5.7).

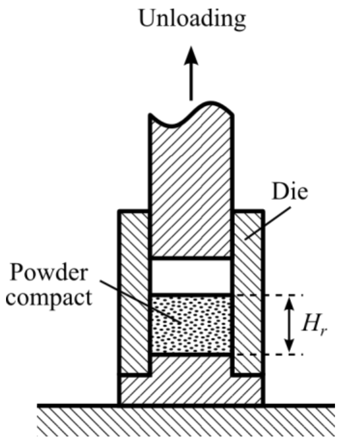

Figure 5.7: Height measurement of in-die relaxed compact porosity
The model constants from Equation (5.13) were estimated using non-linear regression analysis and the values are listed in

Table 5.2. The increased level of residual die pressure from the increased compaction pressure could probably be related to the degree of permanent deformation of the compact when compacted at higher pressure. The powder compacts undergo significant deformation at higher compaction pressure which may lead to an increase in compact stiffness attributed by the porosity of the compact. The decrease in compact porosity increased the bonding strength of the compact and may subsequently increases the residual die wall pressure after the applied compaction pressure was removed.

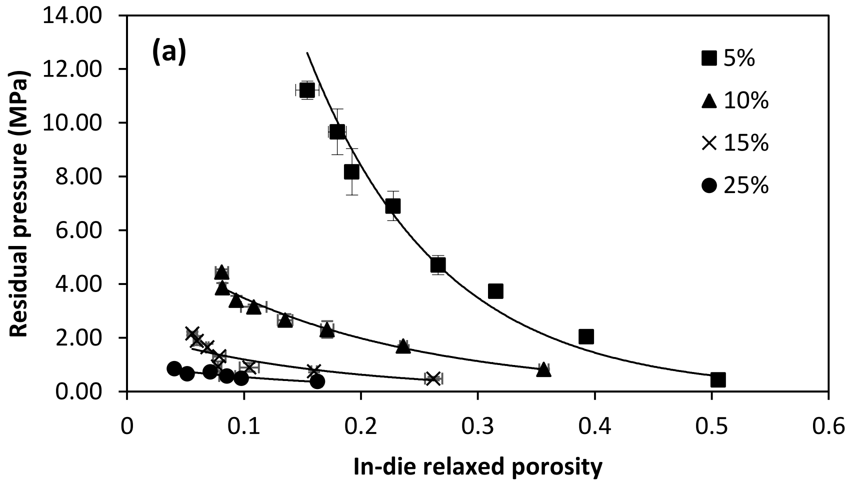

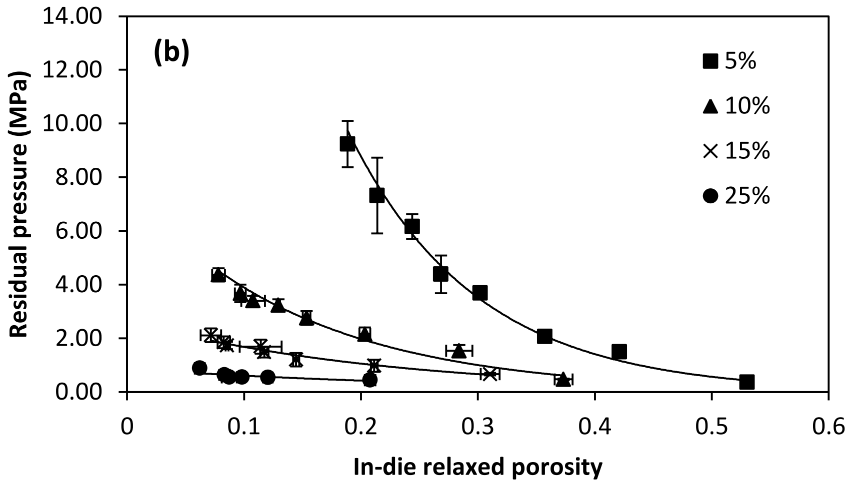

Figure 5.8: Relationship between residual pressure and in-die relaxed porosity with different moisture content with particle size of (a) 150-300 µm and, (b) 300-600 µm. Values in legend indicate the moisture content.

Table 5.2: Values of φ and σ_{res_0} obtained from the fitting of Equation (5.13)

Particle size (µm)	Moisture content (% w.b.)	φ	σ_{res_0} (MPa)	R^2
150-300	5	7.086	33.288	0.9943
	10	5.616	6.084	0.9841
	15	6.439	2.273	0.7849
	25	6.805	1.047	0.9136
300-600	5	8.070	41.079	0.9885
	10	4.936	6.012	0.9886
	15	4.650	2.655	0.9604
	25	3.556	0.862	0.6570

5.4.2.2 *Effect of particle size*

EFB compost powder with different particle size showed no significant difference in residual die wall pressure as evident by the extrapolated value of σ_{res_0} from

Table 5.2. Similar trend was observed by Abdel-Hamid et al. (2011) in the study of pharmaceutical compaction where there was no difference in residual pressure between two different particle size of microcrystalline cellulose. Microcrystalline cellulose particle was reportedly to have an elongated fibrous structure.

5.4.2.3 *Effect of moisture content*

By increasing the moisture content, the residual die wall pressure was reduced for all powders. Similar results were reported before by Abdel-Hamid and Betz (2011a) where the increase in moisture content in most pharmaceutical excipient powder reduced the residual die wall pressure with the exception of pre-gelatinised starch. Abdel-Hamid and Betz (2011a) further theorised that the reduction of residual die wall pressure could be attributed to the lubrication effect of water where the absorbed moisture reduces the particle surface energy and subsequently reduces the adhesion to the die wall. This explanation however, remain inadequate as some material e.g. mannitol showed an increase in coefficient of friction with corresponding to the increase of moisture content in the same study.

The reduced residual die wall pressure could also be attributed by the lowered elastic modulus of compact at higher moisture content which could be explained similarly to the effect of compaction pressure. It has been reported that the pellet compacted with higher compaction pressure and lower moisture content has greater elastic modulus (Carone et al. 2011). Higher elastic modulus implies greater stiffness of the compact and therefore the irrecoverable radial strain resulted from the permanent deformation may result in higher residual pressure exerted on the die wall.

5.4.3 Ejection force

Figure 5.10 shows the plot of the ejection force correspond to the compact contact area against the machine crosshead displacement in reference to the bottom surface of the compact as zero datum point during ejection. The negative value of the displacement indicates the position of the top piston is above the zero reference point (see Figure 5.9). Conversely, the position of the top piston is below the zero reference point when the machine displacement shows a positive value. The compact is fully ejected from the die when the machine displacement approached 7.5 mm. The compact contact area was measured according to the in-die relaxed height.

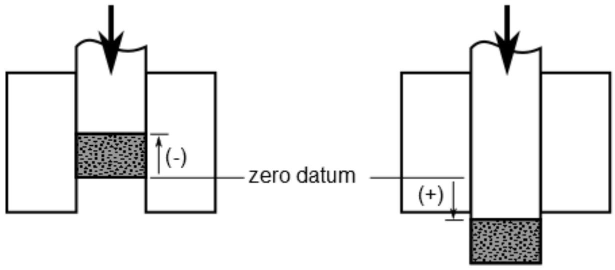

Figure 5.9: Machine crosshead-piston positioning in reference to the bottom surface of the compact

During the ejection of the ground EFB compost powder compact, the friction dramatically increased to a peak value known as the static friction and then reduced to a relatively constant friction force known as dynamic friction when the compact is sliding in the die. The friction force gradually decreased when the compact started to emerge out from the die.

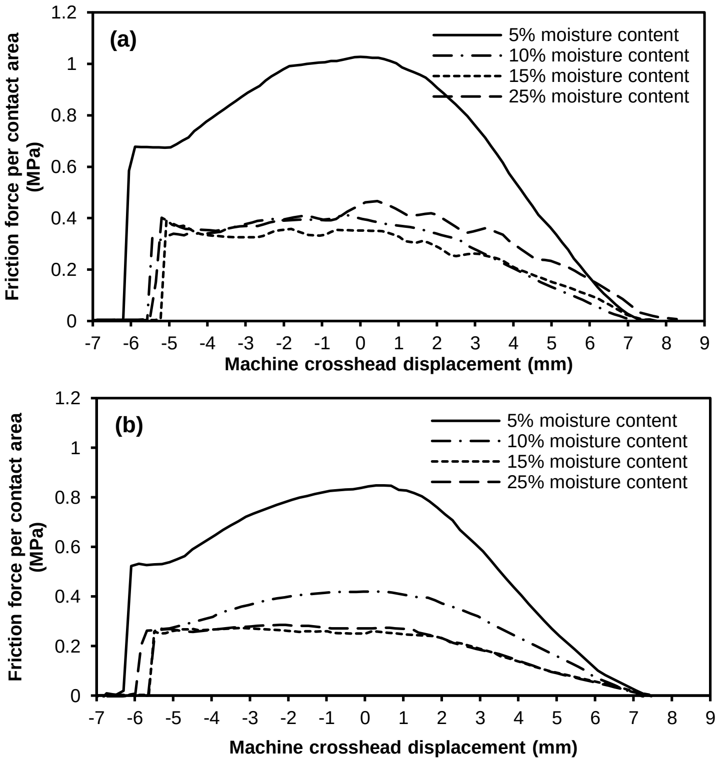

Figure 5.10: Change of friction during the ejection normalised with contact area due to the moisture content of compact with preload of 5000 N for particle size of (a) 150-300 µm and (b) 300-600 µm

The friction force per contact area was found to be increased by increasing the applied compaction force and length of the compact as illustrated in Figure 5.11 and Figure 5.12. The friction force per contact area also observed to be dependent on the moisture content of the compact which correspond to the increased residual die wall pressure. The effect of residual die wall pressure will be discussed later in this chapter. There was an excessive increase in friction during the sliding of compact with moisture content of 5% and 10%. This feature was also observed in the study by Briscoe and Rough (1998) for spray dried alumina powder in an unlubricated die. Interestingly, the excessive increase in friction force during sliding was found to be absent with the increased compact height and shows peak friction force before the sliding occurred.

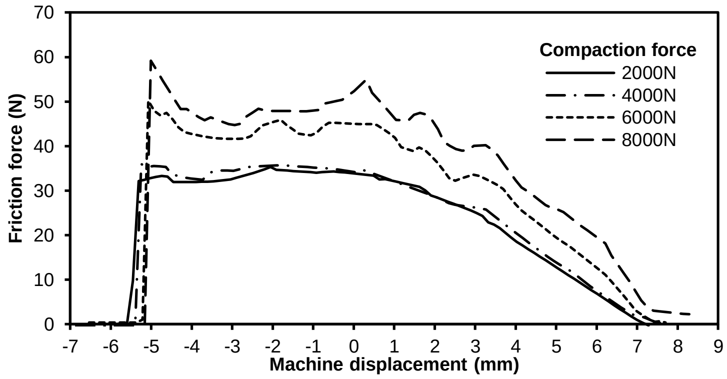

Figure 5.11: Change of friction during ejection of compact with different range of compaction load for particle size of 300-600 µm and 11.5% (w.b.) moisture content

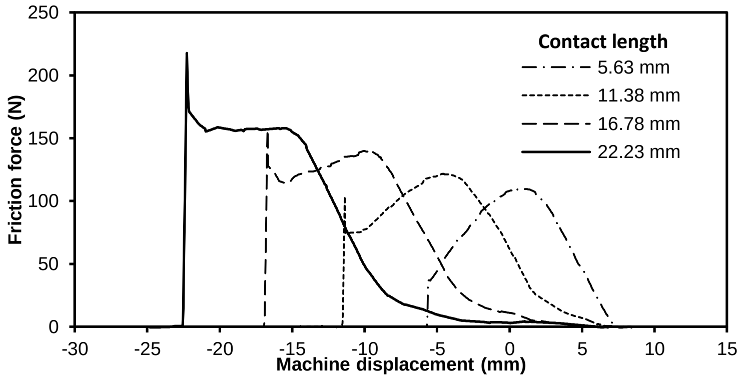

Figure 5.12: Change of friction during ejection of compact with different contact length for particle size of 300-600 µm and 15% (w.b.) moisture content

5.4.4 Coefficient of friction during ejection

Figure 5.13 shows the relationship between the friction force per contact area and the applied compaction axial pressure for moisture content of 5%, 10%, 15% and 25% and particle size of 150-300 µm and 300-600 µm respectively. It appears that the increase in the friction force per contact area was closely proportional to the increase of applied compaction pressure. The increased friction could be correlated to the increased residual pressure which increases with the applied compaction pressure as illustrated in Figure 5.14. Similarly, the friction force reduced when the moisture content increased from 5% to 10% corresponds to the decrease of residual die wall pressure.

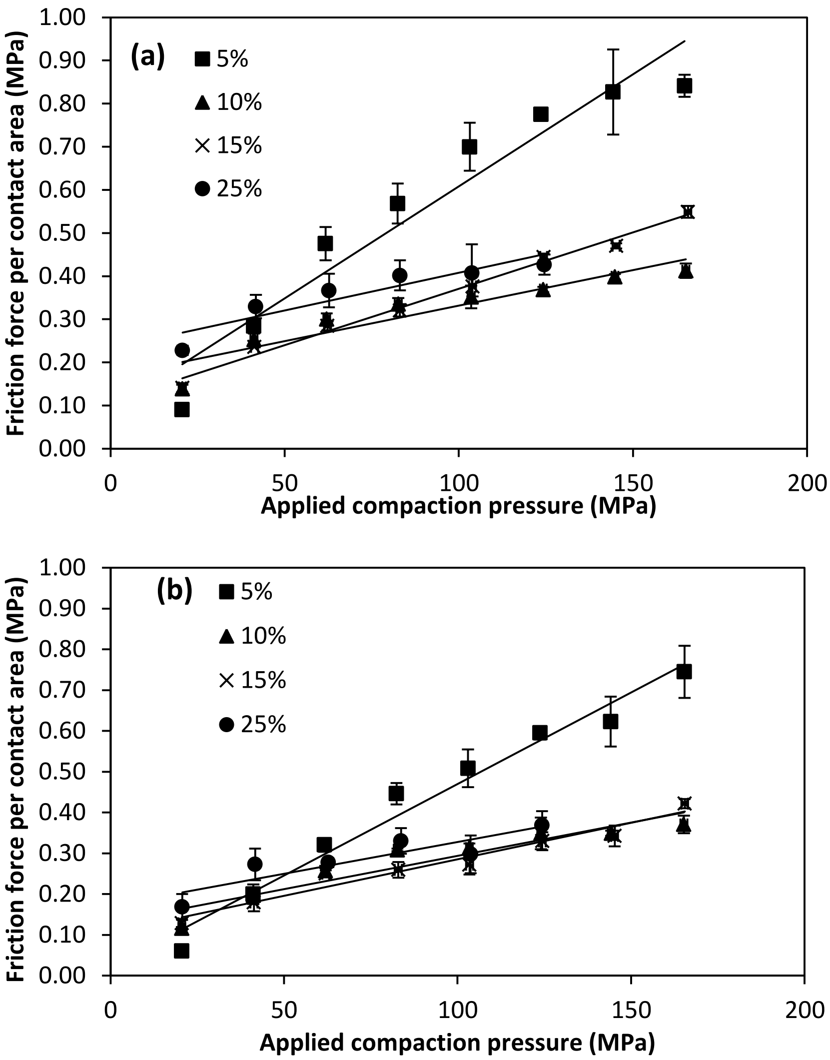

Figure 5.13: Relationship between friction force per contact area and the applied compaction pressure with different moisture content for particle size of (a) 150-300 µm and, (b) 300-600 µm. Values in legend indicate the moisture content.

If the coefficient of friction during ejection is reasonably constant over the pressure range tested, plot of friction force per die wall contact area vs. residual die wall pressure should yield a linear plot. The slope of this line would indicate the coefficient of friction of the compact. However, results show that both particle sizes and all levels of moisture content shows non-linear decrease in friction as the residual pressure increases (Figure 5.14). This suggests that the coefficient of friction during ejection does not remain constant over the pressure range tested.

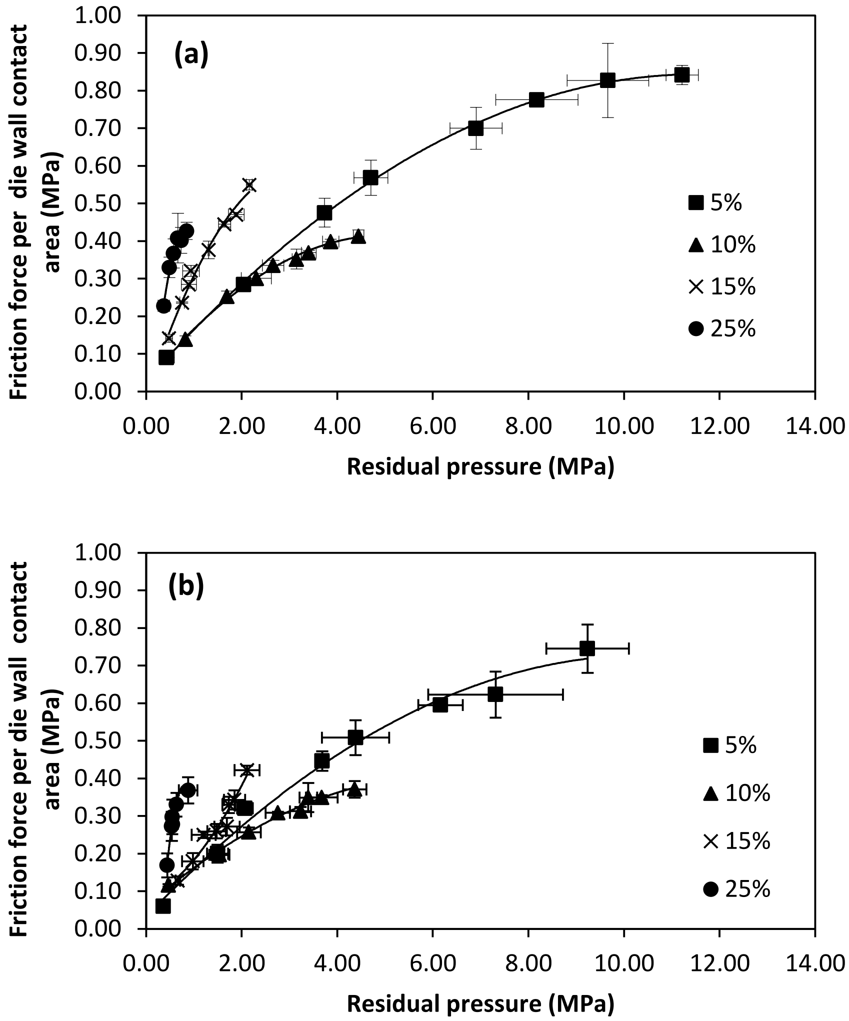

Figure 5.14: Relationship between friction force per contact area and the residual die wall pressure with different moisture content for particle size (a) 150-300 µm and, (b) 300-600 µm. Values in legend indicate the moisture content.

5.4.4.1 *Effect of porosity*

Figure 5.15 shows the relationship between the coefficient of friction during ejection and the in-die relaxed porosity of the compact. It appears that the coefficient of friction during ejection gradually decreased with the decrease in in-die relaxed compact porosity. The relationship between coefficient of friction during ejection and compact porosity was modelled as:

$$\mu_e = \gamma \varepsilon_r + \mu_0 \tag{5.14}$$

where γ is a empirical model constant and μ_0 is the coefficient of friction during ejection when the in-die relaxed compact porosity is zero. The model constants were estimated using linear regression and the values are listed in Table 5.3.

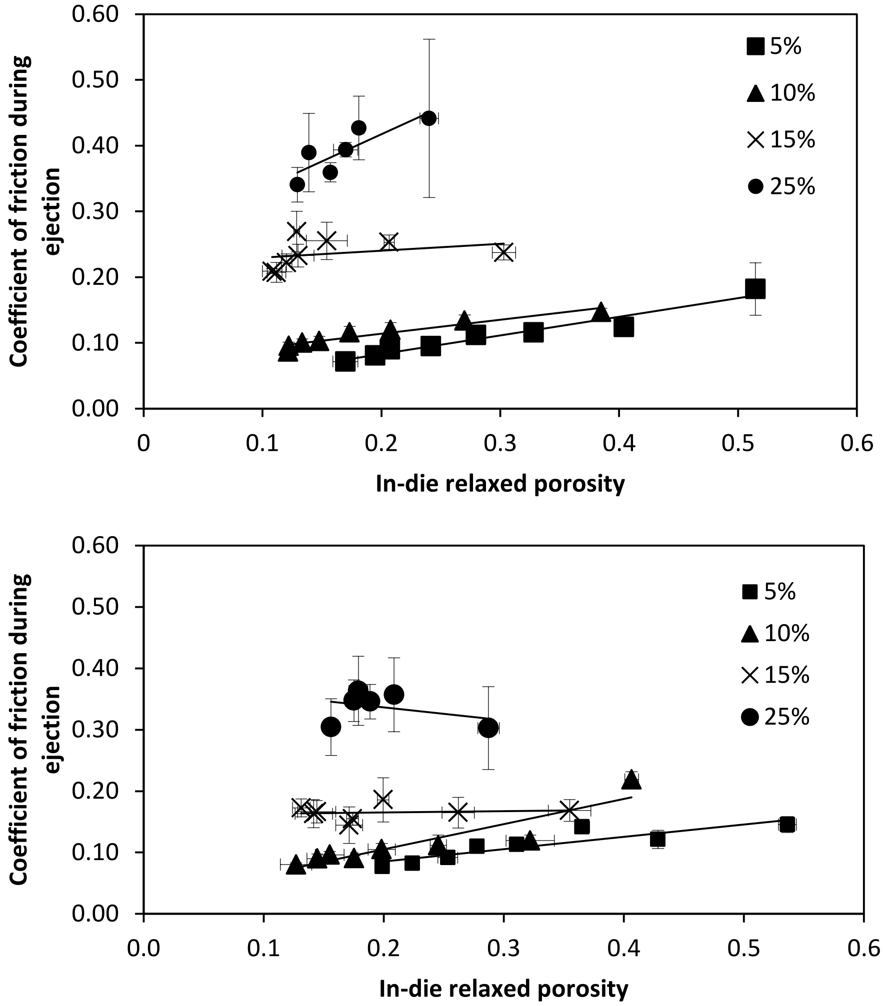

Figure 5.15: Relationship between coefficient of friction during ejection and the in-die relaxed porosity with the different moisture content for particle size of (a) 150-300 µm and, (b) 300-600 µm. Values in legend indicate the moisture content.

The decrease in the coefficient of friction could be attributed to the change of surface morphology. The decrease in compact porosity produced smoother surface which reduce friction contact between the compact and the die wall surface. It is also reported that the average surface roughness of the compact decreased with the increase of the compaction pressure (Yusof et al. 2010; Seitavuopio et al. 2003).

Table 5.3: Values of γ and μ_0 obtained from the fitting of Equation (5.14)

Particle size (µm)	Moisture content (% w.b.)	γ	μ_0
150-300	5	0.198	0.048
	10	0.258	0.082
	15	0.100	0.225
	25	0.749	0.329
300-600	5	0.255	0.053
	10	0.203	0.076
	15	0.020	0.162
	25	-0.192	0.358

5.4.4.2 *Effect of particle size*

The coefficient of friction during ejection appears to be decreased with the change of particle size from 150-300 µm to 300-600 µm despite the coarser surface with larger particle size. The difference in coefficient of friction however, diminished as the moisture content decreases. A decrease in friction force during ejection was observed for coarser particles despite that the residual die wall pressure did not significantly vary with particle size, and thus reduced in the coefficient of friction. This could be attributed by the larger surface area with smaller particles which promotes greater tendency to adhere to the die wall and further exaggerated by the increase in moisture content. Stelte et al. (2011b) also reported that the friction increases with the decrease of particle size of biomass with beech, spruce and, straw.

5.4.4.3 *Effect of moisture content*

By increasing the moisture content, it appears that the coefficient of friction during ejection was found to be increased for both particle sizes. This result however, in contrast with existing studies with most pharmaceutical excipients where the coefficient of friction was reduced due to the water lubrication effect, with exception of mannitol powder (Abdel-Hamid and Betz 2011a). Whereas in biomass densification, Stelte et al. (2011b) demonstrated that increasing the moisture content in beech and spruce resulted in a drop of the friction force. Increasing the moisture content in straw however, resulted in increase of friction force. It is possible that some of the water-soluble carbohydrate content may have solubilised with the presence of moisture and act as natural binder and increased the tendency to adhere to the die wall (Tumuluru 2015). It is also reported that increasing the moisture content above 9% in alfafa grind may tends to choke the pellet mill with 6.1mm die channel size and required larger die channel to tolerate higher moisture as it offered less resistance to the flow of grind particles through it (Tabil and Sokhansanj 1996).

Similarly, the EFB compost was treated with wastewater known as palm oil mill effluent (POME) during the composting process. POME is a viscous brown liquid with high concentration of suspended and dissolved solids discharged from the palm oil mill. When the EFB compost powder was rehydrated with water, some of the POME content may have dissolved and therefore act as a binder that adhere the compact to the die wall. The effect of adhesion in higher moisture content was found to be more pronounce with smaller particle size due to the increased surface area.

5.5 Validation of pellet mill compaction model

As previously shown, the pellet mill compaction model variable parameters of radial-axial transmission ratio K, residual stress σ_{res} and coefficient of friction during ejection μ_e were found to be dependent on the compact porosity ε. The empirical relationship between the model variable parameters and porosity were described in Equation (5.12), (5.13) and (5.14). These equations may be used to modify the pellet mill compaction model from Equation (5.7) expressed as a function of porosity ε_r:

$$\sigma_P = \frac{\sigma_{res_0} e^{-\varphi\varepsilon_r}}{m\varepsilon_r + K_0}\left(\exp(4\frac{H}{D}(\gamma\varepsilon_r + \mu_0)(m\varepsilon_r + K_0)) - 1\right) \tag{5.15}$$

where σ_{res_0}, φ, m, K_0, γ and μ_0 are the parametric constant of the pellet mill compaction model.

Figure 5.16 shows the experimental results of pressure needed to eject the pellet out from the die σ_P as a function of dimensionless compact height $\frac{H}{D}$. The experimental data of σ_P was obtained from Figure 5.12 and calculated as:

$$\sigma_P = \frac{F_f}{\frac{\pi D_{top}^2}{4}} \tag{5.16}$$

Where F_f is the static friction force measured by the first peak in the friction – displacement plot. Equation (5.15) was used to predict σ_P and parameters used in this are listed in Table 5.1,

Table 5.2 and Table 5.3. The predicted σ_P (solid lines) were compared with experimental results (data points) as shown Figure 5.16. It appears that the predicted σ_P were in reasonable agreement with the experimental data. This suggests that the proposed pellet mill compaction model from Equation (5.7) was able to yield reasonable prediction σ_P at various length with the model parameters obtained independently using the instrumented die.

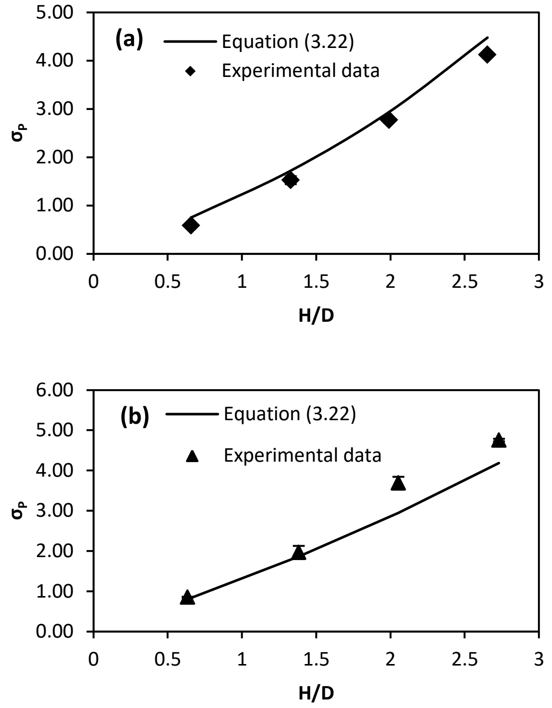

Figure 5.16: Comparison between theoretical (solid line) and experimental results (data points) of pelleting pressure vs $\frac{H}{D}$ plot for (a) 10% moisture content, 300-600 µm particle size, (b) 15% moisture content, 300-600 µm particle size.

5.6 Conclusions

In this chapter, an alternative model describing the pelleting pressure in a function of die channel height was proposed. The proposed model was found able to fit experimental data with the model variable parameters obtained independently by using an instrumented die that incorporates simultaneous radial pressure and axial pressure measurements.

Results show that the radial axial transmission ratio was found to be increased with decreasing compact porosity which corresponds to the compaction pressure. A slight decrease in the transmission ratio was observed with decreasing particle size of the EFB compost powder. The increase in moisture content significantly increased the transmission ratio. Residual die wall pressure was found to be increased by the decrease in compact porosity and the decrease in moisture content possibly due to the increased elastic modulus. No significant changes were observed in the residual die wall pressure with different particle sizes. Regarding friction, the coefficient of friction during ejection was found to be decreased with the decrease in compact porosity due to the changes in surface morphology. An increase in coefficient of friction was observed with finer particle size possibly due to the increased adhesion tendency with large surface contact area between the compact and the die wall. The increase in moisture content may have increased the adhesion of the compact to the die wall which resulted in increased coefficient of friction.

The instrumented die is useful tool with the capability to simultaneously measure radial and axial pressure in a powder compaction. The results from this study showed that it is possible to use the instrumented die to investigate the model parameters from the pellet mill compaction model correspond to the various conditions of compaction pressures, particle sizes and moisture content. With the information obtained from the instrumented die, the proposed model can be made useful in numerically predicting the pelleting pressure. This allows better insight on the ability to optimise the pellet mill design in reference to the processing parameters and material characteristics.

CHAPTER 6:
STEADY-STATE PELLET MILL COMPACTION

6.1 Introduction

Pelletisation is one of the commonly used technique to produce densified biomass products which allows for ease of transportation and storage. To understand and optimising the pelleting process, it is necessary to investigate the influence of the processing conditions and the input material properties such as the compaction pressure, moisture content and particle sizes on the resulting pellet quality. However, optimising the pelleting process based on trial-and-error method can be time consuming and expensive. Laboratory studies using a single pellet press allows for fast and cheap tests in smaller scale which has been primarily used in biomass densification studies. Despite the advances in biomass densification studies, the optimised pelleting conditions obtained from the single pellet press however, may not necessary work with actual pellet mill (Shang et al. 2014). This problem also has been recognised in comparative study between laboratory tests and pilot tests (Puig-Arnavat et al. 2016). Shang et al. (2014) concluded that the static friction to eject the powder compact out from the die appears to be the crucial parameter linking to real production. The friction build up in the die also has been the subject of several studies (Holm et al. 2011; Nielsen, Holm, et al. 2009; Holm et al. 2007; Holm et al. 2006). A new mathematical model describing the pelleting process has been proposed in the previous chapter. The proposed model described friction build up as the pelleting pressure in a function of die channel geometry $\frac{H}{D}$ and material dependent variable parameters such as residual stress σ_{res}, radial-axial transmission ratio K, and coefficient of friction during ejection μ_e.

However, the proposed pelleting model only partially describes the mechanism of the pellet mill compaction process as the compact porosity in the die channel dynamically changes dependent on the condition of the existing compact. Pelleting simultaneously compact and displacing the existing compact out from the die channel. The degree of compaction would be dependent on existing compact in the die channel. The resulting compact porosity may differ and this would cause the friction build up to fluctuate, affecting subsequent compaction. As the pelleting continuously form new layers of compact in the die channel, the compact porosity may deviate to a constant where the pelleting pressure produces the same porosity as the extruded compact (Figure 6.1). This condition would be known as the steady-state pelleting condition. Predicting the pelleting pressure operating at this condition would be crucial in determining the appropriate parameters such as the moisture content, particle size, and die geometry for optimal production of quality pellets.

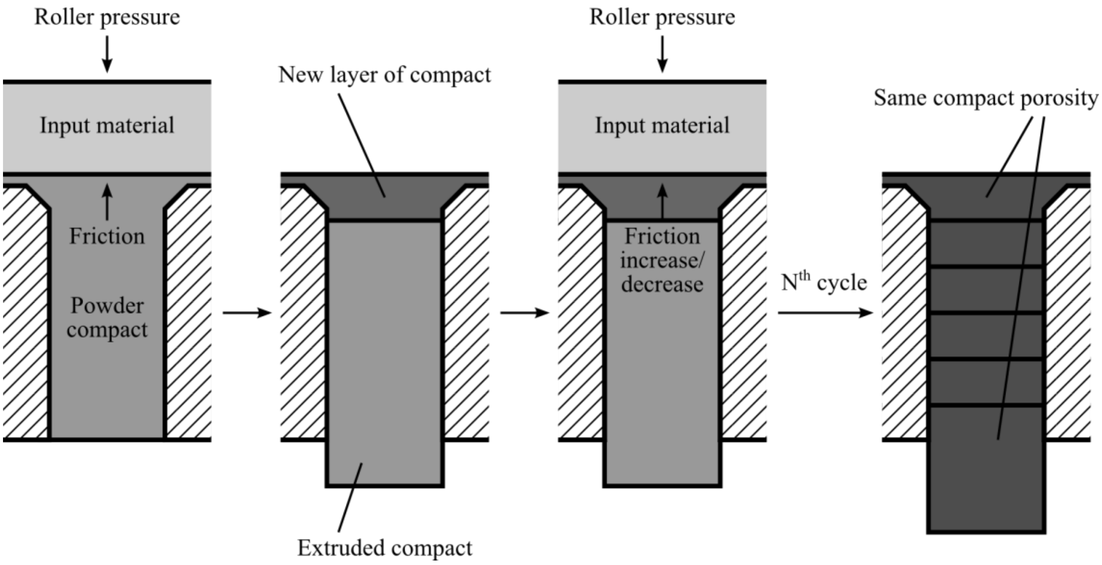

Figure 6.1: Schematic diagram of steady-state pelleting

In this chapter, the steady-state pelleting pressure was solved by implementing porosity-pressure model and the proposed pellet mill compaction model into an iterative analysis approach. Details of the iterative approach will be explained later in this chapter. This approach requires a robust model that can accurately predict the resulting porosity of the compact corresponding to the friction build-up from the die channel. Compaction model that provides the best fit to the compaction results of the ground EFB compost powder was chosen in this analysis. The results obtained from the iteration approach were then compared with data obtained from existing literature.

6.2 Iteration procedure

A flow chart showing the iterative method is presented in Figure 6.2. Given at any die geometry $\frac{\boldsymbol{H}}{\boldsymbol{D}}$ and material properties, the steady-state pelleting condition was solved iteratively by first predicting the input compact porosity $\boldsymbol{\varepsilon}$ with an initial guess of pelleting pressure. The Kawakita model was used to predict the porosity-pressure relationship as the model was able to provide the best fit into the experimental data (R^2 >0.999) as described in the Chapter 3 Section 3.5.3. The predicted compact porosity was then used to calculate the resulting pelleting pressure by using the proposed pellet mill compaction model from Equation (5.15).

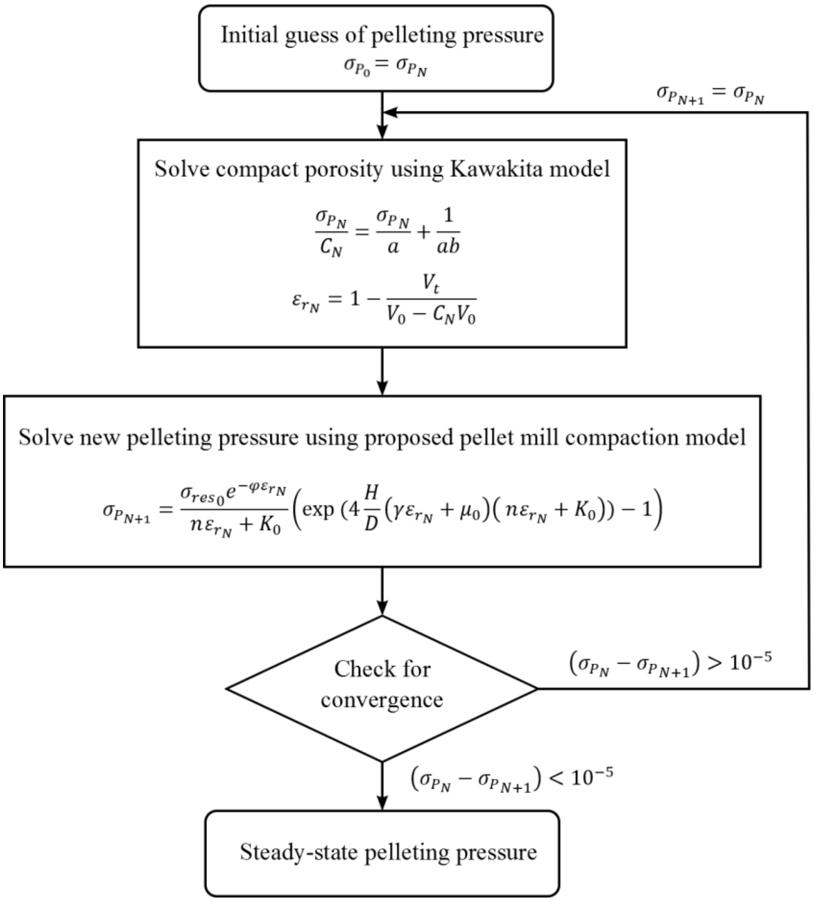

Figure 6.2: Iteration algorithm for solving steady-state pelleting pressure

Table 6.1 lists the values of the empirical parameters from Equation (5.15) corresponding to the EFB powder particle size and moisture content used in the iteration process. The iterative process is continued using the updated value of pelleting pressure until the convergence is attained where the difference between pelleting pressures is less than 10^{-5} MPa. This converged value of pelleting pressure will be known as the steady-state pelleting pressure.

Table 6.1: Values of physical parameter of the pellet mill compaction model used

Particle size (μm)	Moisture content (% w.b.)	Radial-axial transmission ratio $K = n\varepsilon + K_0$		Residual stress $\sigma_{res} = \sigma_{res_0} e^{-\varphi\varepsilon_r}$		Coefficient of friction $\mu = \gamma\varepsilon + \mu_0$	
		n	K_0	φ	σ_{res_0} (MPa)	γ	μ_0
150-300	5	0.0283	0.4652	7.086	33.288	0.198	0.048
	10	-0.4118	0.6216	5.616	6.084	0.258	0.082

	15	-0.7657	0.7037	6.439	2.273	0.100	0.225
	25	-3.3187	0.8305	6.805	1.047	0.749	0.329
300-600	5	-0.0158	0.4068	8.070	41.079	0.255	0.053
	10	-0.7206	0.5394	4.936	6.012	0.203	0.076
	15	-0.7882	0.6361	4.650	2.655	0.020	0.162
	25	-2.5966	0.7641	3.556	0.862	-0.192	0.358

A number of assumptions and limitation made in the current iteration analysis of the steady-state pellet mill compaction including:

1) Negligible gravitational force on the body
2) Constant room temperature
3) Heat generated by friction is neglected
4) Variation of porosities is limited to the boundary conditions from the obtained experimental data.
5) The magnitude of applied pressure in relation to the cross section area of the applied load is constant
1) Calculation of pressure assumes homogenous porosity in all layers *i.e.* each iteration fully displaces with a new single layer of compact to simplify and reduce calculation load.
2) Moisture content and particle size is homogenous

6.3 Results and discussion

The results of the steady-state pelleting pressure obtained from the iteration analysis with respect to the die geometry $\frac{H}{D}$ are shown in Figure 6.3. At a given die geometry $\frac{H}{D}$, the iteration converged into two values, depending on the values of the initial guess of the pelleting pressure:

(a) Below at a certain pressure, the pelleting pressure does not converge, but reduced to zero. This pressure indicates the minimum pelleting pressure required to initiate pelleting for stable pellet formation. This minimum initiation pelleting pressure requirement decreased with the increase of die geometry.

(b) With the initial guess of the pelleting pressure above the minimum pelleting pressure, the iteration would converge to a constant value, known as the steady-state pelleting pressure. The steady-state pelleting pressure increases with the increase in die geometry.

(c) The steady-state pressure line and the minimum initiation pelleting pressure line intercepts at a critical point. Iteration with the die geometry below this point will not converge, which suggests that no stable pellets will be formed.

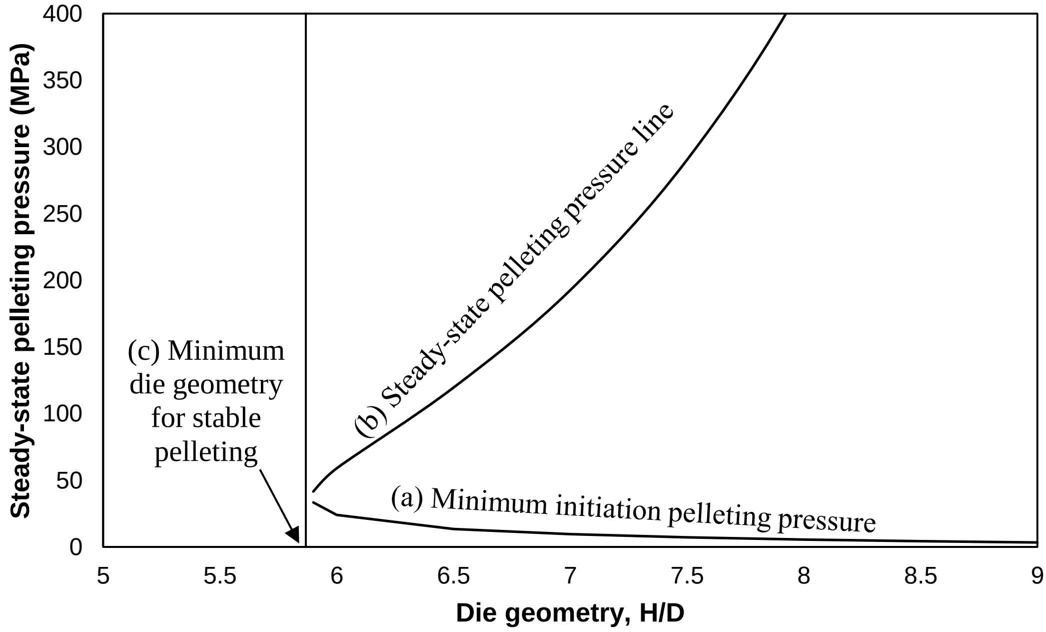

Figure 6.3: Example of relationship between the steady-state pelleting pressure and the die geometry for EFB compost powder with particle size of 150-300 μm and moisture content of 15%

6.3.1 Steady-state pelleting pressure

The effects of moisture content of the EFB compost powder on the steady-state pelleting pressure correspond to the particle size of 150-300 µm and 300-600 µm are shown in Figure 6.4(a) and (b) respectively. The steady-state pelleting pressure appears to increase with the increase in die geometry, and increases rapidly with higher moisture content. The required die geometry for stable pelleting decreased with smaller particle size and with higher moisture content.

Assuming constant die geometry of $\frac{H}{D}$ = 7 and particle size of 150-300 µm, the steady-state pelleting pressure at 25% moisture content are significantly higher than at 15% moisture content, and no steady-state pressure formed at 5% and 10% moisture content. This however, appears to contrast with the results obtained the single pellet press method (Chapter 5) where the ejection force decreased with the addition of moisture. The discrepancy between the predicted steady-state pressure and single press method can be explained with the different die geometry used in the analysis. In single pellet press method, the friction forces measured with the powder compacts ejected at a low height-diameter ratio ($\frac{H}{D}$ < 1) is significantly lower than the die geometry $\frac{H}{D}$ used in actual pellet mill of about 4 to 10.

According to the pellet mill compaction model (Equation (5.7)), the relation between the pelleting pressure and the model variables (coefficient of friction μ, and radial-axial transmission ratio K) is exponential. As of result, an increase in μ and K correspond to the addition of moisture may compound to the exponential increase in pelleting pressure with larger die geometry. On the contrary, for any given infinitely small value of $\frac{H}{D}$, the expression in (Equation (5.7)) is reduced to a linear relation of pelleting pressure vs. residual die wall pressure σ_{res} as the exponential function approaches unity. It is interesting to note that the residual die wall pressure σ_{res} decreased with the increase in moisture content (Chapter 5). This shows that the analysis solely based on the ejection force obtained with low die geometry $\frac{H}{D}$ should approached with caution, as it may not necessary reflect the actual condition of a pellet mill.

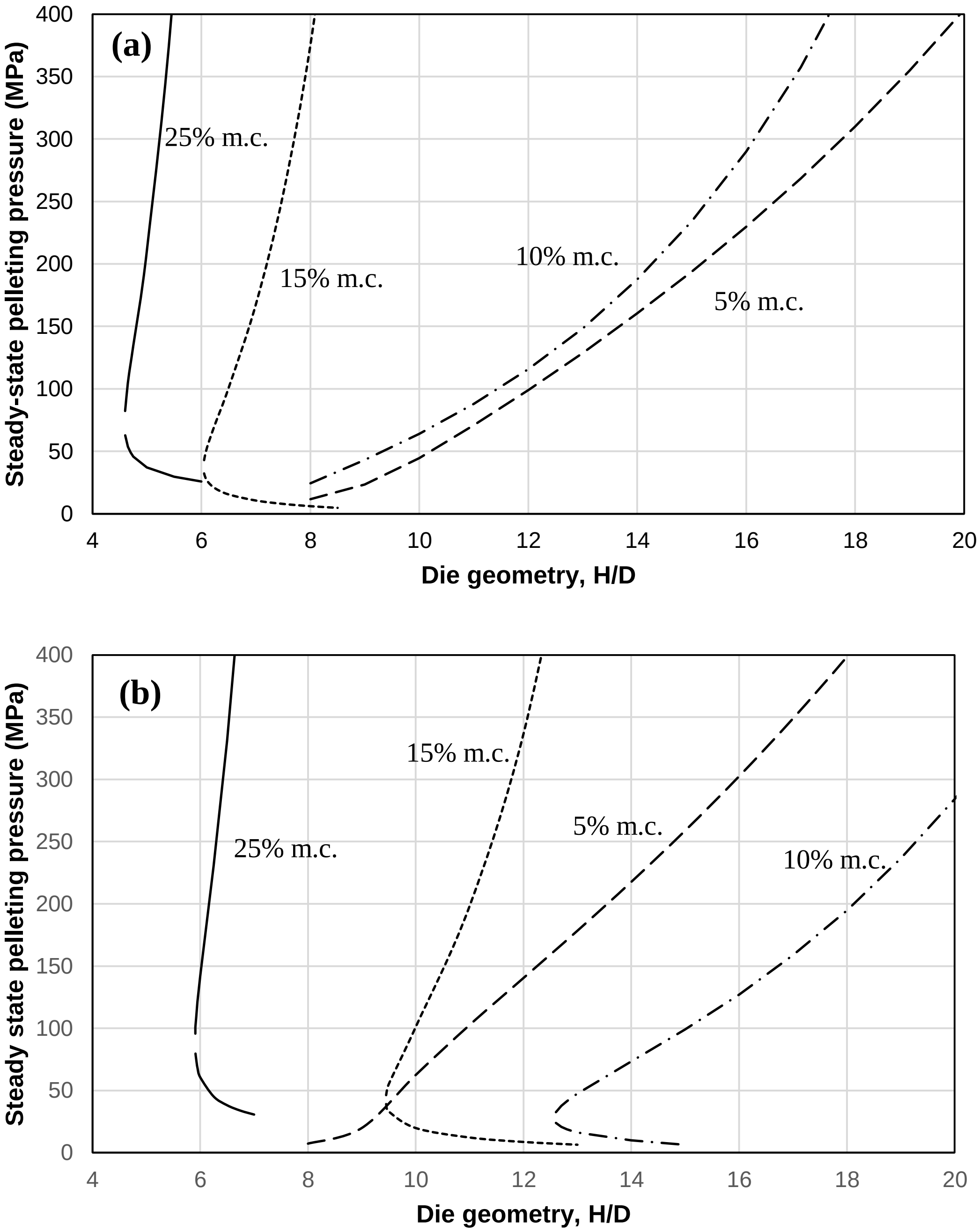

Figure 6.4: Comparison of steady-state pelleting pressure with different moisture content for EFB compost with particle size (a) 150-300 µm and, (b) 300-600 µm. Results for 25% moisture content cropped for clarity.

The rapid increase in steady-state pelleting pressure correspond to the high moisture content could also be used to explain the tendency of clogging in pellet mill due to the excess moisture content as observed in several pilot studies. Clogging may occur when the pelleting pressure from the die exceeded the limit of the roller pressure powered by the motor of the pellet mill (Stelte et al. 2012). Tabil and Sokhansanj

(1996) found that the pelleting using 6.1mm diameter ($\frac{H}{D}$ = 7.31) die would likely to choke with moisture content of the alfafa grind above 9%, while larger die size of 7.8mm (smaller die geometry $\frac{H}{D}$ = 4.10) could handle grind moisture up to 12%. Said et al. (2015) studied the influence of densification parameters on rice straw pellets and found that pelleting with 12% moisture content and die geometry $\frac{H}{D}$ of 4 did not produce any pellets, but increasing the moisture content to 17% would result in clogging of the die hole. This shows that the increased moisture of content and die geometry increased the tendency to cause blockage in the pellet mill. By reducing the moisture content or die geometry, the steady-state pelleting pressure can be decreased which reduces the operation load of the pellet mill.

6.3.2 Porosity and pellet strength

The variation of steady-state pelleting pressure with die geometry and material properties suggest significant impact on the physical property of the produced pellets. Therefore, previous empirical analysis on pressure-porosity and pellet strength-porosity relationship was used to predict the resulting physical property of the pellets from the steady-state pelleting pressure. Figure 6.5 shows the relationship between the in-die compact porosity of EFB compost and the die geometry correspond to the particle size and moisture content. The in-die compact porosity was calculated using the fitted Kawakita model presented in Chapter 3. The in-die compact porosity was chosen since the strength of the EFB compost pellets was analysed in reference to the in-die compact porosity. The relationship between the pellet strength and die geometry will be presented later.

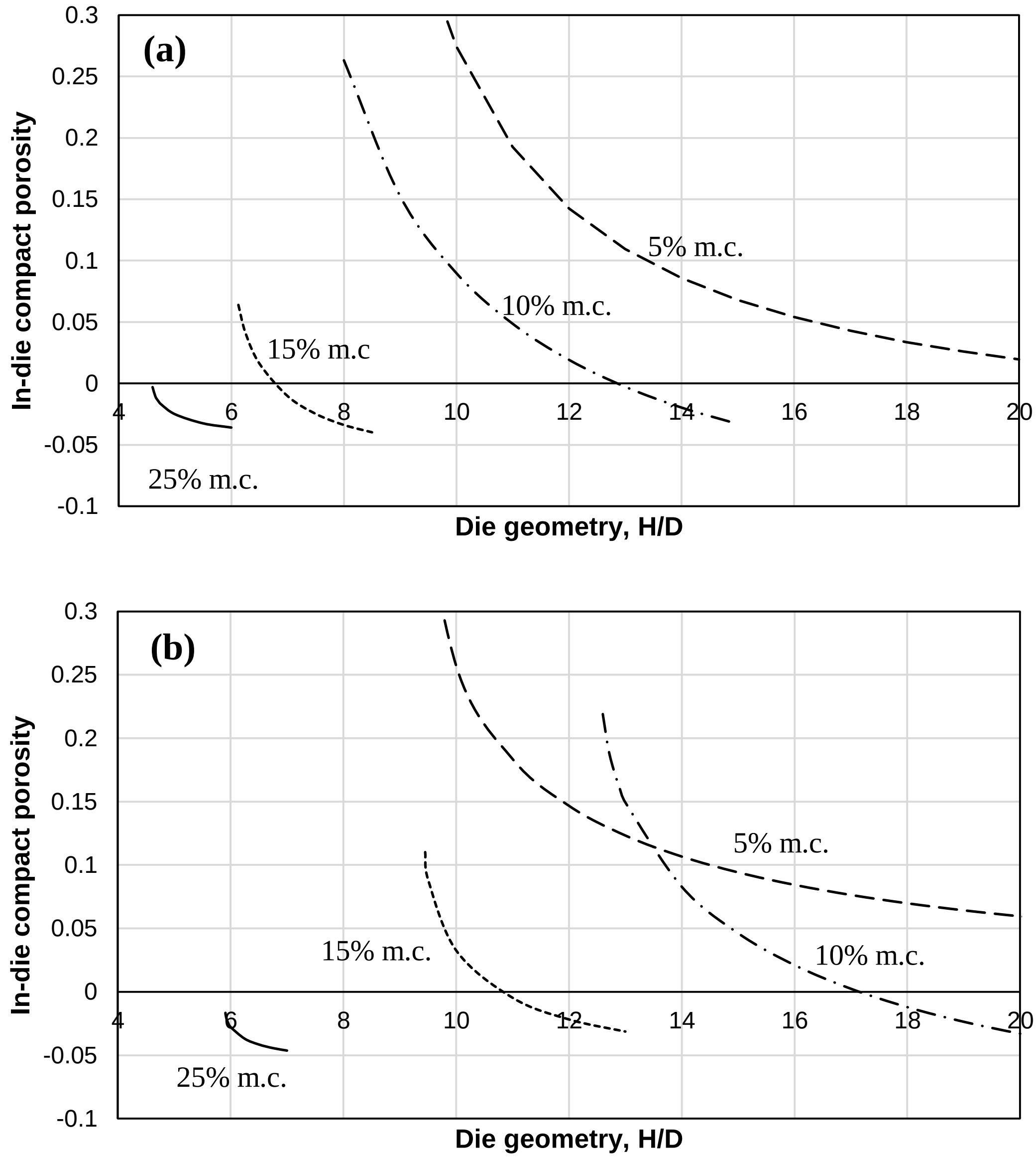

Figure 6.5: Comparison of in-die compact porosity with different moisture content for EFB compost with particle size of (a) 150-300 μm and, (b) 300-600 μm

As expected, the predicted in-die porosity of the EFB compact decreases approached towards zero with the increase in die geometry which corresponds to the increase in steady-state pelleting pressure. Zero porosity can be obtained with shorter die geometry from the resulting increase in moisture content and smaller particle size. This also suggests that pelleting with the die geometry beyond the zero porosity limits would be wasteful as the compaction energy was used to expel moisture from the compact with diminishing improvement on the pellet porosity.

Figure 6.6 shows the relationship between the final pellet strength and die geometry correspond the moisture content and particle size. The final pellet strength was predicted using the fitted Ryskevitch-Duckworth equation (Chapter 4) and the porosity data from Figure 6.5.

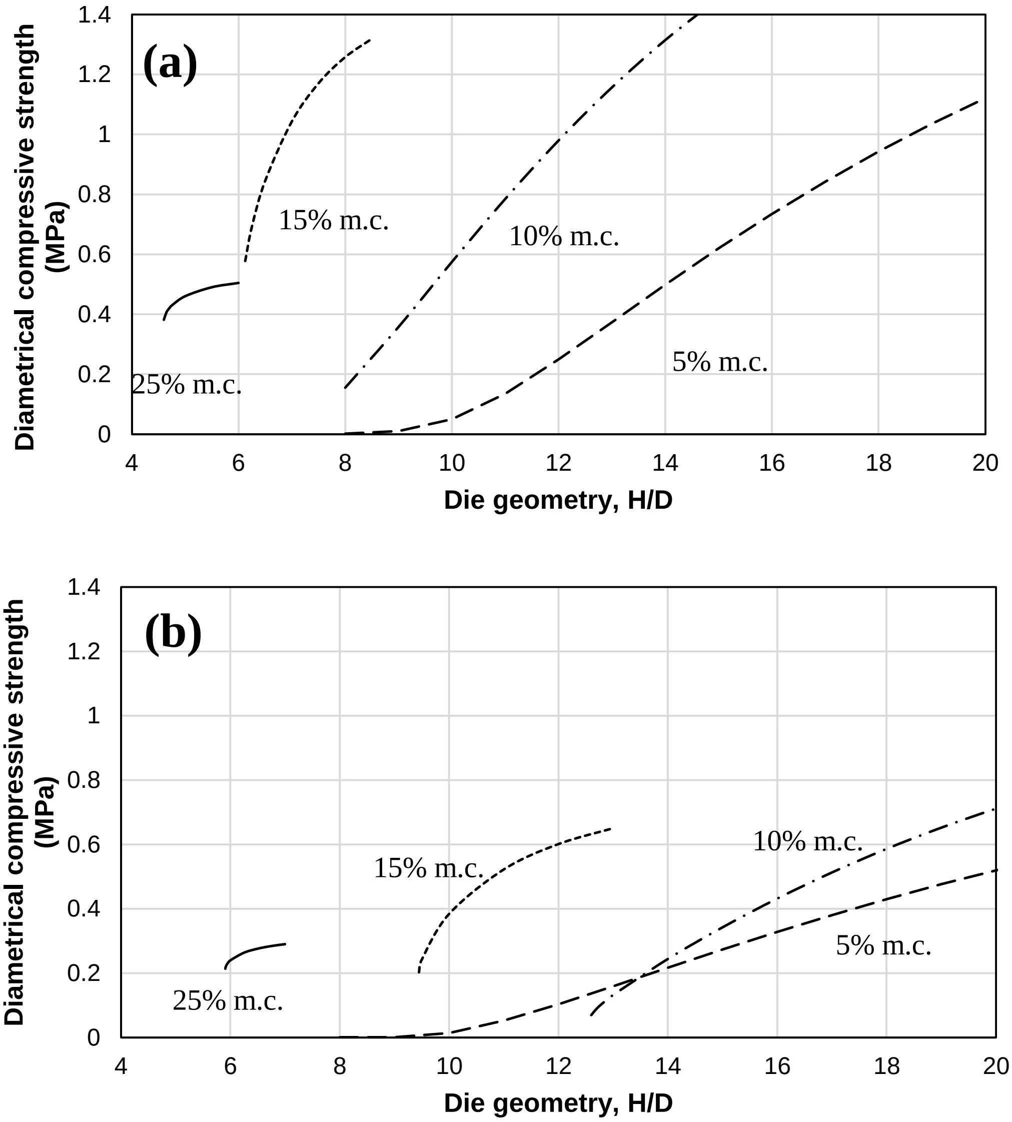

Figure 6.6: Comparison of pellet diametrical compressive strength with different moisture content for EFB compost with particle size of (a) 150-300 µm and, (b) 300-600 µm

Corresponding to the decrease in pellet porosity, the diametrical compressive strength appears to increase with the increase in die geometry and plateau towards the end of the die geometry which is consistent with pilot studies observed by other researchers. Tabil and Sokhansanj (1996) noted that the increase in die geometry $\frac{H}{D}$

from 4.10 to 6.1 increased the pellet durability made of alfalfa grind from 49.8% to 65.8%. Čolović et al. (2010) studied the effect of die geometry on physical quality of pelleted cattle feed and found that increasing the die geometry from $\frac{H}{D}$ 3 to 8 increased the pellet hardness twofold. Addition of moisture also drastically increased the final diametrical compressive strength of the pellets assuming constant die geometry and this was attributed by the rapid increase in steady-state pelleting pressure due the increased adhesion to the die wall surface and in addition to the increased compatibility from the addition of moisture. This was also observed in the studies of (Ishii and Furuichi 2014) where the rice straw pellets shows a twofold improvement on durability by increasing the moisture content from 15% to 20%.

6.4 Conclusions

It has been established that the steady-state pelleting pressure can be predicted using the iterative method presented in this chapter. Using the proposed pellet mill compaction model and empirical model that describe pressure-porosity relationship, the steady-state pelleting pressure was estimated with various conditions of die geometry, moisture content and particle size. The moisture content, die geometry and particle size was found to significantly influence the steady-state pelleting pressure and the pellets strength as of result. Increasing moisture content and die geometry drastically increases the steady-state pelleting pressure and could enhance the pellet strength; however, this would increase the tendency of blockage in the pellet mill if the pellet mill motor fails to overcome the friction induced in the die channel. These results are expected to be useful in selecting the optimal processing conditions for efficient pellet production and quality pellets that closely resembles the actual condition in pellet mills.

CHAPTER 7:
CONCLUSIONS, RECOMMENDATIONS, AND FUTURE WORK

7.1 Conclusions

The aim of this research is sought to investigate the mechanism of pellet mill compaction process and to evaluate the effects of moisture content, particle sizes and the applied compaction pressure on the compactability, compressibility, and nutrient release behaviour of the EFB compost pellets. Ground EFB compost with initial moisture content ranging from 5% to 25% of total mass, and particle size between 150 – 300 μm and 300 – 600 μm were used to study the compaction behaviour. 8 mm diameter EFB compost pellets were produced with the compaction pressure ranging from 10 MPa to 160 MPa. Compression tests and nutrient release tests were then carried out on the produced pellets. These were followed by analytical analysis which describes the compaction behaviour of ground EFB compost, mechanical strength and nutrient release behaviour of EFB compost pellets.

From the literature, a new theoretical model that describes pellet mill compaction process was proposed as $\sigma_P = \frac{\sigma_{res}}{K}\left(e^{4\frac{H}{D}\mu K} - 1\right)$. Instrumented die with the capability for simultaneous measurement of top, bottom axial pressure, and radial pressure was used to obtain the physical parameter of the proposed model. The proposed new pellet mill compaction model was found able to fit into the experimental data with the model variable parameters obtained independently with the instrumented die.

The instrumented die was used to characterise the effect of moisture content, particle size and the applied compaction pressure on the model variable of proposed model. The following conclusions were as:

1) Compaction behaviour of ground EFB compost:

a) The compaction behaviour of the ground EFB compost was studied using the same 8mm instrumented die. The total specific energy required for compacting EFB compost was reduced from 35.2 MJ/t to 8.2 MJ/t with increase of moisture content from 5% to 25% for the particle size of 300-600 µm. Decreasing the particle size of the EFB compost from 300-600 µm to 150-300 µm showed an 6 – 19% reduction in total specific energy.

b) Results showed that the porosity of the produced pellets decreased with the increase in applied compaction pressure. The resulting pellet porosity also appeared to be affected by the initial moisture content and the particle size of the EFB compost. Increasing the moisture content from 5% to 15% resulted in a decrease in pellet porosity after ejection and storage. However, increasing the moisture content to 25% resulted in increased pellet porosity. Coarser particle size also resulted in increased pellet porosity.

c) To characterise the compaction behaviour of the EFB compost, empirical Heckel model and the Kawakita model was used. Both "in die" and "out of die" results of the Heckel and Kawakita models were compared. The Kawakita model provided the best fit with the compaction data of all range of applied compaction pressure and moisture content studied. Reasonable fit was obtained for both "in die" and "out of die" Heckel model, however limited within pressure range before mechanical dewatering occurred at high compaction pressure. In contrast, the Kawakita model appears to be more robust and less sensitive towards the effect of mechanical dewatering at high moisture content. Both models suggest that the compactability of the EFB compost powder increased with the increase in moisture content but showed minor or no significant difference with different particle size.

2) Properties of EFB compost pellets:

   i) Mechanical behaviour

      (1) The effects of storage, applied compaction pressure, moisture content, and particle size on the diametrical compressive strength of EFB compost pellets were studied.

(2) The diametrical compressive strength of the pellets increased with the decrease in pellet porosity of which corresponded to the increased applied compaction pressure, the pellet initial moisture content and particle size.

(3) When measured immediately after ejection, increasing the initial moisture content from 5% to 25% would decrease the diametrical compressive strength from 1.47 MPa to 0.28 MPa for 150-300 µm, and 0.80 MPa to 0.24 MPa for 300-600 µm. EFB compost pellets with coarser particle showed significantly weaker strength.

(4) After storage, the pellets showed significant decrease in strength particularly in pellets with low initial moisture content. Increasing the moisture content however, showed minor degradation or increase in strength after storage, possibly due to new bond formation of solid bridge from the evaporation of dissolved solid. This assumption was supported by the increase in bonding capacity and zero porosity compressive strength after storage with the Ryshkewitch – Duckworth equation.

b) Nutrient release behaviour

i) Rapid laboratory methodology using temperature-controlled incubation method (TCIM) was used to study nutrient release pattern of the EFB compost pellets. Process parameters which could affect the diffusion behaviour such as compaction pressure, moisture content and particle size are investigated.

ii) Spiro and Siddique kinetic model was used in the diffusion study and show good agreement with the experimental results. The diffusion constant was found to be correlated to the diametrical compressive strength. The increase in diametrical compressive strength of the pellets would result in decreased diffusion rate constant of the EFB compost pellets. However, there is no noticeable difference observed for pellets with diametrical compressive strength above 0.2 MPa.

iii) The diffusion rate constant was significantly decreased with smaller particle sizes possibly due to the reduced pathway for diffusion as the pellets were able to retain in shape for a longer period of time when submerged in water.

3) Modelling of pellet mill compaction mechanism:
   a) Radial axial transmission ratio
      i) Increased with decreasing compact porosity which corresponds to the compaction pressure.
      ii) A slight decrease in the transmission ratio with decreasing particle size of the EFB compost powder.
      iii) Significantly increased with the increase in moisture content from 5% to 25%.
   b) Residual die wall pressure
      i) Increased with the decrease in compact porosity and;
      ii) Increased with the decrease in moisture content possibly due to the increased initial modulus.
      iii) No significant change was observed with different particle sizes.
   c) Coefficient of friction
      i) Coefficient of friction during ejection decreased with the decrease in in-die relaxed porosity due to the changes in surface morphology.
      ii) Increased with finer particle size possibly due to the increased adhesion tendency with large surface contact area between the compact and the die wall.
      iii) Increased coefficient of friction during ejection was observed with the increase in moisture content and possibly related to the increased adhesion of the compact to the die wall.

4) Steady-state pellet mill compaction:
   a) Provided prediction of steady-state pellet mill compaction pressure and the resulting porosity and pellet strength
   b) The iteration analysis effectively predicted the trend for variation of pellet mill compaction pressure with varying die geometry, particle size and moisture content.

c) Steady-state pellet mill compaction pressure is dependent on the die geometry and strongly affected by coefficient of friction
d) Primary root cause of clogging in pellet mill with the increase of moisture content was due to the increased adhesion to the die surface corresponding to the increase of coefficient of friction.

7.2 Recommendations

It has been concluded that a controlled release of nutrient can be achieved with a smaller particle size. Increasing the applied compaction pressure would improve the diametrical compressive strength and eventually reduce the diffusion rate of the pellet. However, there will be no significant reduction in diffusion rate above 0.2 MPa of diametrical compression strength. Regardless, pellets should be produced with the highest possible strength to avoid breakage during storage and transportation as this would reduce the efficiency of the EFB compost pellets. Moisture content of 10% to 15% is suggested to produce strong and durable pellets.

7.3 Future work

- Current research was conducted on limited particle size range and diameter of the die instrument due to the upper limit of the compaction force applied with the current compression-tensile testing machine (Lloyd LR10K Plus, UK). Further investigation should consider larger particle size range using different die size with larger testing machine capacity.
- The compaction test was conducted at a fixed room temperature. Research on the effect of temperature on the pellet mill mechanism as well as the densification behaviour of EFB compost should be considered in future studies.
- Current studies on the nutrient release pattern of the EFB compost pellets were conducted using rapid laboratory method with the pellets submerged in distilled water. In future studies, field tests should be considered to correlate the results from the laboratory method. In addition, the concentration of the nutrient released was measured in total according to the electrical

conductivity. Separate measurement of nutrient such as ammonia, nitrate, and nitrite using ion selective electrode (ICE) method would useful to determine the kinetic of each nutrient.

- There is a lack of experimental data in pilot-scale studies that able to correlate with the theoretical results of steady-state pellet mill compaction obtained from the iteration analysis. Future studies should consider pilot tests with actual pellet mill for proper comparison. The material used in the fabricating the instrumented die should reflect on the material used in actual pellet mill.

CHAPTER 8:
REFERENCES

Abdel-Hamid, S., F. Alshihabi, and G. Betz. 2011. "Investigating the Effect of Particle Size and Shape on High Speed Tableting through Radial Die-Wall Pressure Monitoring." *International Journal of Pharmaceutics* 413 (1–2): 29-35. doi: http://dx.doi.org/10.1016/j.ijpharm.2011.04.012.

Abdel-Hamid, S., and G. Betz. 2011a. "Radial Die-Wall Pressure as a Reliable Tool for Studying the Effect of Powder Water Activity on High Speed Tableting." *International Journal of Pharmaceutics* 411 (1–2): 152-161. doi: http://dx.doi.org/10.1016/j.ijpharm.2011.03.066.

Abdel-Hamid, S., and G. Betz. 2011b. "Study of Radial Die-Wall Pressure Changes During Pharmaceutical Powder Compaction." *Drug Development and Industrial Pharmacy* 37 (4): 387-395. doi: 10.3109/03639045.2010.513985.

Abdullah, N, and F Sulaiman. 2013a. "The Oil Palm Wastes in Malaysia." *Chapter* 3: 75-100.

Abdullah, N., and F. Sulaiman. 2013b. "The Properties of the Washed Empty Fruit Bunches of Oil Palm." *Journal of Physical Science* 24 (2): 117-137.

Adapa, P., L. Tabil, and G. Schoenau. 2009. "Compaction Characteristics of Barley, Canola, Oat and Wheat Straw." *Biosystems Engineering* 104 (3): 335-344. doi: http://dx.doi.org/10.1016/j.biosystemseng.2009.06.022.

Adapa, P., L. Tabil, G. Schoenau, and A. Opoku. 2010. "Pelleting Characteristics of Selected Biomass with and without Steam Explosion." *International Journal of Agricultural and Biological Engineering* 3 (3): 62-79. doi: 10.3965/j.issn.1934-6344.2010.03.062-079.

Agnew, J. M., and J. J. Leonard. 2003. "The Physical Properties of Compost." *Compost Science & Utilization* 11 (3): 238-264. doi: http://dx.doi.org/10.1080/1065657X.2003.10702132.

Amira, R. D., A. R. Roshanida, M. I. Rosli, M. F. Zahrah, J. M. Anuar, and C. M. Adha. 2011. "Bioconversion of Empty Fruit Bunches (Efb) and Palm Oil Mill Effluent (Pome) into Compost Using Trichoderma Virens." *African Journal of Biotechnology* 10 (81): 18775-18780.

Andrejko, D., and J. Grochowicz. 2007. "Effect of the Moisture Content on Compression Energy and Strength Characteristic of Lupine Briquettes." *Journal of Food Engineering* 83 (1): 116-120. doi: http://dx.doi.org/10.1016/j.jfoodeng.2006.12.019.

Anuar, M. S., and B. J. Briscoe. 2009. "The Elastic Relaxation of Starch Tablets During Ejection." *Powder Technology* 195 (2): 96-104.

ASTM. 2014. *Standard Test Methods for Specific Gravity of Soil Solids by Water Pycnometer (D854-14)*. American Society for Testing and Materials

Baharuddin, A. S., N. A. Rahman, U. K. Shan, M. A. Hassan, M. Wakisaka, and Y. Shirai. 2013. "Evaluation of Pressed Shredded Empty Fruit Bunch (Efb)-Palm Oil Mill Effluent (Pome) Anaerobic Sludge Based Compost Using

Fourier Transform Infrared (Ftir) and Nuclear Magnetic Resonance (Nmr) Analysis." *African Journal of Biotechnology* 10 (41): 8082-8289.

Baharuddin, A. S., M. Wakisaka, Y. Shirai, S. Abd-Aziz, N. A. Abdul Rahman, and M. A. Hassan. 2009. "Co-Composting of Empty Fruit Bunches and Partially Treated Palm Oil Mill Effluents in Pilot Scale." *International Journal of Agricultural Research* 4 (2): 69-78.

Bernhart, M., O. O. Fasina, J. Fulton, and C. W. Wood. 2010. "Compaction of Poulry Litter." *Bioresource Technology*: 234-238.

Berry, H., and C. W. Ridout. 1950. "The Preparation of Compressed Tablets: Part Iii.—a Study of the Value of Potato Starch and Alginic Acid as Disintegrating Agents." *Journal of Pharmacy and Pharmacology* 2 (1): 619-629. doi: 10.1111/j.2042-7158.1950.tb12981.x.

Bhattacharya, S. C., S. Sett, and R. M. Shrestha. 1989. "State of the Art for Biomass Densification." *Energy Sources* 11 (3): 161-182. doi: 10.1080/00908318908908952.

Briscoe, B. J., and S. L. Rough. 1998. "The Effects of Wall Friction on the Ejection of Pressed Ceramic Parts." *Powder Technology* 99 (3): 228-233. doi: http://dx.doi.org/10.1016/S0032-5910(98)00113-2.

Carone, M. T., A. Pantaleo, and A. Pellerano. 2011. "Influence of Process Parameters and Biomass Characteristics on the Durability of Pellets from the Pruning Residues of Olea Europaea L." *Biomass and Bioenergy* 35 (1): 402-410. doi: http://dx.doi.org/10.1016/j.biombioe.2010.08.052.

Carson, L. C., and M. Ozores-Hampton. 2012. "Methods for Determining Nitrogen Release from Controlled-Release Fertilizers Used for Vegetable Production." *HortTechnology* 22 (1): 20-24.

Cheney, E., and D. Kincaid. 2012. *Numerical Mathematics and Computing*: Cengage Learning.

Chowhan, Z. T., I. C. Yang, A. A. Amaro, and L. H. Chi. 1982. "Effect of Moisture and Crushing Strength on Tablet Friability and in Vitro Dissolution." *Journal of pharmaceutical sciences* 71 (12): 1371-1375.

Chu, K. R., E. Lee, S. H. Jeong, and E. S. Park. 2012. "Effect of Particle Size on the Dissolution Behaviors of Poorly Water-Soluble Drugs." *Archives of pharmacal research* 35 (7): 1187-1195.

Cocolas, H. G., and N. G. Lordi. 1993. "Axial to Radial Pressure Transmission of Tablet Excipients Using a Novel Instrumented Die." *Drug development and industrial pharmacy* 19 (17-18): 2473-2497.

Čolović, R., Đ. Vukmirović, R. Matulaitis, S. Bliznikas, V. Uchockis, V. Juškienė, and J. Lević. 2010. "Effect of Die Channel Press Way Length on Physical Quality of Pelleted Cattle Feed." *Food and Feed Research* 37 (1): 1-6.

Cooper, A. R., and L. E. Eaton. 1962. "Compaction Behavior of Several Ceramic Powders." *Journal of the American Ceramic Society* 45 (3): 97-101. doi: 10.1111/j.1151-2916.1962.tb11092.x.

Crawford, R. J., and D. W. Paul. 1981. "Radial and Axial Die Pressures During Solid Phase Compaction of Polymeric Powders." *European Polymer Journal* 17 (10): 1023-1028.

Cunningham, J. C., I. C. Sinka, and A. Zavaliangos. 2004. "Analysis of Tablet Compaction. I. Characterization of Mechanical Behavior of Powder and

Powder/Tooling Friction." *Journal of Pharmaceutical Sciences* 93 (8): 2022-2039. doi: 10.1002/jps.20110.

Denny, PJ. 2002. "Compaction Equations: A Comparison of the Heckel and Kawakita Equations." *Powder Technology* 127 (2): 162-172.

Department of Statistics. 2013. National Accounts Gross Domestic Products Malaysia. http://www.statistics.gov.my/portal/index.php.

Doelker, E., and D. Massuelle. 2004. "Benefits of Die-Wall Instrumentation for Research and Development in Tabletting." *European Journal of Pharmaceitics and Biopharmaceutics 58*: 427-444.

Duberg, M., and C. Nyström. 1986. "Studies on Direct Compression of Tablets Xvii. Porosity—Pressure Curves for the Characterization of Volume Reduction Mechanisms in Powder Compression." *Powder Technology* 46 (1): 67-75. doi: http://dx.doi.org/10.1016/0032-5910(86)80100-0.

Duckworth, W. 1953. "Discussion of Ryshkewitch Paper by Winston Duckworth." *Journal of the American Ceramic Society* 36: 68.

Eriksson, M., and G. Alderborn. 1994. "Mechanisms for Post-Compaction Changes in Tensile Strength of Sodium Chloride Compacts Prepared from Particles of Different Dimensions." *International Journal of Pharmaceutics* 109 (1): 59-72.

Fasina, O. O. 2008. "Physical Properties of Peanut Hull Pellets." *Bioresource Technology* 99 (5): 1259-1266. doi: http://dx.doi.org/10.1016/j.biortech.2007.02.041.

Fassihi, A. R. 1987. "Kinetics of Drug Release from Solid Matrices: Effect of Compaction Pressure." *International Journal of Pharmaceutics* 37 (1): 119-125.

Fell, J. T., and J. M. Newton. 1970. "Determination of Tablet Strength by the Diametral - Compression Test." *Journal of Pharmaceutical Sciences* 59 (5): 688-691.

Forny, L., A. Marabi, and S. Palzer. 2011. "Wetting, Disintegration and Dissolution of Agglomerated Water Soluble Powders." *Powder Technology* 206 (1): 72-78.

Friedman, S.P., and Y. Mualem. 1994. "Diffusion of Fertilizers from Controlled-Release Sources Uniformly Distributed in Soil." *Fertilizer Research* 39: 19-30.

Fujimoto, K., and T. Togo. 1986. "ゴムの体積弾性率とポアソン比 [Bulk Modulus and Poisson's Ratio of Rubber]." *Nippon Gomu Kyokaishi* 59 (7): 385-398.

Fukami, J., E. Yonemochi, Y. Yoshihashi, and K. Terada. 2006. "Evaluation of Rapidly Disintegrating Tablets Containing Glycine and Carboxymethylcellulose." *International journal of pharmaceutics* 310 (1): 101-109.

García-Gómez, A., M. P. Bernal, and A. Roig. 2005. "Organic Matter Fractions Involved in Degradation and Humification Processes During Composting." *Compost Science & Utilization* 13 (2): 127-135.

Goh, S. M., S. Alten, G. van Dalen, R. S. Farr, C. Gamonpilas, and M. N. Charalambides. 2008. "The Mechanical Properties of Model-Compacted Tablets." *Journal of Materials Science* 43 (22): 7171-7178.

Gupta, A., G. E. Peck, R. W. Miller, and K. R. Morris. 2005. "Effect of the Variation in the Ambient Moisture on the Compaction Behavior of Powder Undergoing Roller-Compaction and on the Characteristics of Tablets Produced from the Post-Milled Granules." *Journal Pharmaceutical Science* 94 (10): 2314-26. doi: 10.1002/jps.20414.

H., Stephen W., S. D. Vivek, and M. Vikas. 2008. "Compression and Compaction." In *Pharmaceutical Dosage Forms - Tablets*, 555-630. CRC Press.

Hara, M. 2001. *Fertilizer Pellets Made from Composted Livestock Manure*: Food & Fertilizer Technology Center Taiwan.

Hashim, K., S. Tahiruddin, and A. J. Asis. 2012. "Palm and Palm Kernel Oil Production and Processing in Malaysia and Indonesia." In *Palm Oil - Production, Processing, Characterization, and Uses*, edited by Oi-Ming Lai, Chin-Ping Tan and Casimir C. Akoh: AOCS press.

Haware, R. V., I. Tho, and A. Bauer-Brandl. 2010. "Evaluation of a Rapid Approximation Method for the Elastic Recovery of Tablets." *Powder Technology* 202 (1): 71-77.

Heckel, R.W. 1961. "Density-Pressure Relationships in Powder Compaction." *Transactions of the Metallurgical Society*: 671-675.

Heriansyah. 2011. "Optimising the Use of Oil Palm by-Product (Efb) as Fertiliser Supplement for Oil Palm" *3rd Palm Oil Summit - Yield Improvement & Carbon Management Bali*,

Hersey, J. A., and J. E. Rees. 1971. "Deformation of Particles During Briquetting." *Nature* 230 (12): 96-96.

Hersey, John A., and J.E. Rees. 1970. "The Effect of Partizle Size on the Consolidation of Powders During Compaction." In *Particle Size Analysis Conference, University of Bradford*.

Higuchi, T., T. Shimamoto, S. P. Eriksen, and T. Yashiki. 1965. "Physics of Tablet Compression Xiv. Lateral Die Wall Pressure During and after Compression." *Journal of Pharmaceutical Sciences* 54 (1): 111-118. doi: 10.1002/jps.2600540126.

Holm, J. K., U. B. Henriksen, J. E. Hustad, and L. H. Sørensen. 2006. "Toward an Understanding of Controlling Parameters in Softwood and Hardwood Pellets Production." *Energy & Fuels* 20 (6): 2686-2694. doi: 10.1021/ef0503360.

Holm, J. K., U. B. Henriksen, K. Wand, J. E. Hustad, and D. Posselt. 2007. "Experimental Verification of Novel Pellet Model Using a Single Pelleter Unit." *Energy & Fuels* 21 (4): 2446-2449. doi: 10.1021/ef070156l.

Holm, J. K., W. Stelte, D. Posselt, J. Ahrenfeldt, and U. B. Henriksen. 2011. "Optimization of a Multiparameter Model for Biomass Pelletization to Investigate Temperature Dependence and to Facilitate Fast Testing of Pelletization Behavior." *Energy & Fuels* 25 (8): 3706-3711. doi: 10.1021/ef2005628.

Hölzer, A. W, and J. Sjögren. 1979. "Instrumentation and Calibration of a Single-Punch Press for Measuring the Radial Force During Tableting." *International Journal of Pharmaceutics* 3 (4): 221-230.

Hölzer, A. W., and J. Sjögren. 1981. "Friction Coefficients of Tablet Masses." *International Journal of Pharmaceutics* 7 (4): 269-277. doi: http://dx.doi.org/10.1016/0378-5173(81)90052-1.

Huckle, P.D., and M. P. Summers. 1985. "The Use of Strain Gauges for Radial Stress Measurement During Tableting." *Journal of Pharmacy and Pharmacology* 37 (10): 722-725.
Husain, Z., Z. Zainac, and Z. Abdullah. 2002. "Briquetting of Palm Fibre and Shell from the Processing of Palm Nuts to Palm Oil." *Biomass and Bioenergy* 22 (6): 505-509.
Igwe, J. C., and C. C. Onyegbado. 2007. "A Review of Palm Oil Mill Effluent (Pome) Water Treatment." *Global Journal of Environmental Research* 1 (2): 54-62.
Ilić, I., B. Govedarica, and S. Srčič. 2013. "Deformation Properties of Pharmaceutical Excipients Determined Using an in-Die and out-Die Method." *International Journal of Pharmaceutics* 446 (1): 6-15.
Ishii, K., and T. Furuichi. 2014. "Influence of Moisture Content, Particle Size and Forming Temperature on Productivity and Quality of Rice Straw Pellets." *Waste management* 34 (12): 2621-2626.
Jaganyi, D., and S. Mdletshe. 2000. "Kinetics of Tea Infusion. Part 2: The Effect of Tea-Bag Material on the Rate and Temperature Dependence of Caffeine Extraction from Black Assam Tea." *Food Chemistry* 70 (2): 163-165.
Jakobsen, S. T. 1996. "Leaching of Nutrients from Pots with and without Applied Compost." *Resources, Conservation and Recycling* 17 (1): 1-11.
Janssen, H. A. 1895. "Versuche Über Getreidedruck in Silozellen." *Zeitschr. d. Vereines deutscher Ingenieure* 39 (35): 1045-1049. doi: citeulike-article-id:7798398.
Johansson, B., and G. Alderborn. 2001. "The Effect of Shape and Porosity on the Compression Behaviour and Tablet Forming Ability of Granular Materials Formed from Microcrystalline Cellulose." *European Journal of Pharmaceutics and Biopharmaceutics* 52 (3): 347-357.
Kalidindi, S. R., A. Abusafieh, and E. El-Danaf. 1997. "Accurate Characterization of Machine Compliance for Simple Compression Testing." *Experimental Mechanics* 37 (2): 210-215. doi: 10.1007/BF02317861.
Kaliyan, N. 2008. "Densification of Biomass." Ph.D., University of Minnesota, Ann Arbor.
Kaliyan, N., and R. V. Morey. 2009. "Densification Characteristics of Corn Stover & Switchgrass." *Transaction of the ASABE* 52 (3): 907-920.
Kaliyan, N., and R. V. Morey. 2010. "Natural Binders and Solid Bridge Type Binding Mechanisms in Briquettes and Pellets Made from Corn Stover and Switchgrass." *Bioresource Technology* 101 (3): 1082-1090. doi: http://dx.doi.org/10.1016/j.biortech.2009.08.064.
Kawakita, K., and K.H. Lüdde. 1971. "Some Considerations on Powder Compression Equations." *Powder Technology* 4 (2): 61-68.
Khan, K. A., and C. T. Rhodes. 1972. "Effect of Compaction Pressure on the Dissolution Efficiency of Some Direct Compression Systems." *Pharmaceutica Acta Helvetiae* 47 (10): 594.
Kleinebudde, P. 1994. "Shrinking and Swelling Properties of Pellets Containing Microcrystalline Cellulose and Low Substituted Hydroxypropylcellulose: I. Shrinking Properties." *International journal of pharmaceutics* 109 (3): 209-219.

Kong, L. J., S. H. Tian, C. He, C. M. Du, Y. T. Tu, and Y. Xiong. 2012. "Effect of Waste Wrapping Paper Fiber as a “Solid Bridge” on Physical Characteristics of Biomass Pellets Made from Wood Sawdust." *Applied Energy* 98: 33-39.

Lachman, L., H. A. Lieberman, and J. L. Kanig. 1986. *The Theory and Practice of Industrial Pharmacy*. United States: Lea & Febiger.

Lai, Z. Y., H. B. Chua, and S. M. Goh. 2013. "Influence of Process Parameters on the Strength of Oil Palm Kernel Shell Pellets." *Journal of Materials Science* 48 (4): 1448-1456. doi: 10.1007/s10853-012-6897-x.

Leigh, S., J. E. Carless, and B. W. Burt. 1967. "Compression Characteristics of Some Pharmaceutical Materials." *Journal of pharmaceutical sciences* 56 (7): 888-892.

Lim, C. Y. 2014. Addressing Palm Oil Concerns. [Digital image]. The Star Online. http://www.thestar.com.my/news/environment/2014/09/08/addressing-palm-oil-concerns/.

Lim, K. H. 1989. "Trials on Composting Efb of Oil Palm with and without Prior Shredding and Liquid Extraction" *International Palm Oil Development Conference*, *Kuala Lumpur*: PORIM.

Liu, Z. G., A. Quek, and R. Balasubramanian. 2014. "Preparation and Characterization of Fuel Pellets from Woody Biomass, Agro-Residues and Their Corresponding Hydrochars." *Applied Energy* 113: 1315-1322.

Maarschalk, K. , K. Zuurman, H. Vromans, and G. K. Bolhuis. 1996. "Porosity Expansion of Tablets as a Result of Bonding and Deformation of Particulate Solids." *International journal of Pharmaceutics* 140: 185-193.

MacBain, R. 1966. *Pelleting Animal Feed*. Chicago, IL.

Mani, S., L. G. Tabil, and S. Sokhansanj. 2004a. "Evaluation of Compaction Equations Applied to Four Biomass Species." *Canadian Biosystems Engineering* 46 (3): 55-61.

Mani, S., L. G. Tabil, and S. Sokhansanj. 2004b. "Grinding Performance and Physical Properties of Wheat and Barley Straws, Corn Stover and Switchgrass." *Biomass and Bioenergy* 27 (4): 339-352.

Mani, S., L. G. Tabil, and S. Sokhansanj. 2006a. "Effects of Compressive Force, Particle Size and Moisture Content on Mechanical Properties of Biomass Pellets from Grasses." *Biomass and Bioenergy* 30 (7): 648-654. doi: http://dx.doi.org/10.1016/j.biombioe.2005.01.004.

Mani, S., L. G. Tabil, and S. Sokhansanj. 2006b. "Specific Energy Requirement for Compacting Corn Stover." *Bioresource Technology* 97 (12): 1420-1426. doi: http://dx.doi.org/10.1016/j.biortech.2005.06.019.

Mantanis, G. I., R. A. Young, and R. M. Rowell. 1994. "Swelling of Wood." *Wood Science and Technology* 28 (2): 119-134.

Marais, A. F., M. Song, and M. M. de Villiers. 2003. "Effect of Compression Force, Humidity and Disintegrant Concentration on the Disintegration and Dissolution of Directly Compressed Furosemide Tablets Using Croscarmellose Sodium as Disintegrant." *Tropical Journal of Pharmaceutical Research* 2 (1): 125-135.

Meakid, E. T. 1934. Pellet Mill. US 1954086 A, filed and issued

Mesnier, X., T. O. Althaus, L. Forny , G. Niederreiter, S. Palzer, M. J. Hounslow, and A. D. Salman. 2013. "A Novel Method to Quantify Tablet Disintegration." *Powder Technology*: 27-34.

Michrafy, A., J. A. Dodds, and M. S. Kadiri. 2004. "Wall Friction in the Compaction of Pharmaceutical Powders: Measurement and Effect on the Density Distribution." *Powder Technology* 148 (1): 53-55.

Michrafy, A., M. S. Kadiri, and J. A. Dodds. 2003. "Wall Friction and Its Effects on the Density Distribution in the Compaction of Pharmaceutical Excipients." *Chemical Engineering Research and Design* 81 (8): 946-952.

Mikkelsen, R. L., H. M. Williams, and A. D. Jr Behel. 1994. "Nitrogen Leaching and Plant Uptake from Controlled-Release Fertilizers." *Fertilizer Research* 37: 43-50.

Mohammad, N., M. Z. Alam, N. A. Kabbashi, and A. Ahsan. 2012. "Effective Composting of Oil Palm Industrial Waste by Filamentous Fungi: A Review." *Resources, Conservation and Recycling* 58: 69-78.

Mohammed, M. A. A., A. Salmiaton, W. A. K. G. Wan Azlina, and M. S. Mohamad Amran. 2012. "Gasification of Oil Palm Empty Fruit Bunches: A Characterization and Kinetic Study." *Bioresource Technology* 110: 628-636. doi: http://dx.doi.org/10.1016/j.biortech.2012.01.056.

Mollan, M. J., and M. Celik. 1995. "The Effects of Humidity and Storage Time on the Behavior of Maltodextrins for Direct Compression." *International journal of pharmaceutics* 114 (1): 23-32.

MPOB. 2015. Economics & Industry Development Division. Accessed February 6, http://bepi.mpob.gov.my/.

Mukhlis. 2006. "Composting of Oil Palm Empty Fruit Bunches with Trichoderma and Organic Nitrogen Supplementation and the Effects of the Compost on Growth of Tomato and Corn." Faculty of Agriculture, University Putra Malaysia. http://psasir.upm.edu.my/6232/.

Munoz-Hernandez, G., J. Domínguez-Dominguez, and O. Alvarado-Mancilla. 2006. "An Easy Laboratory Method for Optimizing the Parameters for
the Mechanical Densification Process: An Evaluation with an
Extruder." *Agricultural Engineering International: the CIGR Ejournal* VIII.

N.Kaliyan, and R. V. Morey. 2009. "Factors Affecting Strength and Durability of Densified Biomass Products." *Biomass and Bioenergy* 33 (3): 337-359. doi: http://dx.doi.org/10.1016/j.biombioe.2008.08.005.

Nahrul, H., A. A. Astimar, M. Anis, M. I. Hakimi, and A. Khalil. 2012. "Vermicomposting of Empty Fruit Bunch with Addition of Palm Oil Mill Effluent Solid." *Journal of Oil Palm Research*: 1542-1549.

Nedderman, R. M. 2005. *Statics and Kinematics of Granular Materials*: Cambridge University Press.

Nelson, E. 1955. "The Physics of Tablet Compression. Viii. Some Preliminary Measurements of Die Wall Pressure During Tablet Compression." *Journal of the American Pharmaceutical Association* 44 (8): 494-497.

Nicklasson, F., and G. Alderborn. 2000. "Analysis of the Compression Mechanics of Pharmaceutical Agglomerates of Different Porosity and Composition Using the Adams and Kawakita Equations." *Pharmaceutical research* 17 (8): 949-954.

Nielsen, N. P. K., D. J. Gardner, T. Poulsen, and C. Felby. 2009. "Importance of Temperature, Moisture Content, and Species for the Conversion Process of Wood Residues into Fuel Pellets." *Wood and Fiber Science* 41 (4): 414-425.

Nielsen, N. P.K., J. K. Holm, and C. Felby. 2009. "Effect of Fiber Orientation on Compression and Frictional Properties of Sawdust Particles in Fuel Pellet Production." *Energy & Fuels* 23 (6): 3211-3216. doi: 10.1021/ef800923v.

Nogami, H., T. Nagai, E. Fukuoka, and T. Sonobe. 1969. "Disintegration of the Aspirin Tablets Containing Potato Starch and Microcrystalline Cellulose in Various Concentrations." *Chemical & Pharmaceutical Bulletin* 17 (7): 1450-1455. doi: 10.1248/cpb.17.1450.

Noyes, A. A., and W. R. Whitney. 1897. "The Rate of Solution of Solid Substances in Their Own Solutions." *Journal of the American Chemical Society* 19 (12): 930-934.

Oertli, J. J. 1980. "Controlled-Release Fertilizers." *Fertilizer Research* (1): 103-123.

Panda, B., and S. Mallick. 2012. "Correlation between Compaction and Dissolution of Metoprolol Tartarate Tablets Prepared by Direct Compression Using Different Polymers." *International Journal Pharmacy & Pharmaceutical Science* 4: 77-88.

Paronen, P. 1986. "Heckel Plots as Indicators of Elastic Properties of Pharmaceuticals." *Drug Development and Industrial Pharmacy* 12 (11-13): 1903-1912. doi: doi:10.3109/03639048609042616.

Patel, N. R., and R. E. Hopponent. 1966. "Mechanism of Action of Starch as a Disintegrating Agent in Aspirin Tablets." *Journal of Pharmaceutical Sciences* 55 (10): 1065-1068.

Pietsch, W. 2008. *Agglomeration Processes : Phenomena, Technologies, Equipment*. 1 ed. Hoboken: Wiley. http://CURTIN.eblib.com.au/patron/FullRecord.aspx?p=482225.

Puig-Arnavat, M., L. Shang, Z. Sárossy, J. Ahrenfeldt, and U. B. Henriksen. 2016. "From a Single Pellet Press to a Bench Scale Pellet Mill — Pelletizing Six Different Biomass Feedstocks." *Fuel Processing Technology* 142: 27-33. doi: http://dx.doi.org/10.1016/j.fuproc.2015.09.022.

Quodbach, J., and P. Kleinebudde. 2015a. "A Critical Review on Tablet Disintegration." *Pharmaceutical Development and Technology*: 1-12.

Quodbach, J., and P. Kleinebudde. 2015b. "Performance of Tablet Disintegrants: Impact of Storage Conditions and Relative Tablet Density." *Pharmaceutical Development and Technology* 20 (6): 762-768.

Quodbach, J., A. Moussavi, R. Tammer, J. Frahm, and P. Kleinebudde. 2014. "Tablet Disintegration Studied by High - Resolution Real - Time Magnetic Resonance Imaging." *Journal of Pharmaceutical Sciences* 103 (1): 249-255. doi: 10.1002/jps.23789.

Rehkugler, G. E., and Wesley F. Buchele. 1969. "Biomechanics of Forage Wafering." *Transaction of the ASAE* 12 (1).

Rhén, C., R. Gref, M. Sjöström, and I. Wästerlund. 2005. "Effects of Raw Material Moisture Content, Densification Pressure and Temperature on Some Properties of Norway Spruce Pellets." *Fuel Processing Technology* 87 (1): 11-16.

Ridgway, K., J. Glasby, and P. H. Rosser. 1969. "The Effect of Crystal Hardness on Radial Pressure at the Wall of a Tabletting Die." *Journal of Pharmacy and Pharmacology* 21 (S1): 24S-29S.

Rumpf, H. 1958. "Grundlagen Und Methoden Des Granulierens." *Chemie Ingenieur Technik* 30 (3): 144-158. doi: 10.1002/cite.330300307.

Ryshkewitch, E. 1953. "Compression Strength of Porous Sintered Alumina and Zirconia." *Journal of the American Ceramic Society* 36 (2): 65 - 68.

Said, N., A. García-Maraver, and M. Zamorano. 2015. "Influence of Densification Parameters on Quality Properties of Rice Straw Pellets." *Fuel Processing Technology* 138: 56-64.

Sartain, J. B., W. L. Hall, R. C. Littell, and E. W. Hopwood. 2004. "New Tools for the Analysis and Characterization of Slow-Release Fertilizers." *Environmental Impact of Fertilizer on Soil and Water* 872: 180-195.

Seitavuopio, P., J. Rantanen, and J. Yliruusi. 2003. "Tablet Surface Characterisation by Various Imaging Techniques." *International Journal of Pharmaceutics* 254 (2): 281-286. doi: http://dx.doi.org/10.1016/S0378-5173(03)00026-7.

Serrano, C., E. Monedero, M. Lapuerta, and H. Portero. 2011. "Effect of Moisture Content, Particle Size and Pine Addition on Quality Parameters of Barley Straw Pellets." *Fuel Processing Technology* 92 (3): 699-706. doi: http://dx.doi.org/10.1016/j.fuproc.2010.11.031.

Shang, L., N. P. K. Nielsen, W. Stelte, J. Dahl, J. Ahrenfeldt, J. K. Holm, M. P. Arnavat, L. S. Bach, and U. B. Henriksen. 2014. "Lab and Bench-Scale Pelletization of Torrefied Wood Chips—Process Optimization and Pellet Quality." *BioEnergy Research* 7 (1): 87-94. doi: 10.1007/s12155-013-9354-z.

Shaw, M. D. 2008. "Feedstock and Process Variables Influencing Biomass Densification."

Sheikh-Salem, M., and J. T. Fell. 1981. "The Influence of Initial Packing on the Compression of Powders." *Journal of Pharmacy and Pharmacology*: 491-494.

Shivanand, P., and O. L. Sprockel. 1992. "Compaction Behavior of Cellulose Polymers." *Powder Technology* 69 (2): 177-184. doi: http://dx.doi.org/10.1016/0032-5910(92)85072-4.

Singh, R. N. 2004. "Equilibrium Moisture Content of Biomass Briquettes." *Biomass and Bioenergy* 26 (3): 251-253.

Sitkei, G. 1987. *Mechanics of Agricultural Materials*: Elsevier.

Spiro, M., and S. Siddique. 1981. "Kinetics and Equilibria of Tea Infusion: Kinetics of Extraction of Theaflavins, Thearubigins and Caffeine from Koonsong Broken Pekoe." *Journal of the Science of Food and Agriculture* 32 (11): 1135-1139. doi: 10.1002/jsfa.2740321115.

Stansbury, R. L. 1971. Method of Preparing Slow Release Fertilizer Compositions. United States Re. 27238, filed November 23, and issued

Steendam, R., H. W. Frijlink, and C. F. Lerk. 2001. "Plasticisation of Amylodextrin by Moisture. Consequences for Compaction Behaviour and Tablet Properties." *European Journal of Pharmaceutical Sciences* 14 (3): 245-254. doi: http://dx.doi.org/10.1016/S0928-0987(01)00171-3.

Stelte, W., J. K Holm, A. R. Sanadi, S. Barsberg, J. Ahrenfeldt, and U. B. Henriksen. 2011a. "A Study of Bonding and Failure Mechanisms in Fuel Pellets from Different Biomass Resources." *Biomass and Bioenergy* 35 (2): 910-918.

Stelte, W., J. K. Holm, A. R. Sanadi, S. Barsberg, J. Ahrenfeldt, and U. B. Henriksen. 2011b. "Fuel Pellets from Biomass: The Importance of the Pelletizing Pressure and Its Dependency on the Processing Conditions." *Fuel* 90 (11): 3285-3290. doi: http://dx.doi.org/10.1016/j.fuel.2011.05.011.

Stelte, W., A. R. Sanadi, L. Shang, J. K. Holm, J. Ahrenfeldt, and U. B. Henriksen. 2012. "Recent Developments in Biomass Pelletization–a Review." *BioResources* 7 (3): 4451-4490.

Stewart, A. 1948. "A Tumbling Test for Pressed Pellets." *Journal of Scientific Instruments* 25: 434-440.

Sun, C. C. 2008. "Mechanism of Moisture Induced Variations in True Density and Compaction Properties of Microcrystalline Cellulose." *International Journal of Pharmaceutics* 346 (1–2): 93-101. doi: http://dx.doi.org/10.1016/j.ijpharm.2007.06.017.

Sun, C. C. 2015. "Dependence of Ejection Force on Tableting Speed—a Compaction Simulation Study." *Powder Technology* 279: 123-126.

Sun, C. C., and D. J. W. Grant. 2001. "Influence of Elastic Deformation of Particles on Heckel Analysis." *Pharmaceutical Development and Technology* 6 (2): 193-200.

Sun, J. 2012. "Effect of Particle Size on Solubility, Dissolution Rate, and Oral Bioavailability: Evaluation Using Coenzyme Q." *International Journal of Nanomedicine* 7: 5733-5744.

Tabil, L. 1996. "Binding and Pelleting Characteristics of Alfalfa."

Tabil, L., P. Adapa, and M. Kashaninejad. 2011. *Biomass Feedstock Pre-Processing – Part 2: Densification, Biofuel's Engineering Process Technology*.

Tabil, L., and S. Sokhansanj. 1996. "Process Conditions Affecting the Physical Quality of Alfafa Pellets." *American Society of Agricultural and Biological Engineers* 12 (3): 345-350.

Takeuchi, H., S. Nagira, H. Yamamoto, and Y. Kawashima. 2004. "Die Wall Pressure Measurement for Evaluation of Compaction Property of Pharmaceutical Materials." *International Journal of Pharmaceutics* 274 (1–2): 131-138. doi: http://dx.doi.org/10.1016/j.ijpharm.2004.01.008.

Thomas, M., and A. F. B. van der Poel. 1996. "Physical Quality of Pelleted Animal Feed 1. Criteria for Pellet Quality." *Animal Feed Science and Technology* 61 (1–4): 89-112. doi: http://dx.doi.org/10.1016/0377-8401(96)00949-2.

Thomas, M., D. J. van Zuilichem, and A. F. B. van der Poel. 1997. "Physical Quality of Pelleted Animal Feed. 2. Contribution of Processes and Its Conditions." *Animal Feed Science and Technology* 64 (2–4): 173-192. doi: http://dx.doi.org/10.1016/S0377-8401(96)01058-9.

Tumuluru, J. S. 2015. "High Moisture Corn Stover Pelleting in a Flat Die Pellet Mill Fitted with a 6 Mm Die: Physical Properties and Specific Energy Consumption." *Energy Science & Engineering* 3 (4): 327-341.

Tumuluru, J. S., C. T. Wright, K. L. Kenney, and R. J. Hess. 2010. "A Technical Review on Biomass Processing: Densification, Preprocessing, Modeling and Optimization." *American Society of Agricultural and Biological Engineers*. doi: doi:10.13031/2013.29874.

Tumuluru, J. S., C. T. Wright, K. L. Kenny, and J. R. Hess. 2010. *A Review on Biomass Densification Technology for Energy Application*. Idaho.

Tye, C. K., C. C. Sun, and G. E. Amidon. 2005. "Evaluation of the Effects of Tableting Speed on the Relationships between Compaction Pressure, Tablet Tensile Strength, and Tablet Solid Fraction." *Journal of Pharmaceutical Sciences* 94 (3): 465-472.

USDA. 2014. Oilseeds: World Markets and Trade. (January 2014). Foreign Agricultural Service. 2/1/2014 http://apps.fas.usda.gov/psdonline/psdDataPublications.aspx.

Van der Voort Maarschalk, K., K. Zuurman, H. Vromans, G. K. Bolhuis, and C. F. Lerk. 1996. "Porosity Expansion of Tablets as a Result of Bonding and Deformation of Particulate Solids." *International journal of pharmaceutics* 140 (2): 185-193.

Walker, A. 2005. *The Encyclopedia of Wood*: London: Quatro Publishing.

Walker, E. E. 1923. "The Properties of Powders. Part Vi. The Compressibility of Powders." *Transactions of the Faraday Society* 19 (July): 73-82. doi: 10.1039/TF9231900073.

Whittington, A. A. 2003. Coating for Fertilizer. United States US2005/0076687A1, filed October 10, and issued

Wu, T. Y., A. W. Mohammad, J. M. Jahim, and N. Anuar. 2010. "Pollution Control Technologies for the Treatment of Palm Oil Mill Effluent (Pome) through End-of-Pipe Processes." *Journal of Environmental Management* 91 (7): 1467-1490.

Xia, X. F., Y. Sun, K. Wu, and Q. H. Jiang. 2014. "Modeling of a Straw Ring-Die Briquetting Process." *BioResources* 9 (4): 6316-6328.

Xu, X. T., R. Q. Huang, H. Li, and Q. X. Huang. 2015. "Determination of Poisson’s Ratio of Rock Material by Changing Axial Stress and Unloading Lateral Stress Test." *Rock Mechanics and Rock Engineering* 48 (2): 853-857.

Yan, W., K. Yamamoto, and K. Yakushido. 2001. "N Release from Livestock Waste Compost Pellets in Barley Fields." *Soil Science and Plant Nutrition* 47 (4): 675-683.

Yan, W., K. Yamamoto, and K. Yakushido. 2002. "Changes in Nitrate N Content in Different Soil Layers after the Application of Livestock Waste Compost Pellets in a Sweet Corn Field." *Soil Science and Plant Nutrition* 48 (2): 165-170.

Yusof, Y. A., S. K. Ng, N. L. Chin, and R. A. Talib. 2010. "Compaction Pressure, Wall Friction and Surface Roughness Upon Compaction Strength of Andrographis Paniculata Tablets." *Tribology International* 43 (5–6): 1168-1174. doi: http://dx.doi.org/10.1016/j.triboint.2009.12.020.

Yusoff, S. 2006. "Renewable Energy from Palm Oil – Innovation on Effective Utilization of Waste." *Journal of Cleaner Production* 14 (1): 87-93. doi: http://dx.doi.org/10.1016/j.jclepro.2004.07.005.

Zafari, A., and M. H. Kianmehr. 2013. "Factors Affecting Mechanical Properties of Biomass Pellet from Compost." *Environmental Technology* 35 (4): 478-486. doi: 10.1080/09593330.2013.833639.